INFORMATION TO USERS

This manuscript has been reproduced from the microfilm master. UMI films the text directly from the original or copy submitted. Thus, some thesis and dissertation copies are in typewriter face, while others may be from any type of computer printer.

The quality of this reproduction is dependent upon the quality of the copy submitted. Broken or indistinct print, colored or poor quality illustrations and photographs, print bleedthrough, substandard margins, and improper alignment can adversely affect reproduction.

In the unlikely event that the author did not send UMI a complete manuscript and there are missing pages, these will be noted. Also, if unauthorized copyright material had to be removed, a note will indicate the deletion.

Oversize materials (e.g., maps, drawings, charts) are reproduced by sectioning the original, beginning at the upper left-hand corner and continuing from left to right in equal sections with small overlaps.

ProQuest Information and Learning
300 North Zeeb Road, Ann Arbor, MI 48106-1346 USA
800-521-0600

Structure/Function Studies on a Bifunctional Enzyme in Tyrosine Biosynthesis

Kevork Mekhssian

A Thesis

in

The Department

of

Chemistry and Biochemistry

Presented in Partial Fulfillment of the Requirements

For the Degree of Master of Science at

Concordia University

Montreal, Quebec, Canada

May, 2003

ABSTRACT

Structure/Function Studies on a Bifunctional Enzyme in Tyrosine Biosynthesis

Kevork Mekhssian

Chorismate mutase – prephenate dehydrogenase (CM-PD) is a bifunctional enzyme that catalyzes two sequential reactions in the tyrosine biosynthetic pathway of *E. coli*. These activities, along with other enzymes of the shikimate pathway are not found in humans and hence are potential targets for the design of inhibitors that can act as antimicrobial agents and herbicides. This thesis probes further the catalytic mechanism of CM-PD.

Three cysteine residues are found within each monomer of dimeric CM-PD. The studies in Chapter 2 help to define their role in the structure of the enzyme, the chemistry of the reactions, and in the relationship between the sites at which the two reactions occur. Site-directed mutagenesis performed on Cys95, Cys169 and Cys215 indicated that only Cys215 is important for the activity of CM-PD and is most important in the binding of prephenate. However, comparative modeling studies indicate that Cys215 may be at the active site of prephenate dehydrogenase and help orient an important catalytic group, His197. Chemical modification of the enzyme with cysteine-specific reagents, iodoacetamide and Ellman's reagent (DTNB), resulted in the loss of both mutase and dehydrogenase activities. Inactivation of wild-type and variant forms of prephenate dehydrogenase suggested that one cysteine (Cys215) is protected against alkylation by NAD^+ plus tyrosine, prephenate and, surprisingly, an inhibitor that mimics the transition state of the mutase reaction. Comparing the effects of alkylation of wild-type and K37Q

by iodoacetamide showed that the protective effects of prephenate and the mutase transition state analog were due to their binding to the mutase site rather than the dehydrogenase site. Time-dependent chemical modification followed by peptide mapping indicated that Cys215 is the most reactive and/or accessible cysteine, followed by Cys95 and Cys169.

In Chapter 3, ESI-mass spectrometry in conjunction with chemical modification studies were used to determine the reactivity and ionization state of Lys37 of CM-PD. The lysine at this position has been proposed to play a role in stabilizing the transition state of the mutase reaction. Reaction of CM-PD with the Lys-specific reagent TNBS resulted in a time-dependent loss of CM activity but not PD activity. The pK_a of Lys37 was determined to be ~ 7.5, by titration of the enzyme with the TNBS as a function of pH. Mass spectrometric analysis of Glu-C digested wild-type and K37Q variant enzyme demonstrated that Lys37 was significantly modified at pH 7.2 and modification was complete by pH 8.5. Reaction of CM-PD with TNBS in the presence of a mutase transition state analog protected the mutase from inactivation and a reduction in modification was also observed by MS. These results along with previous pH rate profiles imply that the pK_a of this reactive lysine is markedly reduced. Analysis of the crystal structures of related CMs complexed with the transition state analog suggest that this may be due to the highly electrostatic environment of Lys37.

ACKNOWLEDGMENTS

First and foremost, I would like to thank Dr. Joanne Turnbull for her guidance and support throughout my studies. Her energy and enthusiasm, dedicated to the learning process of her graduate students contributed greatly to my development as a researcher and have made my studies an enjoyable and positive experience.

I would like to thank my committee members: Dr. Justin Powlowski and Dr. Ann English for their encouragement and advice. Special thanks to Dr. Peter White whose helpful discussion and criticism throughout my project was essential for its success. A very big thank you to Dr. Bernie Gibbs and MDS Pharma Services for giving me the chance to learn more about mass spectrometry. Many thanks to the Chemistry and Biochemistry department, all the professors, technicians and secretaries. Good luck with the move to the new building. I am grateful to all the graduate and undergraduate students that have made my degree at Concordia such a positive experience. In particular, I would like to thank: Raph, Julie "ma poule", John a.k.a. APO, Steve, Kimberley, Tony Lee, David, Andrea and Peter John Wright.

I would like to thank my family: Jean, Taline, Vahe and my sweet sister Stephie, for their love and encouragement. My uncle Tzevac for supporting me throughout my studies. Finally, I would like to thank Tatiana, my girlfriend, whose unconditional love and understanding has been a source of constant support and inspiration during the course of my degree.

To the memories of Nero Sorfazlian and Chake Deukmedjian

TABLE OF CONTENTS

LIST OF FIGURES

CHAPTER 1

CHAPTER 2

CHAPTER 3

LIST OF TABLES

CHAPTER 2

CHAPTER 3

LIST OF ABBREVIATIONS

ACN	acetonitrile
Ala (A)	alanine
BMH	bismaleimidohexane
BMOE	bismaleimidoethane
CD	circular dichroism
CM	chorismate mutase
CM-PD	chorismate mutase – prephenate dehydrogenase
CM-PDT	chorismate mutase – prephenate dehydratase
Cys (C)	cysteine
DMSO	dimethyl sulfoxide
DTNB	5,5'-dithio-bis(2-nitrobenzoic acid)
DTT	dithiothreitol
E. coli	*Escherichia coli*
EDTA	ethylenediamine tetra-acetic acid
ESI	electrospray ionization
Gdn-HCl	guanidinium hydrochloride
HPP	(4-hydroxyphenyl)pyruvate
IAM	iodoacetamide
IPTG	isopropyl-β-D-thiogalactopyranoside
Lys (K)	lysine
MS	mass spectrometry
MW	molecular weight
NEM	N-ethylmorpholine
NAD^+	oxidized form of nicotinamide adenine dinucleotide
PAGE	polyacrylamide gel electrophoresis
PD	prephenate dehydrogenase
TFA	trifluoroacetic acid
TNBS	2,4,6-trinitrobenzene sulfonic acid
Tris	tris(hydroxymethyl)aminomethane
TS	transition state
TSA	transition state analog
Ser (S)	serine
SDS	sodium dodecylsulfate
WT	wild-type

CHAPTER 1

General Introduction

1.0 Biosynthesis of Aromatic Amino Acids

The pathway for aromatic amino acid biosynthesis in *E. coli* and other microorganisms and plants is known as the shikimate pathway (1-4). The shikimate pathway converts derivatives of glucose into chorismate which resides at a branch point in the pathway, and serves as a precursor for the synthesis of phenylalanine, tyrosine and tryptophan as well as for a number of aromatic compounds such as vitamin K, ubiquinone, folate and enterochelin (5, 6).

Many of the enzymes responsible for aromatic amino acid biosynthesis exist as isoenzymes, multifunctional proteins or multienzyme complexes, thus allowing for a diversity of regulation, at both the genetic and protein level. Many of the genes encoding the biosynthetic enzymes for aromatic amino acids are organized in operons which are regulated by three regulatory genes *tyrR*, *trpR* or *pheR* (7, 8). The protein products of these genes combine with the appropriate amino acid co-repressor, resulting in the formation of complexes that bind at the operator loci. Additional regulation is achieved through attenuation at the level of charged tRNA(s) (9). However, the major form of control is achieved through feedback inhibition by phenylalanine, tyrosine and tryptophan of enzymes at the start and at the branch point in the shikimate pathway leading to these products.

1.1 The Pathway to Tyrosine and Phenylalanine Biosynthesis in *E. coli*

The end of the pathway for tyrosine biosynthesis in *E. coli* involves two sequential reactions catalyzed by the enzyme chorismate mutase-prephenate dehydrogenase (CM-PD) (10). CM (EC 5.4.99.5) catalyzes the Claisen rearrangement of chorismate to prephenate, while PD (EC 1.3.1.12) oxidatively decarboxylates prephenate to (4-hydroxyphenyl)pyruvate (HPP) in the presence of NAD^+ (Fig. 1.1). An aromatic aminotransferase then converts HPP to tyrosine (10). CM-PD is highly regulated by the end-product of its pathway, tyrosine (10). However, prephenate dehydrogenase activity is inhibited to a greater extent than the chorismate mutase reaction (11). Moreover, NAD^+ enhances tyrosine inhibition of both mutase and dehydrogenase activities by increasing the enzyme's affinity for the modulator (12, 13).

The first two reactions in the biosynthesis of phenylalanine from chorismate in *E. coli* also involve a bifunctional enzyme, chorismate mutase-prephenate dehydratase (CM-PDT). CM converts chorismate to prephenate, while PDT catalyzes the dehydration and decarboxylation of prephenate to yield phenylpyruvate. This product undergoes a transamination to form phenylalanine (Fig. 1.1). The end-product phenylalanine inhibits both mutase and dehydratase activities, with the dehydratase activity affected significantly more than the mutase (14).

E. coli CM-PD is homodimeric with a molecular weight of 42 kDa per monomer (15-17). The enzyme is considered bifunctional since both activities are associated with each

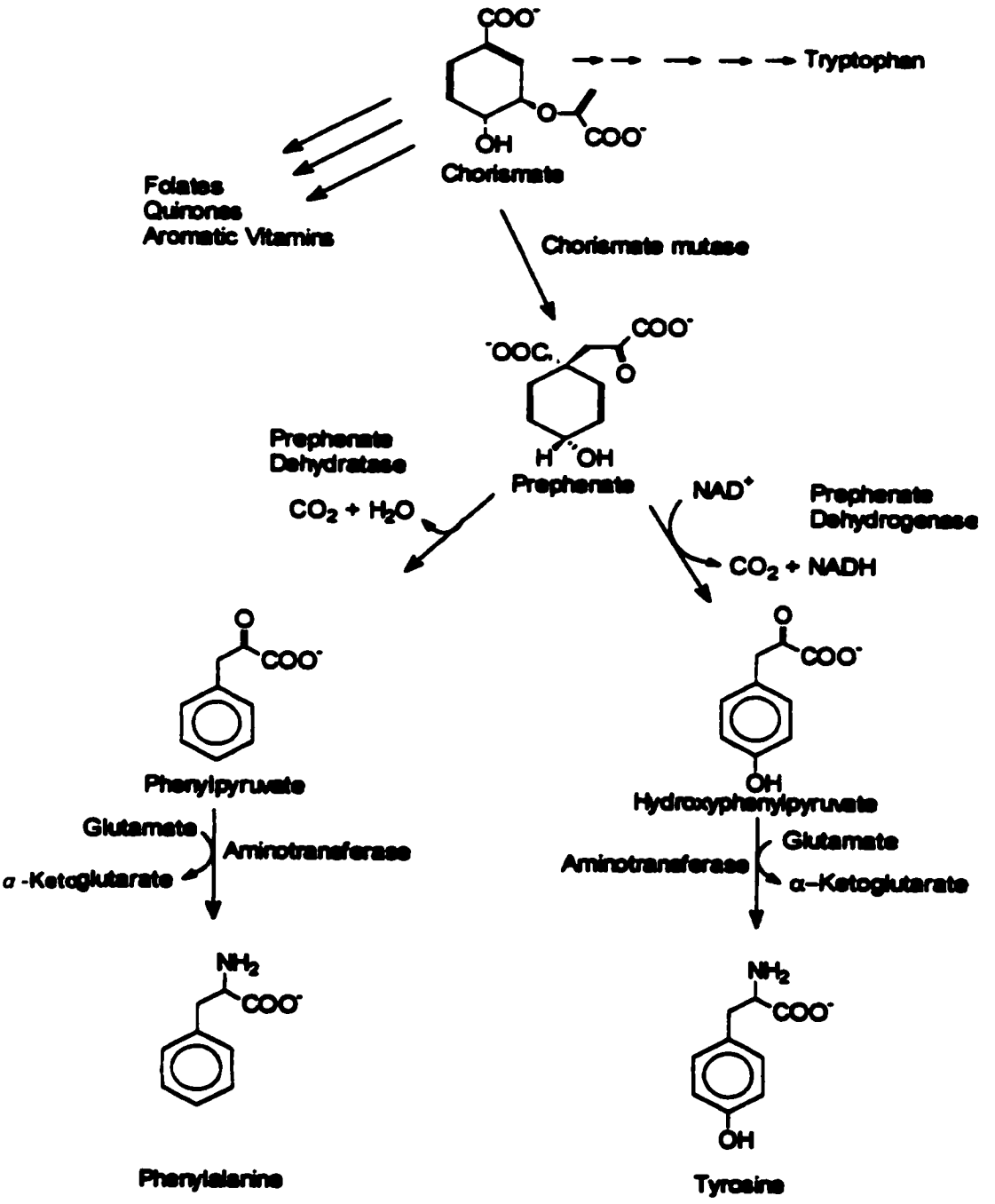

Fig. 1.1 Aromatic amino acid biosynthesis. Figure adapted from D. Christendat (18).

of the polypeptide chains. However, the structural organization of the sites which catalyze the two activities within the enzyme has not been firmly established since there is no crystal structure of this bifunctional enzyme.

Alignment of the primary sequence of *E. coli* CM-PD with that of *E. coli* CM-PDT suggests that the first 100 amino acid residues of the polypeptide chain is responsible for the mutase activity, while the remaining 274 residues comprise the dehydrogenase (8). Since the product of the first reaction, prephenate, is a substrate for the second reaction, there has been much interest concerning the spatial geometry of the active site(s) in which the two reactions occur. There is evidence supporting a common binding site for prephenate and chorismate, as well as evidence for two distinct non-interacting yet closely situated active sites. Studies supporting a single site showed that a variety of inactivating agents such as urea, chemical modifying reagents, extremes in pH and temperature led to parallel loss of both mutase and dehydrogenase activities (16, 19, 20). Kinetic studies showed that the two reactions are catalyzed with similar turnover numbers (21). Moreover, prephenate acting as a substrate in the dehydrogenase reaction or as an inhibitor of the mutase reaction bound with similar affinities (20). Evidence in favor of two distinct active sites or of specific residues involved in catalyzing each of the two reactions, are the observations that the two activities show markedly different pH rate profiles (22) and are inhibited to different degrees by tyrosine (11, 13), and by a family of dicarboxylic acid-containing compounds (malonic acid derivatives) (11). Furthermore, a putative transition state analogue of CM, *endo*-oxabicyclic diacid, has been shown to selectively inhibit the mutase reaction without affecting dehydrogenase activity (11).

Very recently, a *trans*-2,3-pleiadanedicarboxylic acid was synthesized, which specifically inhibits PD without affecting mutase activity (23). The idea of distinct active sites has been supported through recent site-directed mutagenesis studies by Christendat and Turnbull (24, 26). Amino acid substitutions introduced in the PD portion of the enzyme eliminate dehydrogenase activity (H197N) (26) and prephenate binding (R294N) (24) while having no affect on the mutase reaction. Similarly a substitution in the mutase portion (K37Q) has no effect on dehydrogenase activity (26).

There is compelling evidence to suggest that if there are two active sites they are in very close proximity to each other and are structurally interrelated. Computer simulation studies combined with radioactivity channeling experiments showed that some of the prephenate formed from chorismate is converted directly to HPP (20). Christopherson (25) has provided some kinetic evidence by inhibition studies with the malonic acids that the two sites are overlapping. Lastly, protein variants produced by site-directed mutagenesis of residues in the dehydrogenase portion of the molecule (H189N, K178R, and R286A) have been characterized which clearly affect both CM and PD activities (24, 26).

1.2 Chorismate Mutase

The catalytic mechanism of chorismate mutase has been well studied. The rearrangement of chorismate to prephenate can occur in the absence of the enzyme, however the rate of the reaction is accelerated by over a million-fold in the presence of the mutase (29, 30). CM is unique because it is the only known enzyme-catalyzed Claisen rearrangement in

nature. The uncatalyzed reaction of chorismate is an intramolecular mechanism that is believed to proceed via a transition state of chair-like geometry (31) (Fig. 1.2). Chorismate exists in two distinct conformers in aqueous solution, the diequatorial and the diaxial conformer. Proton NMR studies have indicated that 10 to 20% of chorismate, with its hydroxyl and enolpyruvyl group in the diaxial conformer, exists in equilibrium with

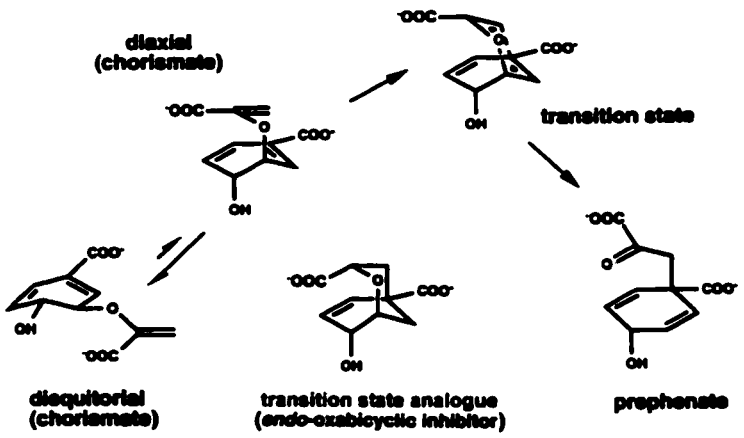

Fig. 1.2. Uncatalyzed rearrangement of chorismate. Adapted from Christendat *et al.* (26)

the more stable diequatorial form (32). The non-enzymatic reaction occurs via the diaxial conformer of chorismate. In aqueous solution, the enolpyruvyl group of the diaxial conformer of chorismate is stabilized by hydrogen bonding to water molecules thus facilitating bond breakage between C-5 and the oxygen of chorismate. Similar to the uncatalyzed rearrangement, chorismate mutase also selectively discriminates against the diequatorial conformer of chorismate (32). The structural features required for catalysis have been determined by the synthesis and characterization of numerous chorismate analogues (33, 34). Neither the 5,6-olefinic nor the 4-hydroxyl are necessary, but mutases

require the allyl vinyl ether and the two carboxylate groups for binding chorismate to the active site (33). Kinetic studies suggest that the mutase reaction catalyzed by the bifunctional enzyme, CM-PD of *E. coli*, is mediated by enzymic acids and bases (22, 35). An enzymic acid has been suggested to either protonate the ether oxygen (O7) or heterolytically cleave the ether bond. It has been proposed that the rearrangement is facilitated by the protonation of the ether oxygen (O7) by an enzymic acid, in conjunction with the attack on the C-1 by an electron pair on the methylene group of the enol pyruvyl side chain (11). In contrast, the monofunctional mutase from *B. subtilis* specifically binds the chair-like conformer of chorismate, which then spontaneously rearranges to prephenate (36, 37).

Crystal structures are available for CM from *S. cerevisiae* (38), *B. subtilis* (39) and the mutase domain of the bifunctional *E. coli* CM-PDT (40) ("mini-mutase") complexed to the mutase transition state analog. While there is little sequence or structural similarity between these three monofunctional mutases, the electronic environment of the active sites appears to be well conserved. Fig. 1.3 shows the structure of the mutase domain of *E. coli* CM-PDT, complexed with the mutase transition state analog.

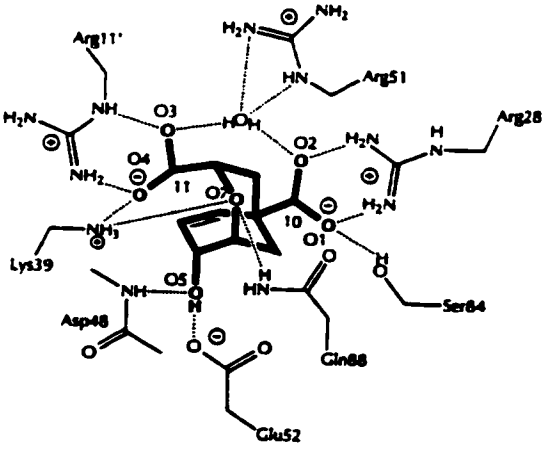

Fig. 1.3 The structure of *E. coli* "mini- mutase" complexed with *endo*-oxabicyclic diacid. This figure was adapted from Lee *et al.* (41).

This transition state analog (*endo*-oxabicyclic diacid) was synthesized by Bartlett and Johnson (42) and was shown to be a potent and selective inhibitor of chorismate mutase; it binds to the enzyme about 250-fold more tightly than chorismate (11, 43). The mutase domains of CM-PD and CM-PDT are highly homologous, hence the structure of the CM portion of CM-PDT has provided valuable insights as to the residues that may participate in the mutase reaction catalyzed by CM-PD. In Fig. 1.3, Lys39 of the "mini-mutase" forms an electrostatic bond with the C11 carboxylate group and a hydrogen bond with O7. By homology, this suggests that Lys37 of CM-PD is important in stabilizing the intermediates in the mutase reaction. Specifically, it may lock the chorismate into the diaxial conformation, facilitating the formation of the transition state, in which the bridge atoms are in the chair-like conformation or protonate the ether oxygen of chorismate in the TS to promote the rearrangement (11). Site-directed mutagenesis performed on CM-PD and the mini-mutase (26, 27, 28) has shown that the cationic residue Lys37 (Lys39 in the mini-mutase) is indeed crucial for CM activity. If this Lys is replaced with Ala or Gln, mutase activity is completely abolished. Interestingly, this mutation in CM-PD has almost no effect on dehydrogenase activity (26).

Another line of evidence that suggests that a cationic residue, possibly Lys37 is involved in chorismate binding stems from the pH dependence of $(V/K)_{chorismate}$. Residues that titrate in this profile are associated with the free enzyme and/or substrate and are essential for substrate binding and/or catalysis. Early work by Turnbull *et al.* (22) showed that the pH dependence of $(V/K)_{chorismate}$ is a bell-shaped curve and indicated the involvement of three ionizable groups (Fig. 1.4). The slope of the acid and alkaline limbs of +1 and –2,

respectively suggest that two groups had to be protonated and one deprotonated. One of these protonated residues may be Lys37.

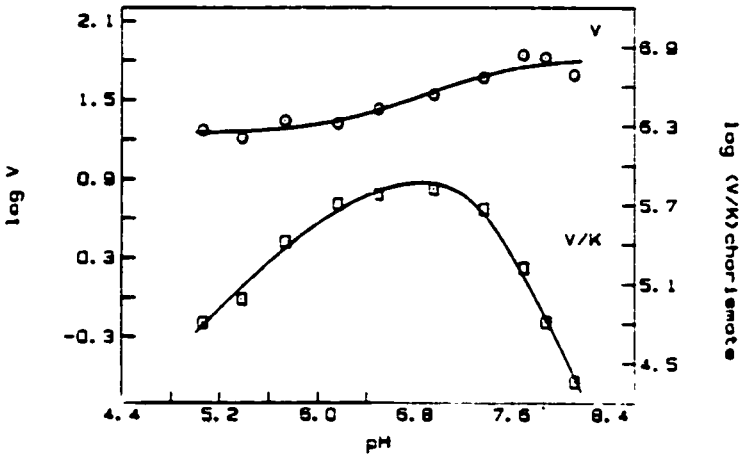

Fig. 1.4 pH profile of V and V/K for the reaction catalyzed by *E. coli* CM (22). This figure was adapted from Turnbull *et al.* (22).

1.3 Prephenate Dehydrogenase

Initial velocity, product and dead-end inhibition studies have established that the kinetic mechanism of PD involves the random addition of prephenate and NAD^+ with binding of substrates in rapid equilibrium and catalysis as the rate-limiting step (21). However, the identity and roles of residues involved in the chemistry of the reaction are still under investigation. Based on the results of pH profiles (22, 46), isotope effects (47, 48), chemical modification of the enzyme with DEPC (35), peptide mapping (35), and site-directed mutagenesis (24, 26), a model for the catalytic mechanism has been put forward (Fig. 2.5). It has been proposed that prephenate and NAD^+ bind to distinct subsites in the PD domain. An enzymic hydrogen bond acceptor (His197, pK 6.7) is believed to polarize

the 4-hydroxyl group of prephenate, lowering the activation barrier to facilitate decarboxylation and hydride transfer of prephenate to NAD^+ (26). The two chemical steps occur simultaneously, driven by the aromaticity of the product and also possibly because the ring carboxylate is near and/or in a hydrophobic pocket promoting decarboxylation (24).

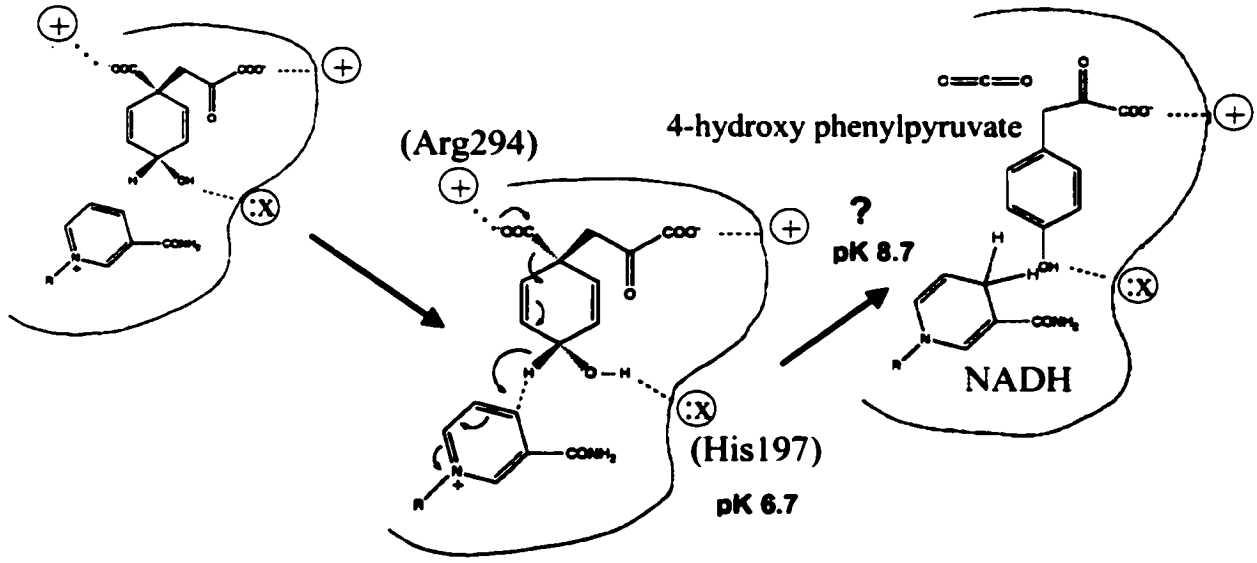

Fig. 1.5 A possible mechanism of the PD reaction involving ionizable amino acid residues at the active site. Unknown group (?) interacts with side chain carboxylate. Adapted from Christendat *et al.* (26).

Studies examining the binding of substrate analogues to WT and variant enzymes have shown that Arg294 interacts with the ring carboxylate of prephenate (24). pH rate profiles have suggested that a group with pK_a of ~8.7 must be protonated in order to bind prephenate to the enzyme - NAD^+ complex. However, this and other residues involved in

the mechanism have not been identified, although there are several residues conserved between PD of *E. coli* CM-PD and several monofunctional PD's.

Tyrosine, the end product of the pathway, inhibits both dehydrogenase and mutase activities in an allosteric fashion (10). However, the mechanism of the inhibition is still under debate. There is evidence using analytical ultracentrifugation that tyrosine inhibits enzyme activity by promoting the formation of an inactive tetramer from the active dimer (13). In contrast, other centrifugation experiments showed no evidence for a quaternary structural change upon inhibition (49, 50). Furthermore, it has been suggested through analysis of kinetic models that there are tertiary structural changes in the enzyme propagated through the subunits that promote the formation of the inactive conformation of CM-PD (51). Very recent work in the Turnbull lab has identified two residues, His245 and His257 that are critical for tyrosine inhibition of both CM-PD activities (T. Lee, unpublished).

1.4 Role of Cysteines in CM-PDT and CM-PD of *E. coli*

Sulfhydryl groups of cysteinyl residues of peptides and proteins are generally the most reactive of all amino acid side-chain functionalities under normal physiological conditions. They may be readily alkylated, acylated, arylated, oxidized, and will form complexes with many heavy-metal ions (52). Sulfhydryl groups are important to both the structure and function of many proteins. In the protonated form they are capable of providing weak hydrogen-bonding in relatively water-free environments, such as those which occur within the protein or at the active sites. But it is their ability to dissociate to

the strongly nucleophilic anion at moderately alkaline pH that renders these groups very reactive towards a variety of reagents (52, 53).

CM-PD of *E. coli* contains 373 amino acids, three of which are cysteines at positions 95, 169 and 215. Two of these cysteines, Cys169 and Cys215, are located in the dehydrogenase domain whereas Cys95 is found in the mutase portion of the enzyme. Previous studies using chemical modification and peptide mapping combined with kinetic studies, indicate that Cys215 is important for maintaining the structural integrity of both the dehydrogenase and mutase active sites (11, 16). In contrast, similar studies using similar techniques have shown that the homologous residue in CM-PDT (Cys216) is critical for prephenate binding but plays no role in the mutase reaction (16, 54, 55). Site-directed mutagenesis has also pinpointed Cys374 as an important residue in the binding of phenylalanine to PDT (56). Furthermore, the monofunctional chorismate mutase from *B. subtilis* contains a Cys residue (Cys75) at the active site, which has been shown by X-ray diffraction studies to interact with the TS analog (57).

1.5 Chemical Modification of Cysteines and Lysines of Proteins

Chemical modification of proteins using group specific reagents has been instrumental in helping to identify enzymic groups important for the biological function of enzymes and proteins (58-61).

However caution must be taken in interpreting data obtained using these reagents keeping in mind the following points: First, the reactivity of a group at a given pH will be a

function of its pK_a and accessibility to the reagent, both of which are governed by the native structure of the protein. However, exceptional reactivity of a given group does not necessarily imply importance to the protein's function. Second, if a group is essential for the function of an enzyme, then inhibition of activity should be stoichiometric with incorporation of reagent into this group. Furthermore, the presence of substrate or product should inhibit such modification and inhibition. Third, inhibition should be invariant with the type of modifying reagent used; therefore, a variety of reagents with different characteristics must be used in such studies. As many of these reagents are bulky and may affect enzyme function due to steric considerations, chemical modification should be used in combination with site-directed mutagenesis to better assess the importance of specific residues. Moreover this traditional approach of residue identification using site-specific reagents has been revitalized by recent advances in protein mass spectrometry, which allow a clearer understanding of the results of modification (62-64).

In this thesis, the role and reactivity of Cys and Lys residues in *E. coli* CM-PD is under investigation. Hence, a brief description of the chemistry of the reagents used to modify these amino acids is necessary for an understanding of the present work:

1) DTNB (Ellman's reagent):

This reagent is very useful as a free sulfhydryl assay reagent due to its high specificity for –SH groups at neutral pH values, its high molar extinction coefficient and its short reaction times (65). DTNB reacts with a free sulfhydryl group to yield a mixed disulfide and 2-nitro-5-thiobenzoic acid (TNB) (Fig. 1.6A). The target of DTNB in this reaction is

the conjugate base (R - S^-) of a free sulfhydryl group. Therefore, the rate of this reaction is dependent on several factors such as the reaction pH, the pK_a of the sulfhydryl group, and steric and electrostatic effects (66). TNB is the "colored" species produced in this reaction and has an extinction coefficient of 14,150 $M^{-1}cm^{-1}$ at 412 nm (66, 67). This reaction is readily reversed by the addition of a reducing agent such as dithiothreitol (DTT) and it is also unstable under acidic conditions, precluding detection of the adduct by mass spectrometry.

2) Iodoacetamide:

Iodoacetamide, a relatively small molecule relative to DTNB, reacts mainly with cysteines but has also been reported to modify histidines and methionines to a lesser extent to yield the corresponding carboxamidomethyl derivative (53, 68). The fastest reaction is usually with sulfhydryl groups and involves nucleophilic attack of the sulfhydryl anion on the reagent, with the iodide group as a leaving group (Fig. 1.6B). The modification with cysteines is irreversible and the alkylation adduct formed (+57 amu) remains intact during mass spectral analysis.

3) Bismaleimidohexane (BMH) and Bismaleimidoethane (BMOE):

Bifunctional cross-linking reagents are compounds that conjugate molecules at specific functional groups, generating a bridge between these residues. The use of bifunctional cross-linking reagents have been instrumental in determining if structural interactions occur between different proteins (69), determining the quaternary structure of a single protein (70) and, when combined with mass spectrometric analysis of proteolytic digests,

identifying residues present at the subunit or protein-protein interfaces (71). For example, cross-linking studies with the cysteine specific reagent bismaleimidohexane (BMH) revealed that the E1 protein of HPV11 existed predominantly as a hexamer when resolved on SDS-PAGE. This result was further confirmed by sedimentation velocity analytical ultracentrifugation performed on HPV 11 E1 (72). BMH is a homobifunctional, sulfhydryl-reactive cross-linker with a spacer arm length of 16.1 Å. It contains two maleimide groups connected by a 6-carbon chain (Fig. 2.6C). A 2-carbon chain separates the maleimide groups in bismaleimidoethane (BMOE), thus producing a shorter linker region (8.0 Å) between reactive groups than with BMH.

4) Trinitrobenzene sulfonic acid (TNBS):

The reaction of 2,4,6-trinitrobenzenesulfonic acid (TNBS) with amino groups has been invaluable in studying the function and reactivity of the ε-amino groups of lysyl residues in proteins (73-75). The reaction of TNBS with the primary amino groups in proteins is shown in Fig. 1.6D. This modification is easy to monitor by spectral analysis. The TNBS adduct of lysine residues absorbs strongly at 346 nm (ε_{346} = 14500 M^{-1} cm^{-1}). The rate of modification is a sensitive indication of the amino group's basicity, which must be in the deprotonated state in order to react with TNBS (53). An important reason for selecting this reagent is that modification is irreversible, so the adduct (+211 amu) can be observed in the mass spectrum of the protein.

Fig. 1.6 Chemical modification of protein sulfhydryl and lysyl groups

Sulfhydryl groups can react with DTNB (A), iodoacetamide (B) or BMH (C) while lysyl groups can react with TNBS (D).

A)

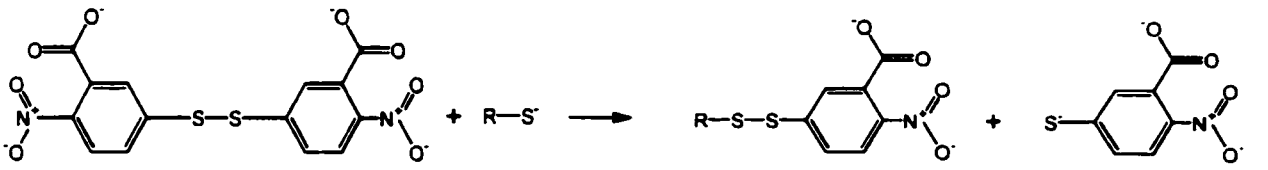

DTNB Cys-residue Yellow anion

B)

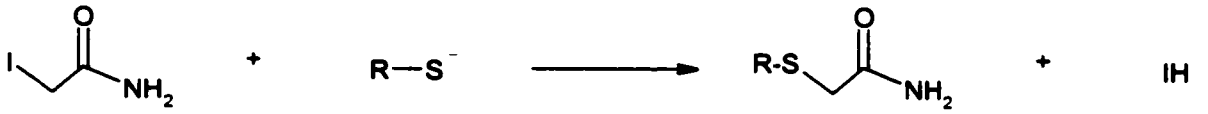

Iodoacetamide Cys-residue IAM adduct
(+57 amu)

C)

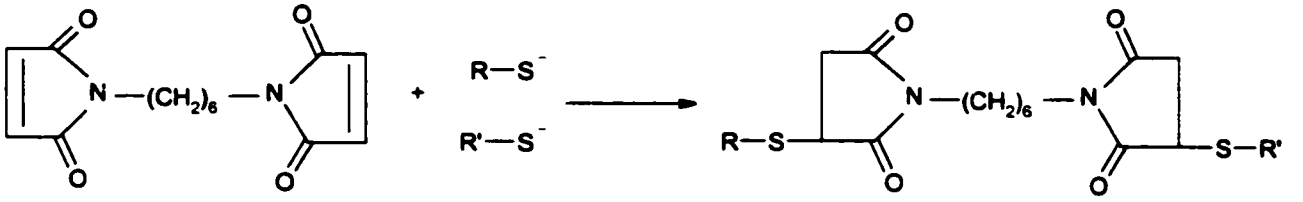

BMH
Spacer arm 16.1 Å

Cys-residues

D)

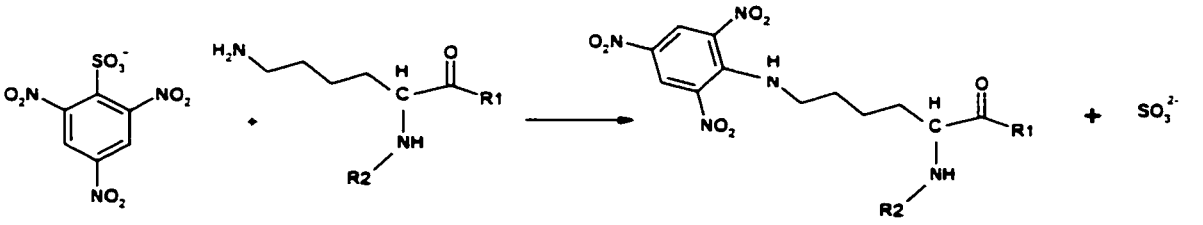

TNBS Lysine residue TNBS adduct
(+211 amu)

1.6 SCOPE OF THIS THESIS

In chapter two, the importance of three Cys residues in the activity of CM-PD are assessed by site-directed mutagenesis and chemical modification of WT and variant forms of the enzyme. Furthermore, this chapter shows the utility of mass spectrometry in verifying the amino acid substitutions and in assessing the reactivity and accessibility of the Cys residues in the native protein.

In chapter three, the pK_a of a key Lys residue in the CM reaction is estimated by monitoring the pH dependence of its reactivity using chemical modification and peptide mapping.

In the absence of a crystal structure these studies provide further insight into the catalytic mechanism of the enzyme and the interdependence of the two sites.

CHAPTER 2

Role of Cysteines in the Structure and Function of *E. coli* Chorismate Mutase - Prephenate Dehydrogenase

2.0 INTRODUCTION

CM-PD from *E. coli* possesses three Cys residues; Cys169 and Cys215 are located in the PD portion of the molecule while Cys95 is associated with the C-terminus of the CM domain. Cys215 is conserved between CM-PD and the related bifunctional *E. coli* enzyme CM-PDT (Cys216), both of which utilize prephenate as a substrate.

Earlier studies examining the reactions of CM-PD with the Cys-modifying reagents iodoacetic acid (11), iodoacetamide (16) and DTNB (11) revealed a time dependent loss of enzyme activity suggesting that at least one Cys, presumably Cys215, was critical for both CM and PD activities. Chemical modification studies and more recent site-directed mutagenesis on *E. coli* CM-PDT have verified the importance of Cys216 in the dehydratase reaction in prephenate binding (55). Recent structural work and kinetic studies on WT and site-directed variants of a monofunctional CM from *B. subtilis* have indicated the involvement of a Cys residue in helping to stabilize the pseudo diaxial form of chorismate in the transition state of the mutase reaction (57, 76). It has also been postulated for CM of *E. coli* CM-PD that an active site nucleophile might assist in the rearrangement through acid/base catalysis (48).

There have been no site-directed mutagenesis studies examining the importance of any Cys residues in *E. coli* CM-PD. The purpose of this chapter is to provide further information as to the roles that these three Cys play in the structure and function of *E. coli* CM-PD. This has been accomplished through kinetic characterization of site-directed

variants of the enzyme and by extending the chemical modification studies to those of the variant forms of the proteins performed in the presence or absence of substrates and substrate analogs. Furthermore, a 3D structural model for the PD portion of *E. coli* CM-PD has been generated using an internet-based comparative modeling software package. From these studies we propose a role for Cys215 in *E. coli* CM-PD.

2.1 EXPERIMENTAL PROCEDURES

2.1.1 Materials

Chorismate was isolated from *Klebsiella pneumonia* 62-1 as described by Rieger and Turnbull (77), prephenate was prepared as previously described (78), and NAD^+ (grade I) was obtained from Boehringer-Mannheim. Stock solutions of these substrates were prepared in water or in an appropriate buffer and the pH adjusted to 7.5 before storage at –20 °C. Their exact concentrations were determined using published extinction coefficients (79) and enzymatic end-point analysis (44). (3-endo-8-exo)-8-hydroxy-2oxa (3.3.1) non-6-ene-3,5-dicarboxylic acid bis (dicyclohexylammonium) salt, (endo-oxabicyclic diacid) (42) was a generous gift from Dr. Paul Bartlett of the University of California, Berkeley, and was stored at –86 °C as a stock solution of 2 mM in water. L-tyrosine was purchased from ICN Biochemicals Inc. Oligonucleotides of standard purity were obtained from Biocorp Inc. QuikChange XL site-directed mutagenesis kit was from Stratagene and restriction enzymes were from MBI Fermentas. Q-Sepharose Fast Flow anion exchange resin was from Amersham Biosciences as were NAP pre-packed Sephadex G-25 size exclusion buffer exchange columns. Iodoacetamide, 5,5'-dithio-*bis*-(2-nitrobenzoic acid) (DTNB) and Trypsin (modified bovine; sequencing grade) were purchased from Sigma. Dithiothreitol (DTT) and acetonitrile (HPLC grade) were from Fisher. Trifluoroacetic acid (TFA) (HPLC grade), Bis-Maleimidohexane (BMH) and Bis-Maleimidoethane (BMOE) were from Pierce. All other chemical reagents were obtained commercially and were of the highest quality available.

2.1.2 Source of Recombinant WT and Variant CM-PD of *E. coli*

Recombinant wild-type (WT) CM-PD of *E. coli* was prepared by D. Christendat (26) by subcloning *tyrA* (the gene encoding CM-PD) from plasmid pKB45 (80) into an inducible expression vector pSE380 (Novagen) to yield pVIV1 (26). Construction of variant C169A was performed with the QuikChange XL site-directed mutagenesis kit (Stratagene) following the manufacturer's instructions. The oligonucleotide sequences used to generate this variant were as follows (underlined sequences correspond to mutated bases; italic corresponds to silent mutation): C169A (**TGT** to **GCT**), 5'-CCTTTACCGAAAGAT**GCT**ATTCTG*GTCGAC*CTGGCATCAGTG-3' (sense) and 5'-CACTGATGCCAG*GTCGAC*CAGAATA**GC**ATCTTTCGGTAAAGGC-3' (antisense). The mutant was initially screened for the addition of a unique restriction site, *Sal*I. Variants C95A, C215A and C215S were constructed by D. Christendat as described in Christendat *et al.* (26). All mutations were confirmed by DNA sequencing at the Centre for Structural and Functional Genomics (Concordia University) using the CEQ 2000XL DNA sequencer. DNA was prepared for sequencing using a Promega Wizard™ plasmid preparation kit.

2.1.3 Expression and Purification of WT and Variant Forms of *E. coli* CM-PD

CM-PD was purified by the method of Christendat *et al.* (26) with slight modifications. WT enzyme was expressed in *E. coli* strain XL2-Blue (Novagen) following transformation by pVIV1. The resulting strain was grown in LB medium containing 50 μg/ml ampicillin to an OD_{600} nm of 0.8 before induction with 0.5 mM IPTG. The cells were harvested 4 h after induction with a yield of 10 g of wet weight/L culture and stored

frozen at –20 °C until further use. The cell pellet was resuspended with stirring for 15 min on ice in **buffer A** (0.1 M NEM, pH 7.5, 1 mM EDTA, 10 % (v/v) glycerol, 1 mM DTT containing 0.4 mg/ml lysozyme, and 50 mM NaCl). The suspension was then sonicated on a Branson sonicator 250 with a macro tip, setting 3.0 at constant duty cycle for 6 bursts of 30 s each. The lysate was centrifuged with a Beckman L5-50B ultracentrifuge using the Ti-45 rotor at 35 000 rpm for 45 min at 4 °C and then subjected to ammonium sulfate fractionation (32-50%) (80). The protein mixture was dialyzed overnight against 4 L of **buffer B** (0.1 M NEM, pH 7.4, 1 mM EDTA, 1 mM DTT, 1 mM sodium citrate, and 10% glycerol). The dialyzed protein was applied to a Q-Sepharose Fast Flow column (2.6 x 30 cm) equilibrated with buffer B. After washing the column with 5 volumes of buffer B, CM-PD was eluted with a linear gradient of 0 – 0.3 M KCl (3x bed volume) in the same buffer. Enzymatically active fractions were pooled, dialyzed and chromatographed on Sepharose-AMP by the method of Turnbull *et al.* (17) with one modification: the pH of the dialysate was kept at 7.4 rather than adjusted to pH 6 prior to chromatography. The active fractions were pooled and stored as ammonium sulfate precipitate at 4 °C. All protein variants were expressed in KB357, an *E. coli* strain that lacks functional *tyrA* and *pheA* genes (81). The proteins were purified as previously described for the WT enzyme except the Sepharose-AMP column was not used and the gradient volume for eluting protein from the Q-Sepharose column was doubled to 6x bed volume.

2.1.4 SDS-Polyacrylamide Gel Electrophoresis

Denaturing SDS-PAGE was performed with a 15% polyacrylamide gel following the method of Laemmli (82). Protein samples were diluted 1:2 (v/v) into 2X SDS sample loading buffer (1.5 M Tris-HCl, 4% SDS, 20% glycerol) and incubated in a boiling water bath for 2 min prior to loading on a gel. The gel was electrophoresed at 100 V as samples migrated through the stacking gel, and then the voltage was increased to 200-220 V as the samples entered the resolving gel. Electrophoresis continued until the Bromophenol Blue tracking dye migrated off the resolving gel. Bio-Rad broad range molecular weight protein standards were used to estimate the molecular weight of proteins in the samples.

Protein was visualized by staining the gels with Coomassie Brilliant Blue R-250. Alternatively, gels were stained by silver nitrate using the "microwave" method as following: the gel was placed in 50 ml 50% methanol and heated in the microwave for 1 min, then shaken for 1 min at room temperature. After repeating this step a second time, methanol was decanted and replaced with 50 ml silver stain solution (2 ml of 20% silver nitrate solution added dropwise to 10.5 ml 0.36% NaOH, 0.7 ml 30% NH_4OH, diluted to 50 ml with doubly distilled (dd) H_2O). The gel was shaken for 2-3 min at room temperature, the solution discarded then the gel was washed 4-5 times with ddH_2O. After decanting the water, the gel was placed in development solution (1.25 ml of 1% citric acid, 0.125 ml 37% v/v formaldehyde (Fisher), diluted to 250 ml in ddH_2O). The gel solution was microwaved for 20 s and then shaken for 3-5 min or until bands reach the desired staining intensity. The development solution was discarded then the gel washed quickly with ddH_2O and the staining reaction quenched in 10% methanol.

2.1.5 Determination of Enzyme Activity and Protein Concentration

Mutase and dehydrogenase activity assays were conducted at various stages of the purification procedure by adding 1 ml of either CM or PDH mix, respectively, to 1 cm quartz cuvettes (pathlength 1 cm). The assay mixtures were equilibrated at 30 °C for 1 min, and then the reactions were initiated by the addition of enzyme. Assays were conducted at 30 °C in a double-beam spectrophotometer (GBC UV/VIS model 918) fitted with a thermostatically controlled (Peletier) cuvette holder. CM mix contained 100 mM Tris-HCl (pH 7.5), 1 mM EDTA, 1 mM DTT, and 0.5 mM chorismate. Mutase activity was determined by measuring the disappearance of chorismate at 274 nm as outlined in Turnbull *et al.* (7). PDH mix contained 100 mM Tris-HCl (pH 7.5), 1 mM EDTA, 1 mM DTT, 2 mM NAD^+ and 0.5 mM prephenate. Dehydrogenase activity was followed by continuously monitoring the formation of NADH from NAD^+ at 340 nm in the presence of prephenate. An extinction coefficient of 6400 $M^{-1}cm^{-1}$ was used which takes into account the contribution of 4-hydroxyphenylpyruvate at 340 nm (12). Reaction rates for CM and PD were calculated from the linear portion of progress curves using the software supplied by the spectrophotometer manufacturer. A unit of enzyme is defined as the amount of enzyme required to produce 1 μmol of product or to catalyze the disappearance of 1 μmol of substrate per min at 30 °C. Protein concentration was estimated using the Bio-Rad Protein Assay Kit (Bio-Rad Laboratories) with bovine serum albumin (Sigma) as a standard and by recording the absorbance at 280 nm using $E^{0.1\%}_{280} = 0.818$ as reported for WT enzyme (83).

2.1.6 Determination of Kinetic Parameters for WT and Variant Forms of CM-PD

WT CM-PD and Cys variants were buffer exchanged into Buffer K (pH 7.5) composed of 0.1 M NEM, 1 mM EDTA, 20% glycerol and 5 mM DTT. Substocks of all three substrates, prephenate, NAD^+ and chorismate, were prepared at the desired concentration by diluting into ice-cold ddH_2O. Reactions were performed at 30 °C by diluting 2 X 3C buffer (0.2 M MES, 0.102 M NEM, 0.102 M diethanolamine, 2 mM EDTA and 2 mM DTT, pH 7.2) with 290 µl of water, 100 µl each of NAD^+ and prephenate at varying concentrations, and 10 µl (1 µg for WT, C95A, C169A, 4.5 µg for C215A and 6.25 µg for C215S) of protein for a total reaction volume of 1.0 ml. The assays were performed in 1 ml quartz cuvettes as follows: First, 2 X 3C buffer, water and substrates were equilibrated together at 30 °C for 1 min. Second, the reaction was initiated with the addition of enzyme. At each step, components were rapidly mixed by inversion of the cuvette. Enzyme activities were monitored as described in section 2.1.5. Initial velocity studies were conducted by varying one substrate at concentrations below to above its K_m value while keeping the second substrate fixed at a saturating level. Hence, reactions were performed using 10-12 concentrations of prephenate while holding NAD^+ constant at 2 mM. Similarly, 8-11 different concentrations of NAD^+ were used while keeping prephenate constant at 1 mM. For variants C215A and C215S, higher concentrations of substrate were used to ensure saturation. The initial velocity data (y) obtained by varying the concentration of chorismate, prephenate or NAD^+ (S) were fitted to the Michaelis-Menten (eq 2.1) using non-linear least squares analysis (GraFit 3.0) to yield values for the maximum velocity (V) and the Michaelis constant (K_m).

$$y = \frac{V\,[S]}{K_m + [S]} \qquad (2.1)$$

Turnover numbers were calculated using subunit molecular weight of 42.0 kDa. Initial velocity data were also plotted graphically in double reciprocal form using Microsoft Excel 2000 to observe any departures from linearity.

2.1.7 pH Dependence of WT and C215S Dehydrogenase Activity

The pH dependence of the values of V and $(V/K)_{prephenate}$ for WT and C215S dehydrogenase were determined from pH 5.9 to 9.3 by varying the concentration of prephenate at a fixed concentration of NAD^+ (5 mM). This was accomplished by performing activity assays in 2 X 3C buffer at 30 °C as outlined in 2.1.6. Over the pH range of 5.9-9.3 for which the initial velocities were measured, the ionic strength of this reaction buffer remains essentially constant (84). The final pH was determined on assay mixtures pooled after the reaction and equilibrated at 30 °C in a water bath.

The variation of the values for V and V/K as a function of pH was fitted to the log form of Eq. 2.2 or Eq. 2.3 (below) using GraFit 5.0.

$$y = ((Lim1 + Lim2 * 10^{pH - pKa1}) / (10^{pH - pKa1} + 1) - ((Lim2 - Lim3) * 10^{pH - pKa2}) / (10^{pH - pKa2} + 1))) \qquad (2.2)$$

$$y = ((Limit * 10^{pH - pKa1}) / (10^{(2* pH - pKa1 - pKa2)} + (10^{pH - pKa1} + 1)) \quad (2.3)$$

y represents the value of *V* or *V/K* at a particular pH value, *Limit* represents the pH-independent value of the parameters, K_1 and K_2 are dissociation constants for groups on the enzyme.

2.1.8 Analytical Methods

2.1.8.1 Mass Spectrometry

2.1.8.1.1 Verification of Amino Acid Substitutions by Mass Spectrometry

WT and variant CM-PD were buffer exchanged into 0.1 M ammonium bicarbonate (pH 8.5) then 100 µl aliquots (15-35 µg) of protein were digested overnight at 37 °C with 1-2 µl (0.5-1.0 µg) of modified bovine trypsin (Sigma). The reaction mixtures were lyophilized to dryness using a SpeedVac. The samples were then redissolved just prior to analysis in 50 µl of ACN:H_2O (1:1) + 0.1% TFA and injected by direct infusion (4 µl/min) into a PE Sciex QSTAR Mass Spectrometer with an IonSpray source and a time-of-flight (TOF) mass analyzer (accuracy of ± 0.01 amu). Prior to injection the mass spectrometer was calibrated using two standards, Cesium iodide (CsI, m/z = 132.9054) and an octapeptide (m/z = 829.5398). Spectra were analyzed using MDS Sciex Bioanalyst software. All QSTAR MS experiments were performed at MDS Pharma Services (Montreal) under the supervision of Dr. Bernard Gibbs.

2.1.8.1.2 LC-ESI-MS of Native WT and Variant CM-PD

All HPLC separations were performed with a Vydac C_{18} (5-μm d_p) column: 250 x 4.6 mm. An HP 1090 Series II/M HPLC system with binary DR5 solvent delivery and HP 1050 multiple wavelength diode-array UV-visible absorbance detector was used for all LC separations. The gradient used for native protein solutions was: 0-22 min (20 to 75% B) where **B** is 100% ACN + 0.05% TFA and **A** is 100% dH_2O +0.05% TFA. A flow rate of 1.00 ml/min was used. Stock preparations of CM-PD (WT and variants) were diluted 10-fold with ACN:H_2O:TFA (50:50:0.05). Samples were then injected manually using a 100 μl glass Hamilton syringe. Peaks were monitored by UV absorbance at 280 nm.

Electrospray mass spectra were obtained using a Finnigan SSQ 7000 single-quadrupole mass spectrometer (Concordia University). Analysis was performed on-line by splitting the LC eluent into a 50-mm i.d. bare-fused silica capillary, reducing flow rates to approximately 40 μl/min. Positive ion detection was used in all cases, scanning over a m/z range of 200-2200 at a rate of 1-2 scans/s. The following conditions were used in all analyses: 4.5 kV spray voltage, 210-250 °C capillary temperature, 30 psi sheath gas pressure, no auxillary gas used, electron multiplier set at 1200 V, centroid mode. After acquisition, the molecular weights of the proteins were obtained by using the deconvolution software, Xcalibur.

2.1.8.2 Circular Dichroism Spectroscopy

2.1.8.2.1 Far-UV CD

Far-UV CD spectroscopy was used to compare the overall secondary structure of WT and variant proteins. Measurements were recorded at room temperature from 184-260 nm using a Jasco-710 spectropolarimeter with a 0.01 cm circular cell. Buffer exchanged proteins were diluted to 1 - 2 mg/ml in 5 mM sodium phosphate buffer, pH 7.2. The following parameters were used: 5 scans averaged, 50 nm/min scan rate, 0.2 nm step resolution, 0.25 s response, 1 nm bandwidth, and sensitivity of 50 mdeg. Each spectrum was normalized for protein concentration and the observed ellipticity was background-corrected against the spectrum obtained for buffer.

2.1.8.2.2 Near-UV CD

Near-UV CD spectroscopy was used to compare the tertiary structure of WT and C215A variant proteins. Near-UV CD monitors the absorption of aromatic amino acids. Phenylalanines absorb in the range 255-270 nm, tyrosines in the range 275-282 nm and tryptophans at $\lambda > 280$ nm (85). Measurements were recorded at room temperature from 250-320 nm using a 1 cm circular cell. Buffer exchanged WT and variant CM-PD were diluted to 1 - 2 mg/ml in 5 mM sodium phosphate buffer, pH 7.2, then ten scans (averaged) were recorded using the parameters noted in 2.1.8.2.1

2.1.9 Cross-Linking of WT CM-PD with Bifunctional Reagents

CM-PD (7 μM monomer) in 0.1 M sodium phosphate buffer, pH 7.0, was incubated with 35 μM of cross-linking reagent (BMH or BMOE) in DMSO. Following 1 h incubation at

room temperature, the reaction was quenched by the addition of 5 mM DTT. The different samples were then loaded onto a 15% acrylamide gel (82) and stained with silver nitrate using the "microwave" method, as described in 2.1.4.

2.1.10 Comparative Modeling

Attempts to model the tertiary structure of *E. coli* CM-PD were accomplished by using the 3D homology modeler, 3D-jigsaw (www.bmm.icnet.uk/servers/3djigsaw). This program is an automated system that builds three-dimensional models of proteins based on homologues of known sequence (86). The primary sequence of protein was submitted online. The program looks for homologous templates in sequence databases like the Protein Families Database of Alignments (PFAM) and the Protein Data Bank (PDB) and splits the query sequence into domains. The domains of interest were then submitted for modeling against the best template. The models were viewed and analyzed by Swiss-PdbViewer v.3.7.

2.1.11 Chemical Modification of WT and Variant CM-PD

2.1.11.1 Enzyme Preparation for Cys Modification Studies

Aliquots of ammonium sulfate precipitated WT and Cys variants were centrifuged for 2 min at 14,000 rpm in a bench-top microcentrifuge at 4 °C. The supernatant was decanted and the pellet was resuspended in 0.5 ml of the appropriate buffer containing 20 mM DTT. That sample was allowed to incubate for 1 h on ice to ensure reduction of the three Cys residues of CM-PD. The DTT was then removed by exchanging the protein into 1 ml

of the same buffer without DTT using NAP-5 columns. Protein concentration was then determined using the BioRad assay kit and then small aliquots were stored at –86 °C until use.

2.1.11.2 Chemical Modification of WT and Variant CM-PD by DTNB

2.1.11.2.1 Quantification of Cys

WT or variant CM-PD (4.76 μM monomer; 15 μM Cys) in 50 mM NEM, pH 7.7, 1 mM EDTA and 25% glycerol were incubated with 1.75-fold excess DTNB (25 μM) at 25 °C. Quantification of DTNB-modified Cys was carried out by monitoring the time-dependent increase in the absorbance at 412 nm using an extinction coefficient of 14,150 $M^{-1}cm^{-1}$ for the released TNB^{2-} chromophore (66, 67). The recorded absorbance was corrected for the blank (buffer and DTNB only). For quantitation of free sulfhydryls under denaturing conditions, proteins were incubated overnight in 6 M GdHCl in 50 mM NEM (pH 7.7). The extinction coefficient used in this case was 13,700 $M^{-1}cm^{-1}$ (66, 67). For modification reactions conducted in the presence of ligands, WT and variants were preincubated for 5 min at 25 °C with or without 1 mM prephenate, 2 mM NAD^+, 2 mM NAD^+ + 1 mM tyrosine, and 10 μM mutase transition state (TS) analog, prior to the treatment with 25 μM DTNB.

2.1.11.2.2 Inactivation of CM-PD by DTNB

CM-PD WT and variants (6.67 μM monomer; 20 μM Cys) in 50 mM NEM (pH 7.7), 1 mM EDTA and 25% glycerol were incubated with 1.75-fold excess DTNB (35 μM) at 25 °C. Control samples were incubated under the same conditions except that DTNB was

omitted. At timed intervals after the addition of DTNB, aliquots of the reaction mixture were assayed for residual CM and PD activities as described in 2.1.5.

2.1.11.3 Chemical Modification of WT and Variant CM-PD by Iodoacetamide

WT and variant CM-PD (12 μM monomer; 36 μM Cys) in 200 mM Tris (pH 7.5) and 2 mM EDTA were reacted in the dark (using microfuge tubes covered with aluminium foil) at 25 °C with either 2 mM, 5 mM, 10 mM or 20 mM iodoacetamide (IAM) prepared in the same buffer. Control samples were incubated under the same conditions except that IAM was omitted. At timed intervals after the addition of IAM, aliquots of the reaction mixture were assayed for PD and CM activities in 1 ml of PDH or CM mix, as described in section 2.1.5, containing 25 mM DTT. For studies in the presence of various ligands, WT and variants were preincubated for 5 min at 25 °C with or without 1 mM prephenate, 2 mM NAD^+, 1 mM tyrosine, 2 mM NAD^+ + 1 mM tyrosine, and 25 μM mutase TS analog, prior to treatment with 10 mM IAM.

2.1.12 Time-Dependent Modification with Iodoacetamide and Peptide Mapping of CM-PD Tryptic Digest

WT CM-PD (23 μM monomer) in 100 mM Tris, pH 7.5 was incubated in the dark at 25 °C with 10 mM IAM prepared in the same buffer. At different time intervals, the reaction was quenched with the addition of 25 mM DTT. The mixture was then buffer exchanged using a NAP-5 column into 0.1 M ammonium bicarbonate, pH 8.5. This step eliminates the excess iodoacetamide and DTT in the reaction mixture. Protein was then digested overnight at 37 °C with modified bovine trypsin (Sigma) (20:1). Digested protein was

lyophilized to dryness using a SpeedVac, redissolved in ACN:H_2O (1:1) + 0.1% TFA and injected by direct infusion into a Sciex QSTAR ESI Mass Spectrometer.

The peptides, generated by tryptic digest of WT and variant CM-PD and observed by MS, were mapped using Peptident (www.expasy.ch) (87). This web based proteomics tool allows the identification of proteins using peptide mass fingerprinting data. Experimentally measured, user-specified peptide masses are compared with the theoretical peptides calculated for all proteins in the SWISS-PROT/TrEMBL databases. The program not only returns a list of likely protein identifications, but also any hits with peptides that are known to carry any of more than 20 different types of discrete post-translational modifications. The mass effects of several chemical protein modifications, such as oxidation of methionine, or desired alkylation products of Cys residues can also be considered by the program.

2.2 RESULTS

2.2.1 Expression and Purification of WT and Variant CM-PD

SDS-PAGE analysis of purified *E. coli* CM-PD (WT and Cys variants) is shown in Fig. 2.1. All proteins were resolved as single bands corresponding to a monomer molecular weight of 42 kDa with greater than 90% purity as judged by Coomasie staining.

2.2.2 Verification of Amino Acid Substitutions by Mass Spectrometry

Verification of the correct amino acid substitution for all four variants of Cys was accomplished by tryptic digest and mass spectrometry, as described in 2.1.8.1.1. The sequence coverage for the detected peptides was more than 80% for all proteins. Table 2.1 shows the list of all the peptides detected by mass spectrometry.

Cys95, Cys169 and Cys215 were resolved on three separate peptides from the tryptic digest of WT CM-PD (Fig. 2.2). Cys95 was present in P(93-112): TLCPSLRPVVIVGGGGQMGR, a doubly charged peak with an m/z 999.0317. Cys169 was present in P(168-178): DCILVDLASVK, a doubly charged peak with an m/z 588.3169. Finally, Cys215 was present in P(210-218): QVVVWCDGR, a doubly charged peak with an m/z 531.2647.

The tryptic digest of all four variant proteins gave an identical peptide map except for the peptide housing the amino acid substitution. In the tryptic digest of C95A, P(93-112) was

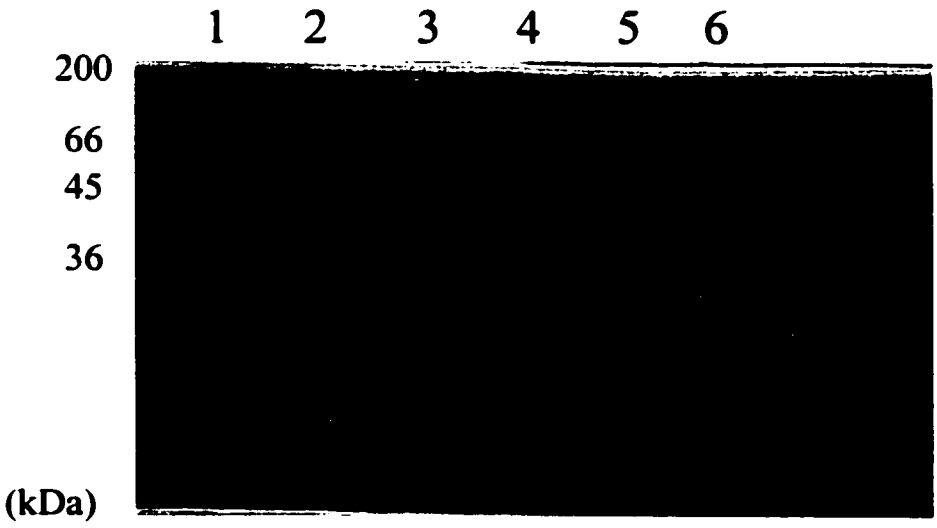

Fig. 2.1 SDS-PAGE analysis of purified WT and Cys variants of *E. coli* CM-PD

Analysis was performed under reducing conditions on a 15% polyacrylamide gel. Lane 1, **MW standards**; lane 2, **WT**; lane 3, **C95A**; lane 4, **C169A**; lane5, **C215A**; lane 6, **C215S**. About 20 μg of each CM-PD protein was loaded on the gel.

Table 2.1 List of peptides generated by Trypsin[1] digestion of WT and variant CM-PD and detected by QSTAR ESI MS[2]

Mass	Position	Amino Acid Sequence
1002.553	1-9	MVAELTALR
960.440	10-17	DQIDEVDK
854.559	18-25	ALLNLLAK
1184.665	27-37	LELVAEVGEVK
1189.649	40-49	FGLPIYVPER
863.417	50-57	EASMLASR
1906.005	59-76	AEAEALGVPPDLIEDVLR
404.221	78-80	VMR
1057.420	81-89	ESYSSENDK
1996.071	**93-112**	TLCPSLRPVVIVGGGGQMGR **(WT)**
1964.099	**93-112**	TLAPSLRPVVIVGGGGQMGR **(C95A)**
535.301	113-116	LFEK
1166.612	117-126	MLTLSGYQVR
1210.573	127-135	ILEQHDWDR
2631.430	136-161	AADIVADAGMVIVSVPIHVTEQVIGK
663.432	162-167	LPPLPK
1174.627	**168-178**	DCILVDLASVK **(WT)**
1142.655	**168-178**	DAILVDLASVK **(C169A)**
1060.512	**210-218**	QVVVWCDGR **(WT)**
1028.540	**210-218**	QVVVWADGR **(C215A)**
1044.535	**210-218**	QVVVWSDGR **(C215S)**
2248.143	219-236	KPEAYQWFLEQIQVWGAR
424.255	237-239	LHR
1941.973	240-256	ISAVEHDQNMAFIQALR
887.490	287-294	LELAMVGR
2096.025	295-312	LFAQDPQLYADIIMSSER
472.232	320-322	YYK
1447.719	324-336	FGEAIELLEQGDK
982.487	337-344	QAFIDSFR
1406.637	346-356	VEHWFGDYAQR
752.345	357-362	FQSESR
499.348	363-366	VLLR

[1] Trypsin is a pancreatic serine endoprotease which hydrolyzes peptide bonds specifically at the carboxyl side of arginine and lysine residues.

[2] Digestion of WT and variant CM-PD and analysis by MS are described in section 2.1.8.1.1

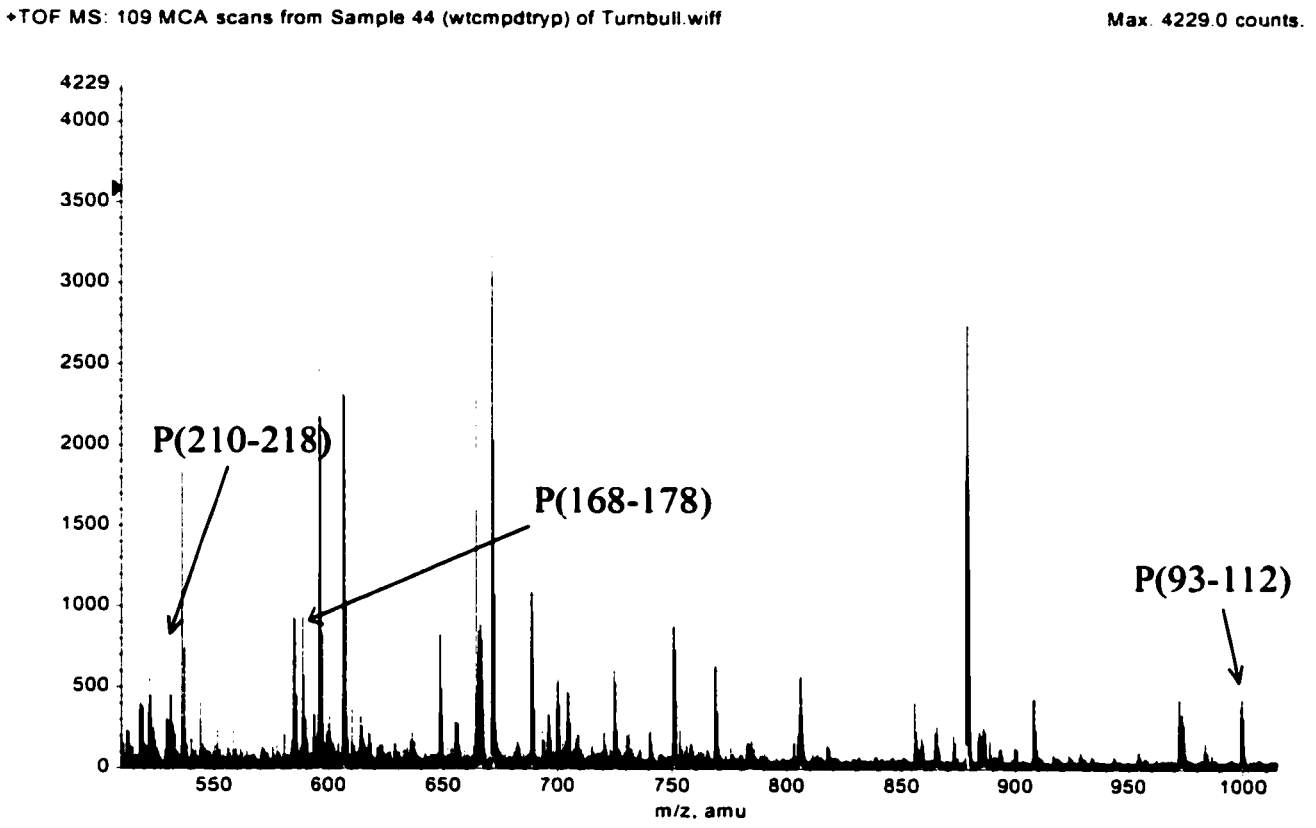

Fig. 2.2 ESI mass spectrum of WT CM-PD tryptic digest.

100 µl aliquot (30 µg) of WT CM-PD was digested overnight with 2 µl (1 µg) of modified trypsin (30:1) at 37 °C. The reaction mixture was lyophilized, then redissolved in ACN:H_2O (1:1) + 0.1% TFA and injected by direct infusion into a QSTAR ESI mass spectrometer. The three Cys containing peptides were resolved as doubly charged peaks at: m/z 999.03 for P(93-112), m/z 588.31 for P(168-178) and m/z 531.26 for P(210-218).

a doubly charged peak with an m/z 983.0378 (Fig. 2.3). Its difference in mass of 31.9878 Da relative to WT enzyme agreed with the difference in mass between Cys (103.0092 Da) and Ala (71.0371 Da). In the tryptic digest of C169A, P(168-178) was present as a doubly charged peak with an m/z 572.3343 (Fig. 2.4), a mass difference of 31.9652 Da again verifying a Cys to Ala substitution. In the tryptic digests of C215A and C215S, P(210-218) was present as doubly charged peaks with m/z 515.2722 and 523.2714, respectively (Fig. 2.5). The difference in mass between WT and C215A (31.98 Da) and WT and C215S (15.98 Da) were in excellent agreement with the theoretical mass difference between Cys and Ala (31.97 Da) and Cys and Ser (15.97 Da).

2.2.3 Determination of Molecular Weight and Post-Translational Modification of WT and Variant CM-PD by Mass Spectrometry

LC-MS was performed on undigested samples of WT and variant CM-PD as described in 2.1.8.1.2. The charge envelope of WT CM-PD is shown in Fig. 2.6A. This mass envelope spanned an unusually large m/z range (800-2200) and seemed to include many envelopes indicating that the enzyme could be present in different unfolded states. Deconvolution of the charge envelope yielded two peaks with identical intensities (Fig. 2.6B). The first peak had a mass of 42,044 Da, in excellent agreement with a value of 42,045 Da predicted from the primary sequence of WT CM-PD. The second peak had a mass of 41,914 Da, which corresponded to the enzyme without the N-terminal methionine (Δm = 130 amu).

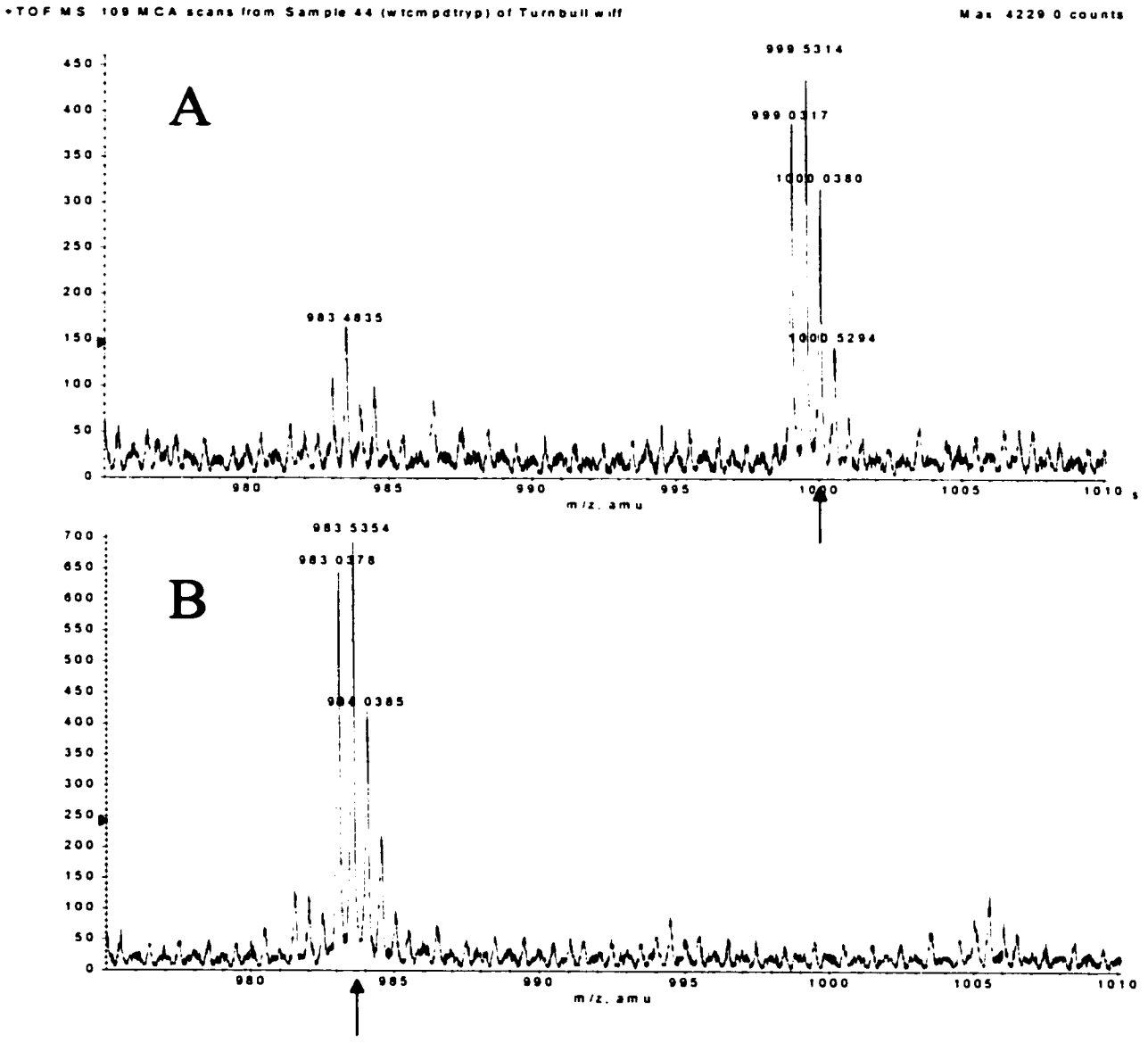

Fig. 2.3 ESI mass spectra of tryptic digests of WT and C95A CM-PD.

Digestion and MS were performed as described in section 2.1.8.1.1. This figure illustrates the region of the peptide map showing P(93-112) for both WT (**A**) and C95A (**B**) CM-PD. This peptide (indicated by arrow) was resolved as doubly charged peaks at m/z 999.53 and m/z 983.53, respectively. The difference in mass corresponds to Cys to Ala substitution.

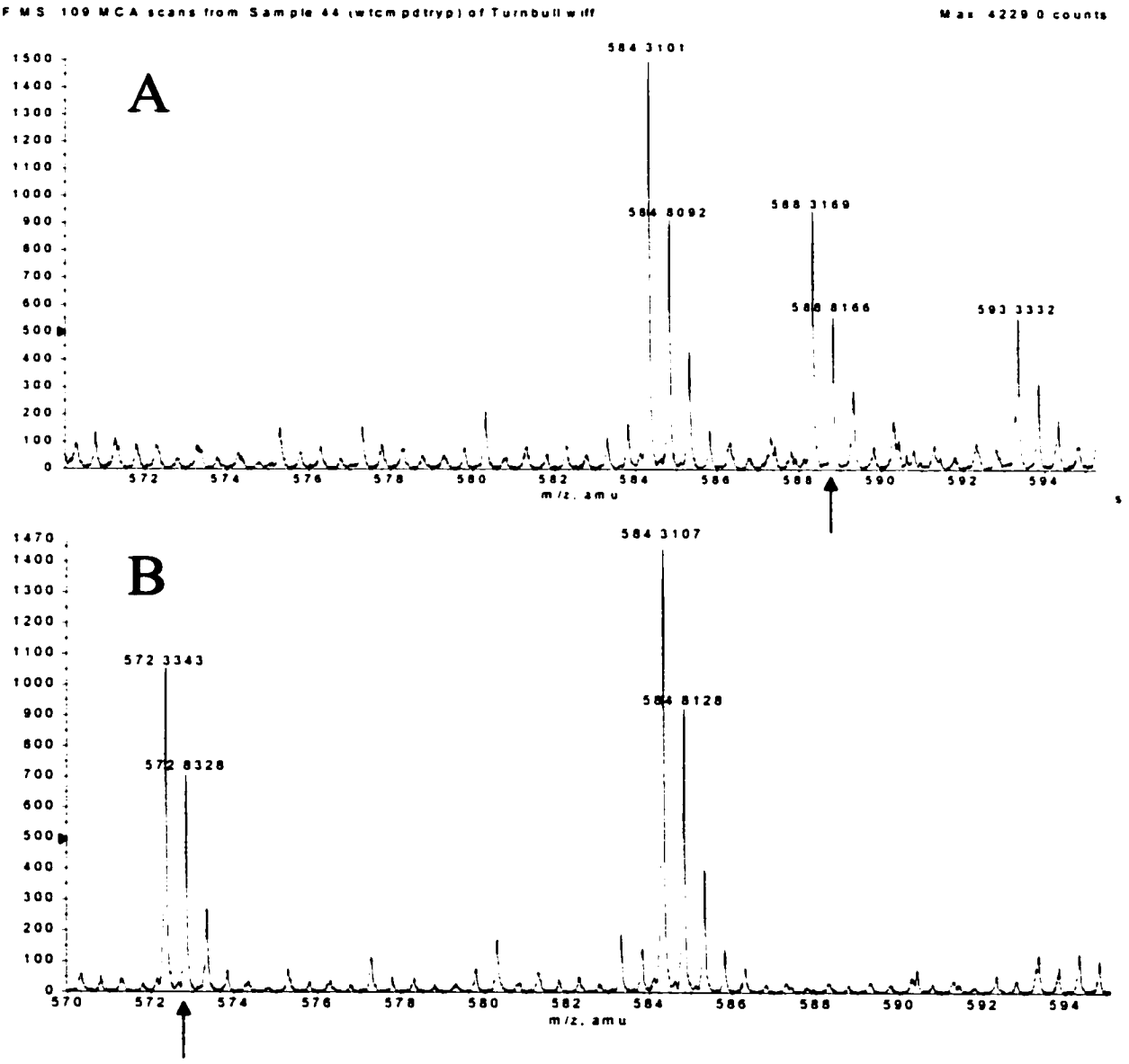

Fig. 2.4 ESI mass spectra of tryptic digests of WT and C169A CM-PD.

Digestion and MS were performed as described in section 2.1.8.1.1. This figure illustrates the region of the peptide map showing P(168-178) for both WT (**A**) and C169A (**B**) CM-PD. This peptide (indicated by arrow) was resolved as doubly charged peaks at m/z 588.31 and m/z 572.33, respectively. The difference in mass corresponds to Cys to Ala substitution.

Fig. 2.5 ESI mass spectra of tryptic digests of WT, C215A and C215S CM-PD Digestion and MS were performed as described in section 2.1.8.1.1. This figure illustrates the region of the peptide map showing P(210-218) for WT (**A**), C215A (**B**) and C215S (**C**) CM-PD. This peptide (arrow) was resolved as doubly charged peaks at m/z 531.26, 515.27, and 523.27 respectively. The difference in mass between WT and C215A corresponds to Cys to Ala substitution whereas the difference between WT and C215S corresponds to Cys to Ser substitution.

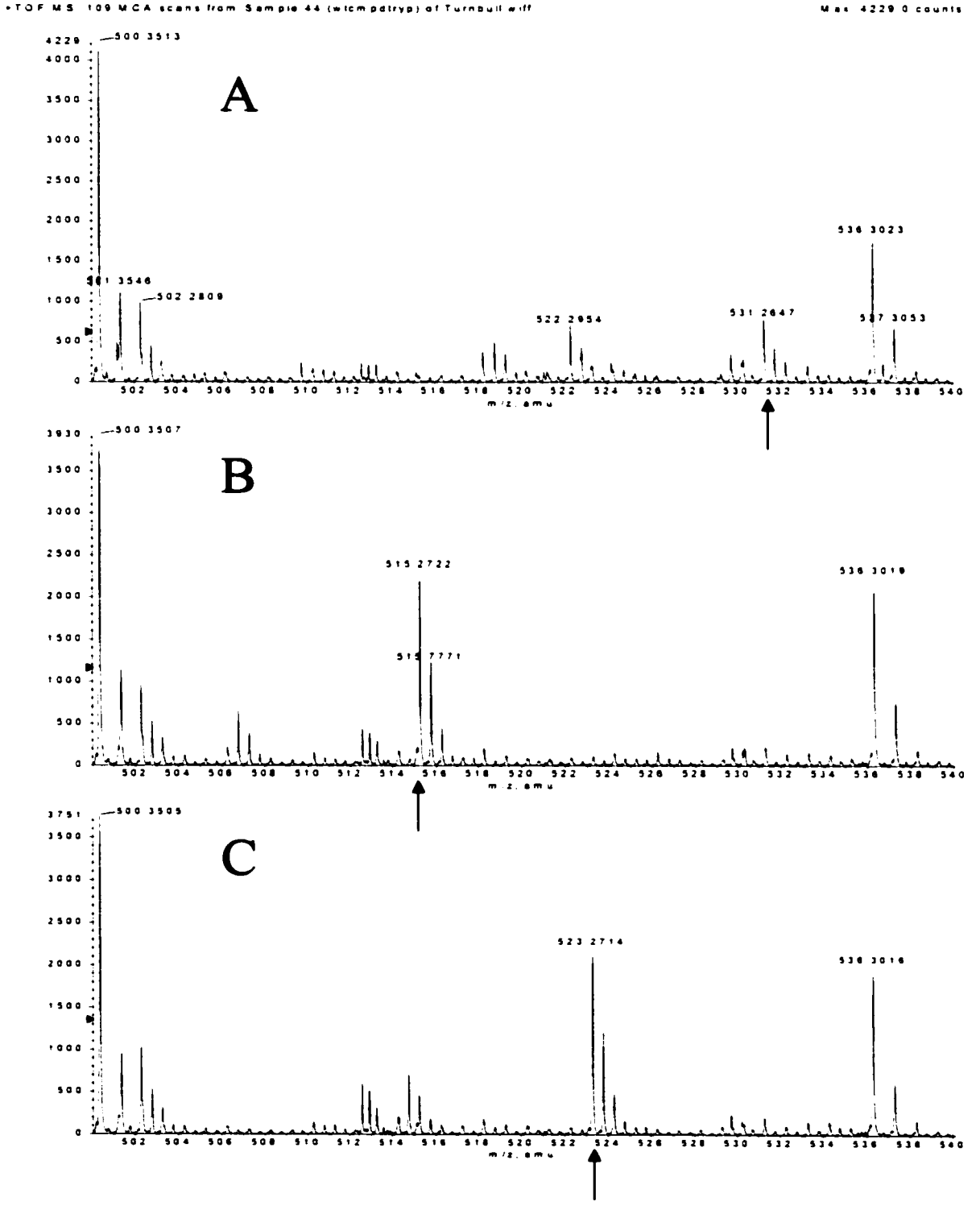
+TOF MS 109 MCA scans from Sample 44 (wtcmpdtryp) of Turnbull.wiff
Max 4229.0 counts
A
500.3513
501.3546
502.2809
522.2654
531.2647
536.3023
537.3053
B
500.3507
515.2722
515.7771
536.3019
C
500.3505
523.2714
536.3016
m/z, amu

Fig. 2.6 ESI mass spectrum of *E. coli* WT CM-PD.

MS was performed by diluting WT CM-PD 10-fold with ACN:H2O + 0.05% TFA to yield a final concentration of 20 μM. 100 μl aliquot was injected into an HPLC system online with a Finnigan SSQ 7000 single-quadrupole mass spectrometer as described in section 2.1.8.1.2. This figure illustrates the charge envelope of WT CM-PD from m/z 800 to 2200 (**A**). Deconvolution of this spectrum yielded two peaks corresponding to mass values of 41914 and 42044 Da (**B**).

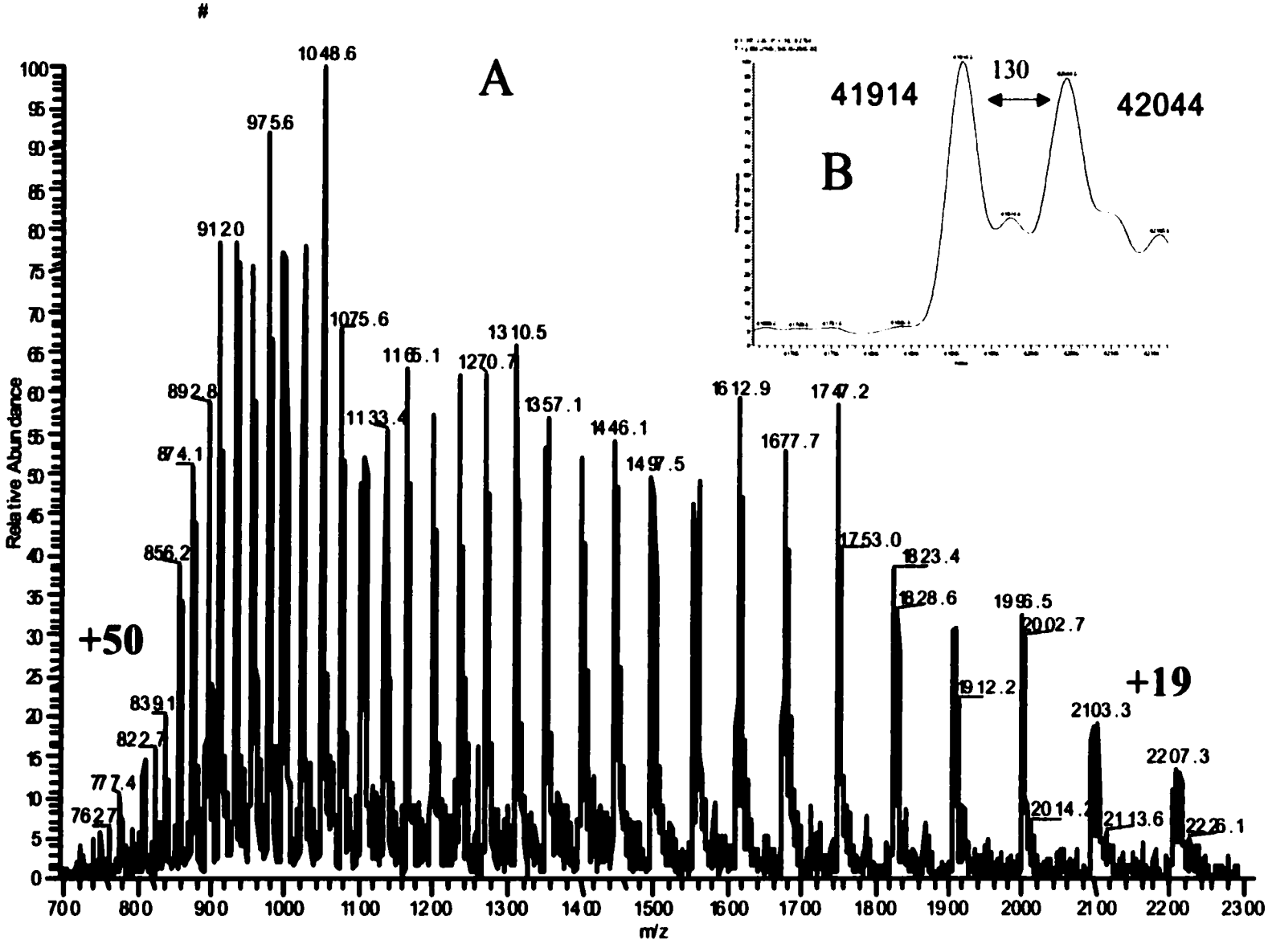
A
B
41914
130
42044
+50
+19
Relative Abundance
m/z
1048.6
975.6
912.0
1075.6
1310.5
1165.1
1270.7
892.8
1133.4
1357.1
1446.1
874.1
1497.5
1612.9
1747.2
1677.7
856.2
1753.0
1823.4
1828.6
1995.5
2002.7
839.1
822.7
1912.2
2103.3
2207.3
777.4
762.7
2014.2
2113.6
2226.1

Similar trends were also noted for the Cys variants, C95A (Fig. 2.7) and C215A (Fig. 2.8). In both cases, the first peak yielded a $\Delta m = 32$ compared to WT enzyme, verifying the Cys to Ala substitutions. The second peak corresponded to the N-terminally cleaved form of the enzyme.

2.2.4 Kinetic Analysis of WT and Variant CM-PD

Substrate saturation curves were constructed for both WT and variant forms of CM-PD at 30 °C. Initial velocities of the mutase-catalyzed reaction were recorded with chorismate as the variable substrate, whereas initial velocities of the dehydrogenase reaction were recorded with prephenate or NAD^+ as the variable substrate. The fixed substrate in the dehydrogenase reaction was maintained at saturating levels. The reactions catalyzed by both enzymes followed hyperbolic kinetics over the substrate concentration range reported (data not shown). Fitting the data to the Michaelis-Menten equation (2.1.6) yielded the kinetic parameters listed in Table 2.2.

The kinetic parameters for the CM and PD reactions catalyzed by C95A and C169A variant proteins were similar to those obtained for WT enzyme. In contrast, replacing Cys215 with Ala markedly affected prephenate binding, yielding a 20-fold increase in K_m for prephenate in the dehydrogenase reaction. Replacing Ala with Ser restored much of the binding affinity for prephenate. Turnover numbers for the reactions catalyzed by both variants at position 215 were similar, with a 2-fold decrease compared to WT dehydrogenase.

Fig. 2.7 ESI mass spectrum of *E. coli* C95A CM-PD.

MS was performed by diluting C95A CM-PD 10-fold with ACN:H2O + 0.05% TFA to yield a final concentration of 6.7 μM. 100 μl aliquot was injected into an HPLC system online with a Finnigan SSQ 7000 single-quadrupole mass spectrometer as described in section 2.1.8.1.2. This figure illustrates the charge envelope of C95A CM-PD from m/z 800 to 2200 (**A**). Deconvolution of this spectrum yielded two peaks corresponding to mass values of 41878 and 42007 Da (**B**).

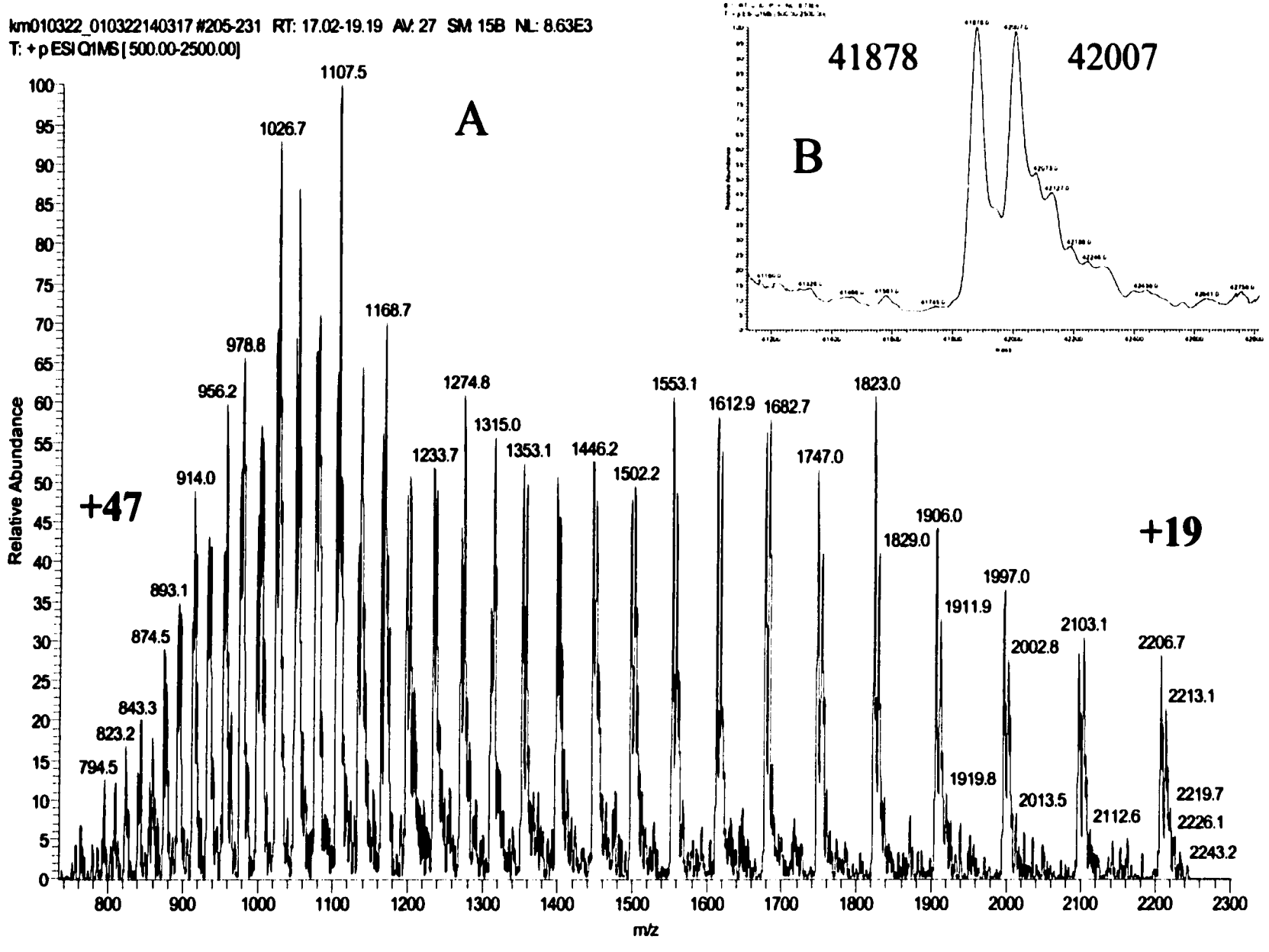
km010322_010322140317 #205-231 RT: 17.02-19.19 AV: 27 SM: 15B NL: 8.63E3
T: + p ESI Q1MS [500.00-2500.00]
A
B
41878
42007
+47
+19
Relative Abundance
m/z
1107.5
1026.7
1168.7
978.8
956.2
1274.8
1315.0
1553.1
1612.9
1682.7
1823.0
1233.7
1353.1
1446.2
1502.2
1747.0
914.0
893.1
874.5
843.3
823.2
794.5
1906.0
1829.0
1997.0
1911.9
2103.1
2002.8
2206.7
2213.1
1919.8
2013.5
2112.6
2219.7
2226.1
2243.2

Fig. 2.8 ESI mass spectrum of *E. coli* C215A CM-PD.

MS was performed by diluting C215A CM-PD 10-fold with ACN:H2O + 0.05% TFA to yield a final concentration of 33 μM. 100 μl aliquot was injected into an HPLC system online with a Finnigan SSQ 7000 single-quadrupole mass spectrometer as described in section 2.1.8.1.2. This figure illustrates the charge envelope of C215A CM-PD from m/z 800 to 2200 (**A**). Deconvolution of this spectrum yielded two peaks corresponding to mass values of 41881 and 42011 Da (**B**).

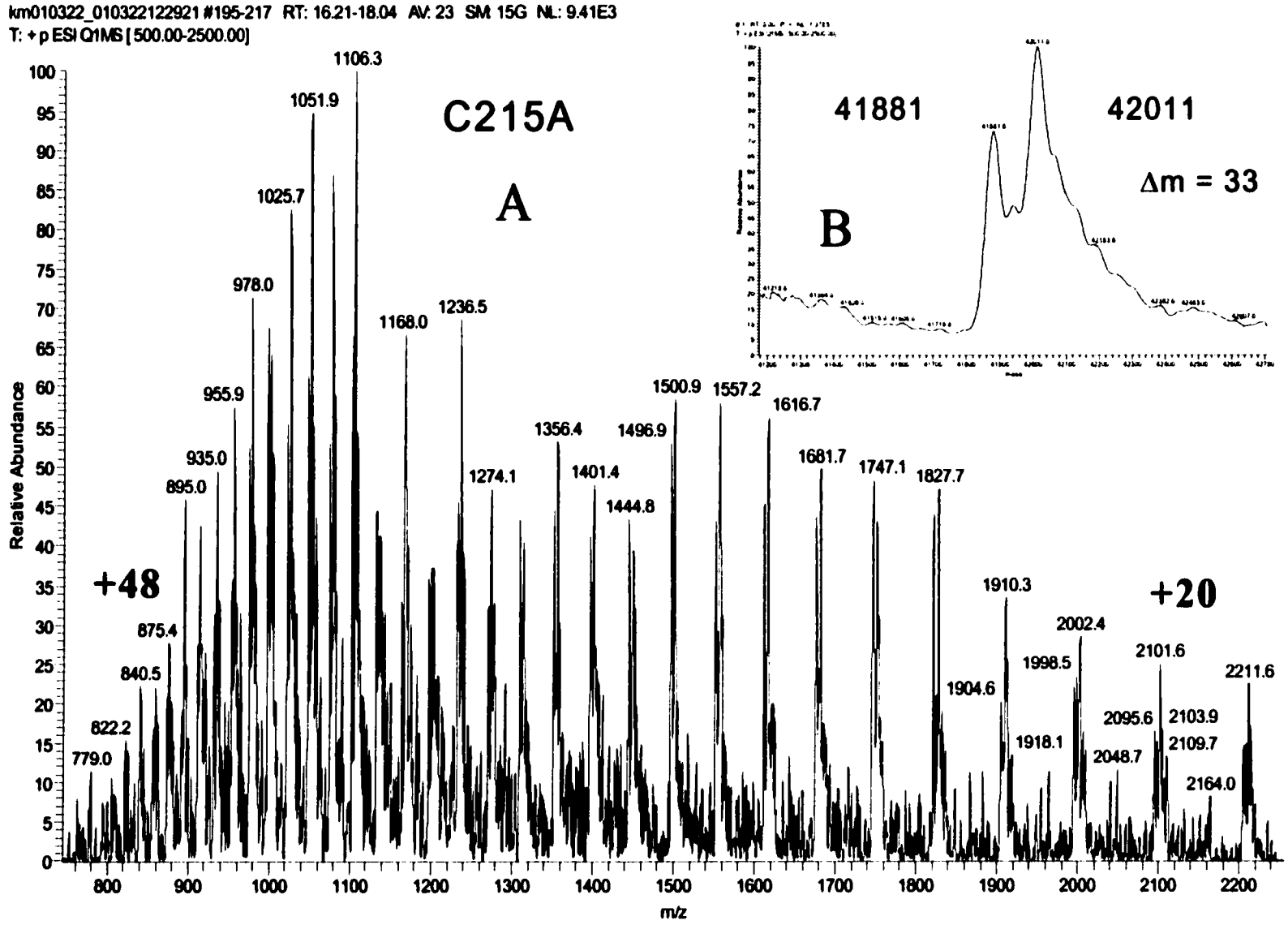
km010322_010322122921 #195-217 RT: 16.21-18.04 AV: 23 SM: 15G NL: 9.41E3
T: + p ESI Q1MS [500.00-2500.00]
C215A
A
B
41881
42011
Δm = 33
+48
+20
Relative Abundance
m/z
779.0
822.2
840.5
875.4
895.0
935.0
955.9
978.0
1025.7
1051.9
1106.3
1168.0
1236.5
1274.1
1356.4
1401.4
1444.8
1496.9
1500.9
1557.2
1616.7
1681.7
1747.1
1827.7
1904.6
1910.3
1918.1
1998.5
2002.4
2048.7
2095.6
2101.6
2103.9
2109.7
2164.0
2211.6

Table 2.2 Kinetic data for WT and variant CM-PD measured at pH 7.2 and 30 °C

Protein	Mutase Activity			Dehydrogenase Activity					
	Chorismate			Prephenate			NAD^+		
	K_m (μM)	k_{cat} (s^{-1})	k_{cat}/K_m ($M^{-1}s^{-1}$)	K_m (μM)	k_{cat} (s^{-1})	k_{cat}/K_m ($M^{-1}s^{-1}$)	K_m (μM)	k_{cat} (s^{-1})	k_{cat}/K_m ($M^{-1}s^{-1}$)
WT	21 ± 4	15 ± 0.6	$7.1x10^5$	37 ± 2	20 ± 0.3	$5.4x10^5$	140 ± 10	17 ± 0.4	$1.3x10^5$
C215A	340 ± 50	2.3 ± 0.1	$6.7x10^3$	640 ± 80	9.4 ± 0.4	$1.5x10^4$	380 ± 30	4.8 ± 0.1	$1.3x10^4$
C215S	600 ± 80	12 ± 0.9	$2.0x10^4$	120 ± 10	9.9 ± 0.3	$8.3x10^4$	290 ± 20	9.6 ± 0.3	$3.4x10^4$
C169A	38 ± 6	15 ± 0.5	$4.0x10^5$	25 ± 1	18 ± 0.2	$7.2x10^5$	240 ± 20	18 ± 0.6	$7.4x10^4$
C95A	60 ± 12	15 ± 0.9	$2.5x10^5$	32 ± 2	13 ± 0.2	$3.8x10^5$	180 ± 10	14 ± 0.2	$7.7x10^4$

Substitution at position 215 also affected CM activity. Replacing Cys215 with Ala affected K_m for chorismate in the mutase reaction with a 16-fold increase over the value observed for WT enzyme. Surprisingly, replacing Ala with Ser reduced chorismate binding even further, yielding a 30-fold increase in K_m for chorismate compared to WT enzyme. The turnover number for the mutase-catalyzed reaction decreased from 15 s^{-1} for WT enzyme to 2.3 s^{-1} for C215A. For C215S, this value was restored to levels reported for WT enzyme. From these results we can conclude that Cys215 is the only cysteine important for enzyme activity and interestingly, mutations at this position affect both CM and PD.

2.2.5 pH Dependence of the Dehydrogenase Reaction Catalyzed by WT and C215S CM-PD

To determine if the pH dependence of the dehydrogenase reaction was affected by the mutation, pH rate profiles were compared between the WT enzyme and C215S from pH 5.9 to 9.3. For both WT and variant enzymes, the effect on the dehydrogenase reaction was determined by varying the prephenate concentration at a fixed concentration of NAD^+ (5 mM). This level was presumed saturating over the entire pH range since the K_m for NAD^+ of WT CM-PD is pH independent from pH 5.6 to pH 9.5 (22). The $V/K_{prephenate}$ profile for WT is bell-shaped with slopes of +1, 0 and −1 and illustrates the fall-off in the rate of reaction of prephenate with the enzyme-NAD^+ complex at both high and low pH values (Fig. 2.9). The variation of log V with pH gives rise to a profile illustrating two groups titrating on the acid limb (Fig. 2.10). They must be deprotonated to participate in catalysis and/or product release. Fit of the data to the appropriate equation (2.2, 2.3)

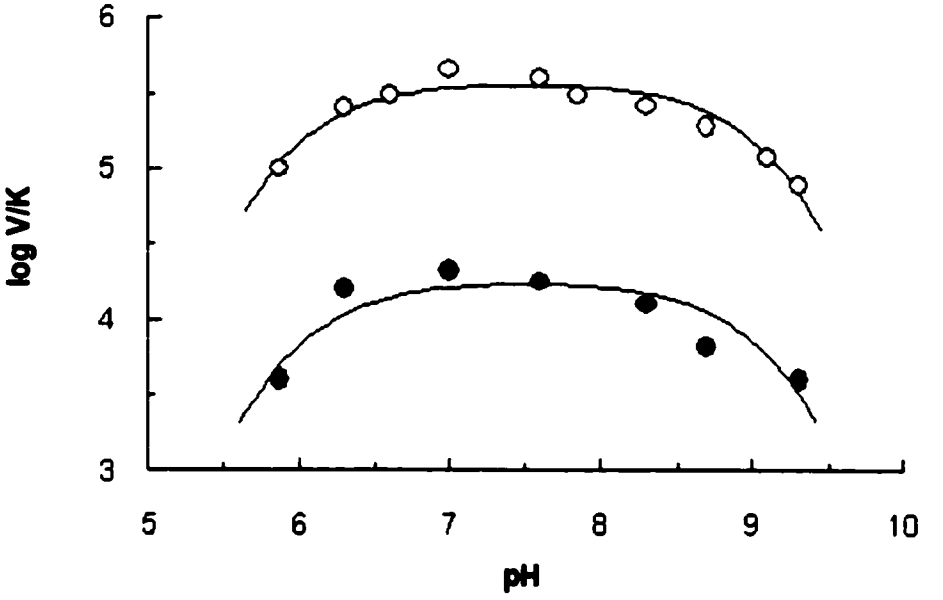

Fig. 2.9 Variation with pH of log $(V/K)_{prephenate}$ for the reaction catalyzed by WT (o) and C215S (●) prephenate dehydrogenase.

The unit for $(V/K)_{prephenate}$ is $M^{-1}s^{-1}$. The curve represents the best fit of the data to Eq. 2.2, with the parameters given in Table 2.3.

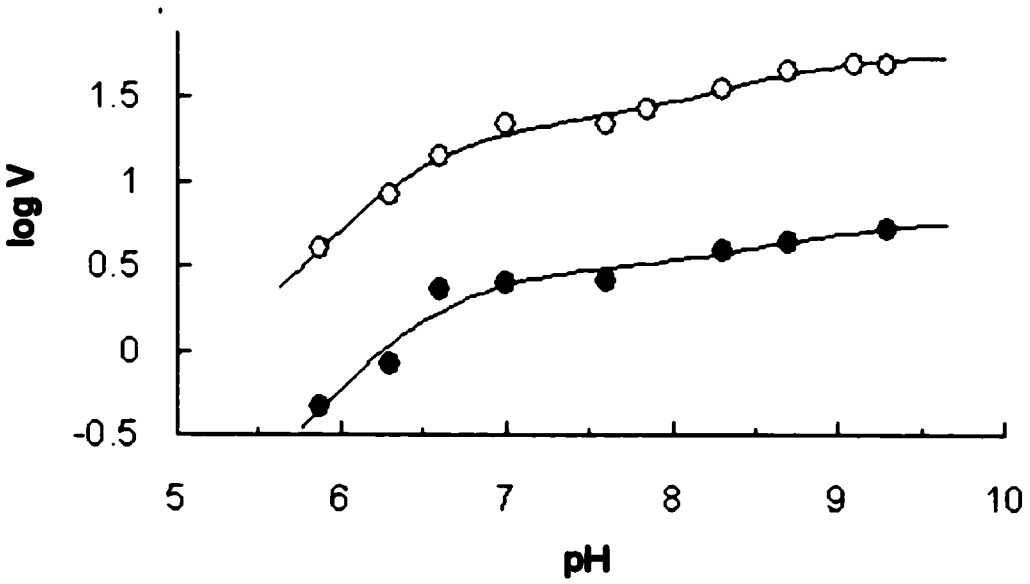

Fig. 2.10 Variation with pH of log V for the reaction catalyzed by WT (o) and C215S (●) prephenate dehydrogenase.

The unit for V is s^{-1}. The curve represents the best fit of the data to Eq. 2.3, with the parameters given in Table 2.3.

yielded the parameters in Table 2.3. The *V/K* values for the WT enzyme are in agreement with those previously determined (22, 46) and are keeping with the idea that a group with pK_a of about 8.4 must be protonated and involved in binding prephenate to the enzyme-NAD^+ complex.

To determine if Cys215 is this important binding group titrating in the log *V/K* profile, we repeated these experiments with C215S protein. C215S was chosen instead of C215A since it possessed a lower K_m for prephenate. Both log $(V/K)_{prephenate}$ and log *V* profiles were similar in shape to the ones obtained for WT enzyme (Fig. 2.9 and 2.10). The data were fit to the appropriate equations to yield pK values similar to WT enzyme (see Table 2.3). The observation that the basic limb of log $V/K_{prephenate}$ was not lost implies that Cys215 is not the group titrating with a $pK_a \sim 8.4$.

2.2.6 Circular Dichroism Spectroscopy

The far-UV CD spectra obtained at room temperature for WT and all the Cys variant forms of CM-PD are shown in Fig. 2.11. Two local minima at 208 nm and 222 nm were observed and are typical for proteins containing a significant content of α-helical structure (85). The spectra were virtually superimposable which indicated that there were no global secondary structural changes in protein structure caused by the mutations.

Near-UV CD monitors the absorption of aromatic amino acids and is very sensitive to any change in the environment of these chromophores (85). Fig. 2.12 shows the near-UV CD spectra obtained at room temperature for WT CM-PD and C215A (the variant displaying

Table 2.3 Values for pK_a and pH-independent kinetic parameters associated with the reaction catalyzed by WT and C215S PD[a]

PD	Parameter determined	pH-independent value of parameter	pK_{a1}[b]	pK_{a2}[b]
WT	V (s^{-1})	22.9 ± 1.1 56.2 ± 1.1	6.07 ± 0.26	8.35 ± 0.41
	V/K ($M^{-1}s^{-1}$ x 10^6)	0.38 ± 0.04	6.27 ± 0.15	8.44 ± 0.14
C215S	V (s^{-1})	3.16 ± 0.3 5.88 ± 0.4	5.95 ± 0.25	8.47 ± 0.34
	V/K ($M^{-1}s^{-1}$ x 10^6)	0.018 ± 0.001	6.23 ± 0.21	8.28 ± 0.20

[a] Parameters were determined by fitting data to equations 2.2 and 2.3

[b] pK_{a1} and pK_{a2} represent the apparent dissociation constants for the groups on the enzyme

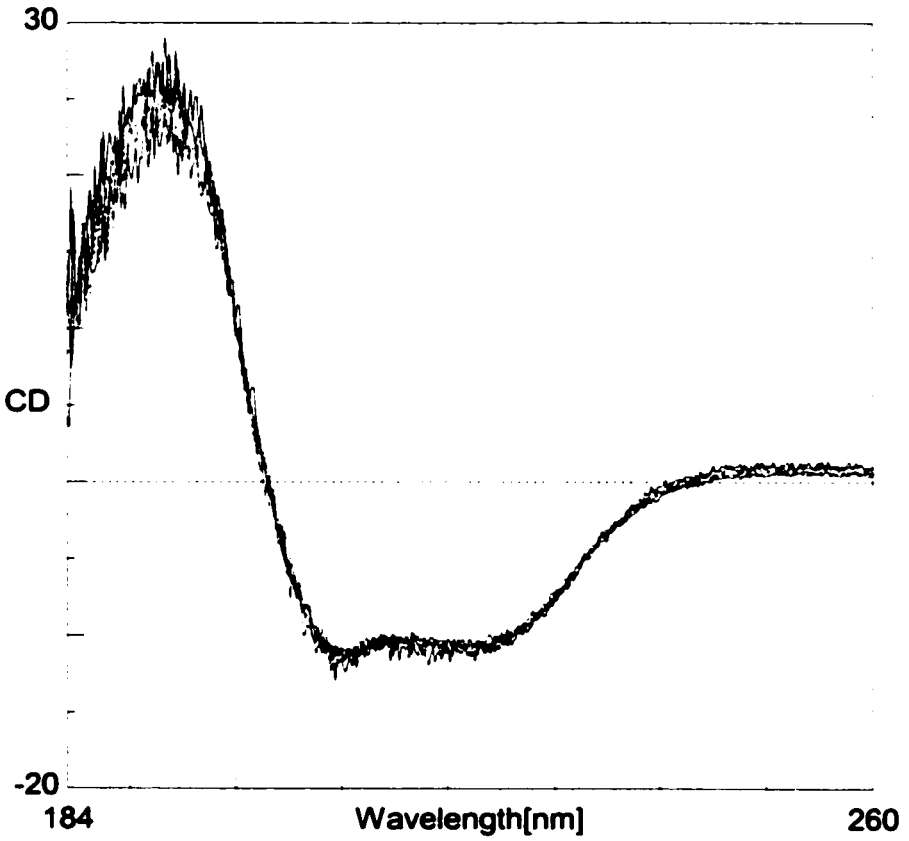

Fig. 2.11 Far-UV circular dichroism of *E. coli* WT and Cys variant proteins (C95A, C169A and C215A/S) CM-PD at 25 °C. Spectra were obtained as described in 2.1.8.2.1.

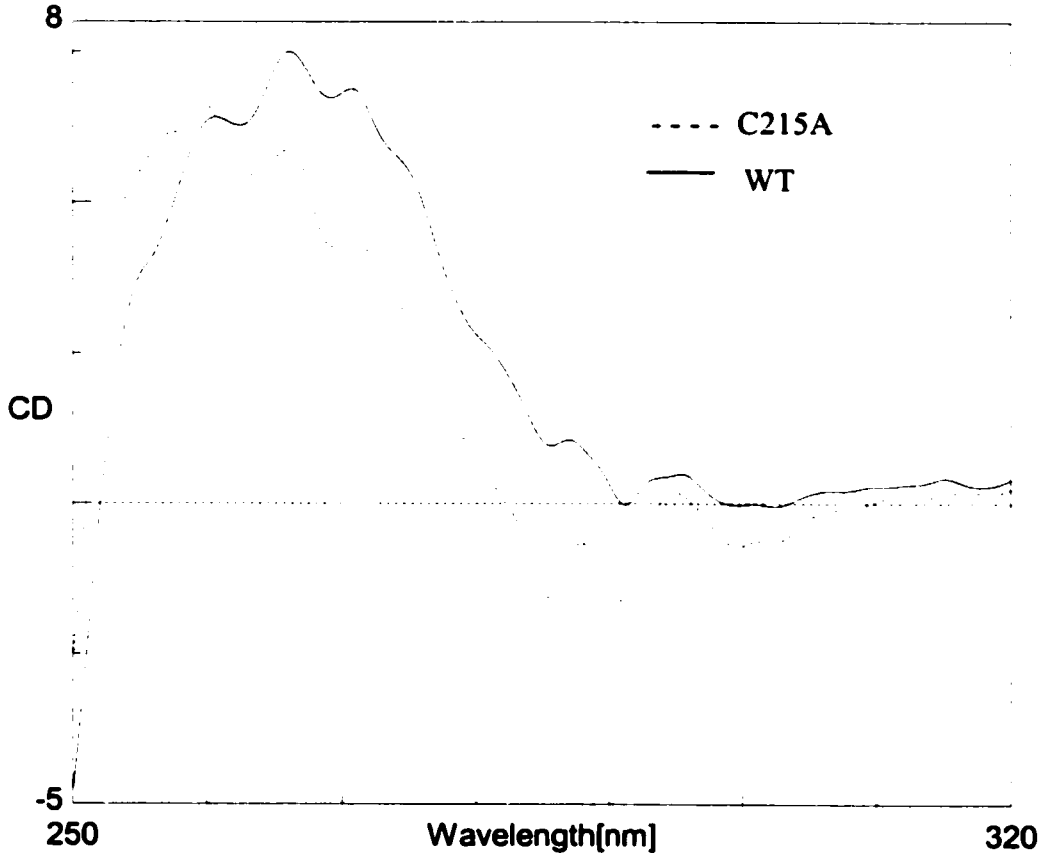

Fig. 2.12 Near-UV circular dichroism of *E. coli* WT and C215A CM-PD at 25 °C.

Spectra were obtained as described in 2.1.8.2.2.

the greatest change in kinetic parameters). Relative to WT enzyme, the spectrum of the variant protein is displaced downward possibly due to a slightly lower protein concentration relative to WT protein. However, the peaks between 280 and 300 nm are notably sharper for C215A relative to WT enzyme. This difference could be due to an increase in the asymmetric environment of tryptophan(s) residues. Overall, we can conclude that there were only small global tertiary structural changes in protein structure caused by the C215A mutation.

2.2.7 Comparative Modeling

The primary sequence of CM-PD of *E. coli* (373 a.a.) was submitted online to the comparative modeling program, 3D-Jigsaw. The results showed a split in the sequence into two recognizable domains: 1) chorismate mutase domain, 2) NAD (P)-binding Rossman fold domain. The latter domain was best aligned against 6-phosphogluconate dehydrogenase of *Trypanosoma brucei* (1pgj.pdb). PD (a.a. 99 to 273) was modeled against this template and is shown in Fig. 2.13. The model produced a high α-helical content, which agrees with previous studies by secondary structure prediction programs (88) and circular dichroism (Fig. 2.11). Two of the three Cys of *E. coli* CM-PD (Cys169, Cys215) are located in the PD portion of CM-PD. Further examination of the surroundings of Cys215 revealed the presence of a pocket housing Cys215 along with other important residues involved in catalysis (His197) (26), prephenate binding (Arg294) (24) and tyrosine binding (His257) (T. Lee, unpublished) (Fig. 2.14). The proximity of Cα of Cys215 to Cα of His197 (3.2 Å), suggests that Cys215 might be involved in correctly orienting this important catalytic His.

Fig. 2.13 3D-Jigsaw model of PD domain of *E. coli* CM-PD.

Figure was generated as described in 2.1.10.

Fig. 2.14 3D-Jigsaw model of PD domain of *E. coli* CM-PD.

Enlargement of PD model showing Cys215 and other residues important for catalysis (His197), prephenate binding (Arg294) and tyrosine binding (His257). On the basis of the modeling, Phe200 is presently targeted for site-directed mutagenesis.

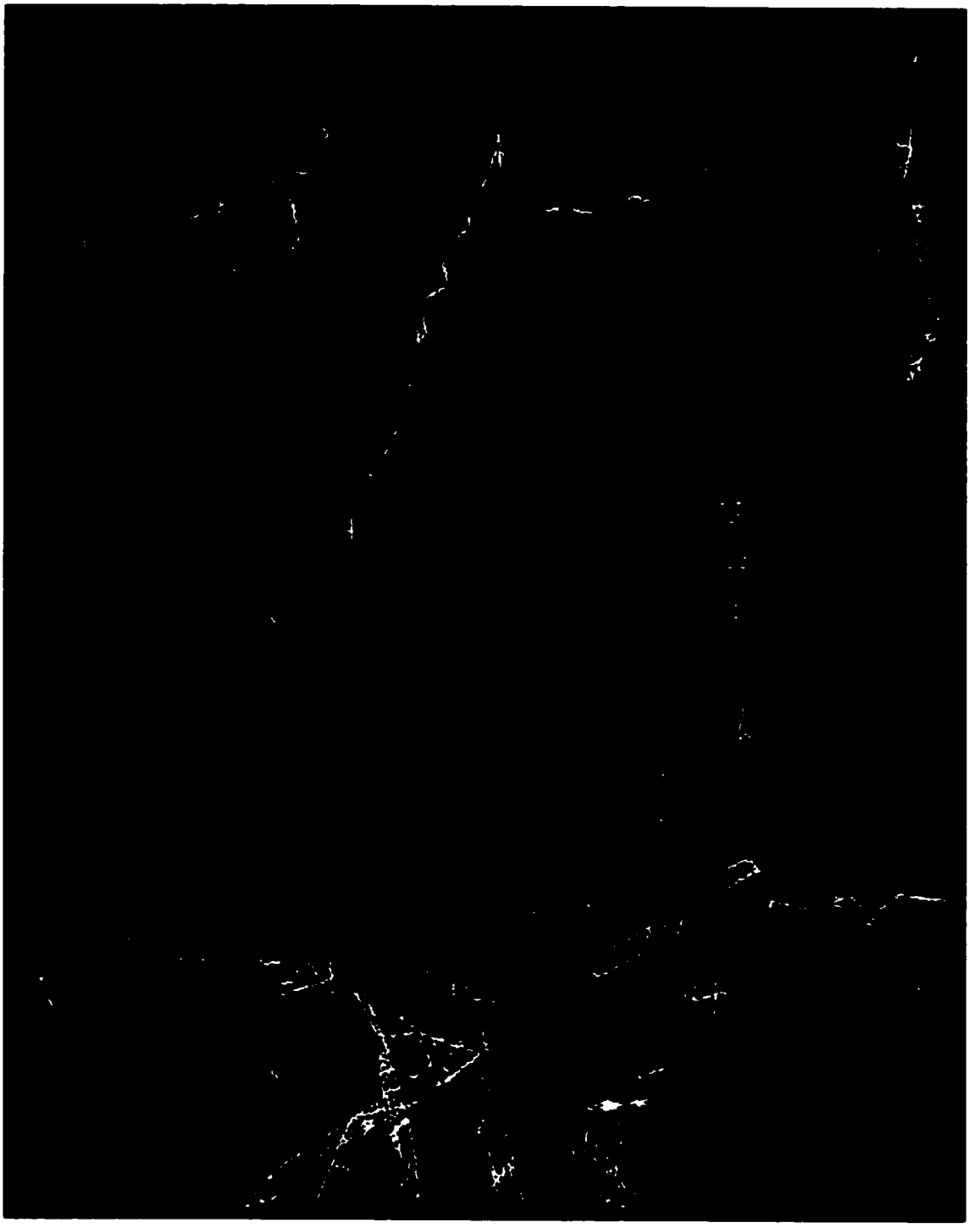

2.2.8 Chemical Modification of WT and Variant CM-PD

Chemical modification of Cys was used as a complementary technique to site-directed mutagenesis to determine the importance of Cys residues in maintaining enzyme activity. Moreover, as there is no crystal structure for CM-PD, examining the effects of two different Cys-specific reagents, DTNB and iodoacetamide, could yield information about the reactivity and accessibility of the different Cys in CM-PD.

2.2.8.1 Chemical Modification of WT and Variant CM-PD by DTNB

2.2.8.1.1 Quantification of Cys

To confirm the number of sulfhydryl groups that were present in the native and denatured enzyme, CM-PD was reacted with a Cys-specific reagent, DTNB, also known as Ellman's reagent (65). The reaction of DTNB with CM-PD in the presence and absence of 6 M Gdn-HCl is shown in Fig. 2.15. In the presence of the denaturing agent, complete reaction was achieved in 3 min with 2.80 Cys reacting per subunit. This result is in good agreement with the expected value of 3 Cys per subunit of enzyme.

When native enzyme was incubated with DTNB under conditions outlined in 2.1.11.2.1, only 1.90 residues per subunit reacted in 1 h (Fig. 2.15). This reaction was characterized by the fast modification of one group, followed by the slower reaction of a second group. Both groups reacted more slowly in the native than in the denatured enzyme. These results indicate that one of the three cysteines is not accessible or reactive to DTNB modification.

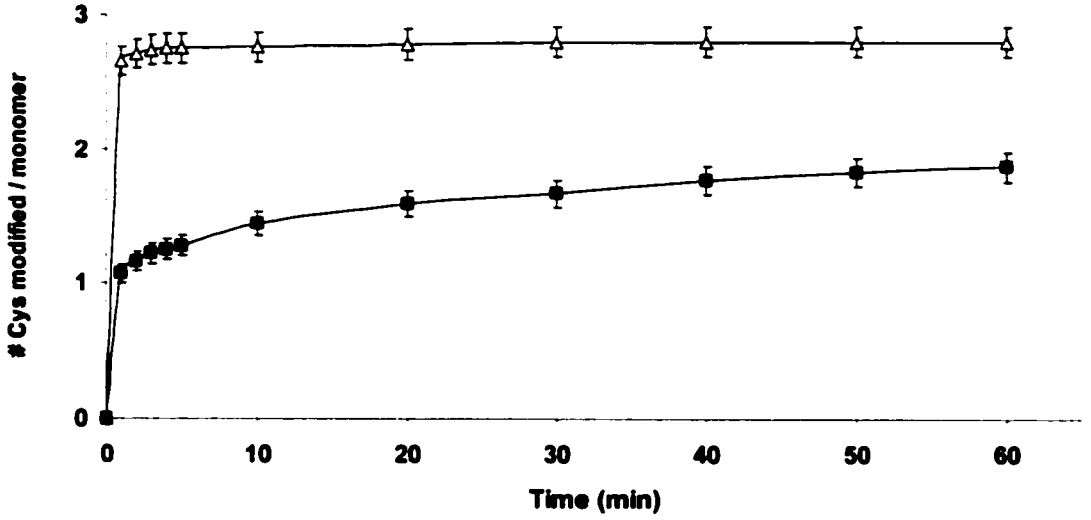

Fig. 2.15 Reaction of WT CM-PD with DTNB.

CM-PD (4.76 μM monomer, 15 μM Cys) in 50 mM NEM (pH 7.7), 1 mM EDTA and 25% glycerol was reacted with 1.75-fold excess DTNB (25 μM) at 25 °C in the presence (Δ) or absence (■) of 6 M Gdn-HCl prepared in the same buffer. Error bars represent the standard deviation from the mean of N data sets (N=2).

To determine which of the three Cys was not reactive to DTNB modification, all four variants were reacted with the reagent in the presence and absence of 6 M Gdn-HCl (Fig. 2.16). Modification of WT, C215A, C215S and C95A proteins under native versus denaturing conditions indicated that in the folded protein there was one Cys, which did not react with DTNB. By contrast ~two Cys were modified in C169A regardless of the conditions clearly indicating that Cys169 is inaccessible to DTNB modification.

Preincubation of various ligands with WT CM-PD prior to the addition of DTNB had similar effects on the rate of modification with DTNB (Fig. 2.17). In the absence of ligands, two Cys per subunit were modified. In the presence of NAD^+, the number of Cys modified per monomer decreased to 1.5. However in the presence of tyrosine, the protection effect of NAD^+ was increased, presumably by enhancing the binding of this cofactor (12, 13) and hence yielding one Cys/monomer modified. Only one sulfhydryl group reacted with DTNB in the presence of prephenate. Interestingly the mutase TS analog afforded protection against modification similar to prephenate. These results suggested that the presence of these ligands protected one Cys from DTNB modification.

The Cys, protected against modification, was identified by repeating these studies with the Cys variants (Fig. 2.18). Modification of C95A and C169A in the presence and absence of ligands showed similar trends to those obtained for WT enzyme. Prephenate, mutase TS analog and NAD^+ + tyrosine, showed some degree of protection against DTNB modification. However, the degree of protection varied from 0.3 to 0.8 groups per subunit, unlike WT enzyme where one cysteine was protected against modification.

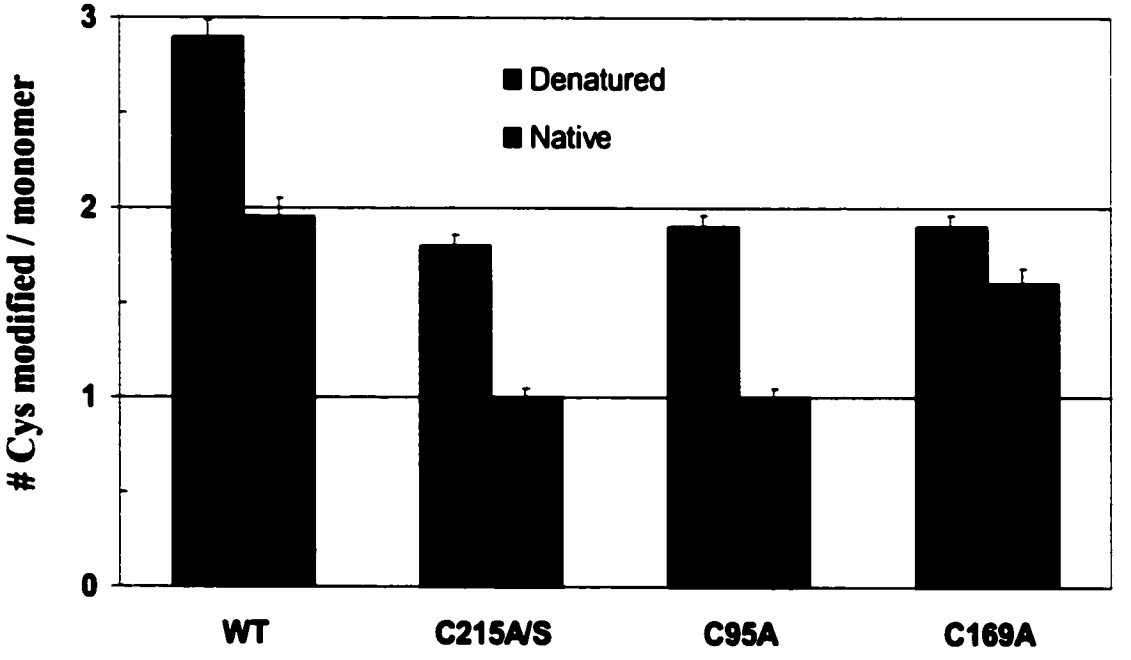

Fig. 2.16 Reaction of WT and variant CM-PD with DTNB. WT and variants (4.76 μM monomer, 15 μM Cys) in 50 mM NEM (pH 7.7), 1 mM EDTA and 25% glycerol were reacted with 25 μM DTNB at 25 °C in the (a) presence or (b) absence of 6 M Gdn-HCl prepared in the same buffer. For presentation purposes, results for C215A and C215S (<5% variation) were averaged and presented together (N = 2).

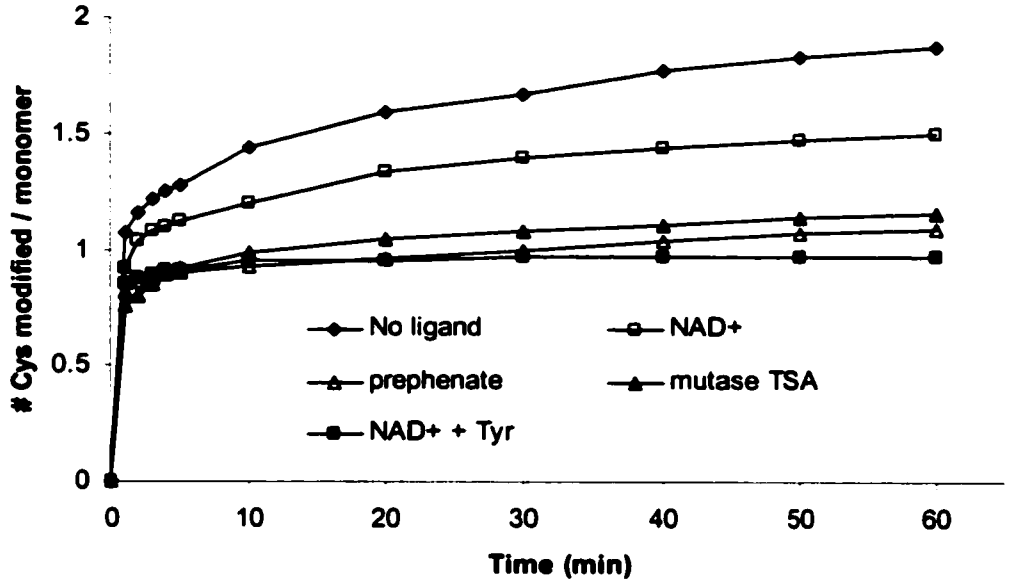

Fig. 2.17 The effect of different ligands on modification by DTNB of WT CM-PD.

Ligands included: 1 mM prephenate; 2 mM NAD^+; 2 mM NAD^+ + 1 mM tyrosine; 10 μM mutase TS analog. Conditions of modification were identical to Fig. 2.15 (N=2).

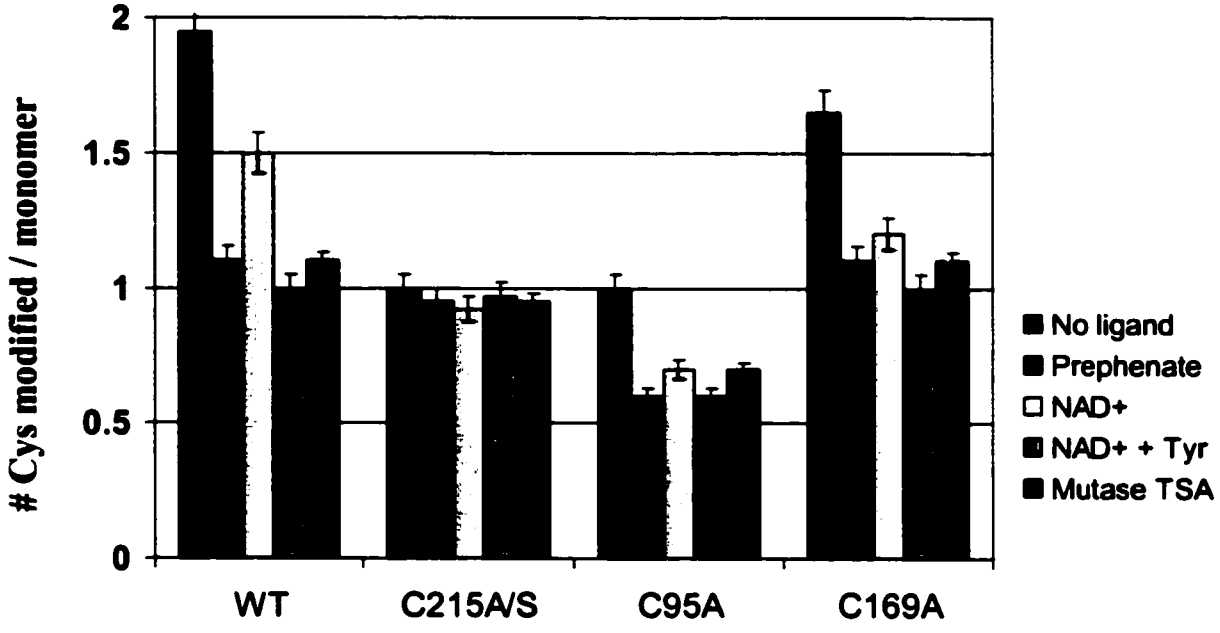

Fig. 2.18 The effect of different ligands on DTNB modification of WT and Cys variant CM-PD.

Ligands included: 1 mM prephenate; 2 mM NAD^+; 2 mM NAD^+ + 1 mM tyrosine; 10 μM mutase TSA. The conditions of modification were identical to that of Fig. 2.15. The # of Cys modified was the value extrapolated after treatment of enzyme (+ ligand) with DTNB for 60 min (N=2).

Studies performed on C215A/S showed no difference in the number of groups modified in the presence or absence of ligands. These results suggest that Cys215 is the group protected from DTNB modification by interacting with substrates and substrate analogs.

2.2.8.1.2 Inactivation of CM-PD Activity by DTNB

Enzyme inactivation studies were conducted under the same conditions as in the modification experiments. The effect of DTNB modification on the activity of WT CM-PD is shown in Figure 2.19. A rapid loss of approximately 60% of mutase activity and 30% of dehydrogenase activity was observed in the first 10 min of the reaction, corresponding to the modification of 1.3 Cys per monomer. Inactivation of the remaining activity occurred at a slower rate as the total reaction approached two groups per subunit. This suggests that a faster reacting group is essential for both enzyme activities. Moreover, the more rapid inactivation of the mutase compared to the dehydrogenase under the same conditions indicates that these two sites are somewhat distinct.

When WT CM-PD was modified with DTNB for 1 h and then the enzyme incubated with excess DTT (10 mM) at room temperature for 60 min, both activities were recovered in parallel to about 85% of initial activity (data not shown). This suggests that the loss of activity is primarily due to the modification of Cys rather than any other enzyme group or conformational change due to the modification.

The effect of DTNB modification on the CM and PD activities of the Cys variants is shown in Fig. 2.20A and 2.20B, respectively. In Fig. 2.20A, we observe a rapid loss of

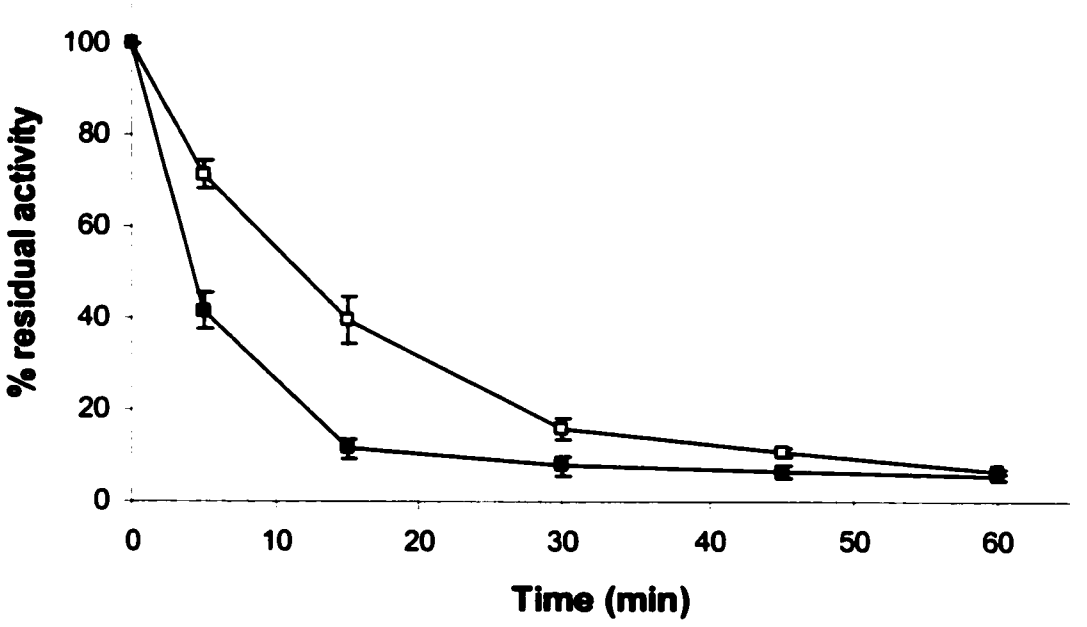

Fig. 2.19 Inactivation of WT CM-PD by DTNB.

Enzyme (6.67 μM monomer; 20 μM Cys) in 50 mM NEM (pH 7.7), 1 mM EDTA and 25% glycerol was reacted with 1.75-fold excess DTNB (35 μM) at 25 °C. Activity assays for CM (■) and PD (□) were performed as described in 2.1.5. (N=2).

mutase activity for C95A and C169A comparable to the inactivation of WT enzyme. However, reaction of DTNB with C215A and C215S leads to about 30% loss of mutase activity. This result supports the idea that Cys215 is the fast reactive group. The partial loss in activity (30%) is most probably due to the modification of a second slower reacting group.

In Figure 2.20B, the loss of dehydrogenase activity of C95A was similar to that observed for WT enzyme. In contrast, the rate of inactivation for C169A was faster than WT. This result is rather surprising given that the kinetic parameters for the reaction catalyzed by C169A and WT enzymes are nearly identical. This could be explained if the mutation at position 169 causes some conformational changes that make the reactive groups more susceptible to modification by DTNB. Interestingly, the C215A and C215S variants lost only 20% of initial activity after 1 h of incubation with DTNB. This indicates that modification of Cys215 is responsible for the loss of dehydrogenase activity since in the absence of this Cys activity is not markedly affected.

Studies were performed on WT and variant forms of CM-PD to determine which of the ligands would protect the active site against inactivation by DTNB. These experiments will also indicate whether or not the reactive groups are located at or near the binding site of the ligands. Preincubation of various ligands with WT CM-PD prior to reaction with DTNB are shown in Fig. 2.21A and 2.21B.

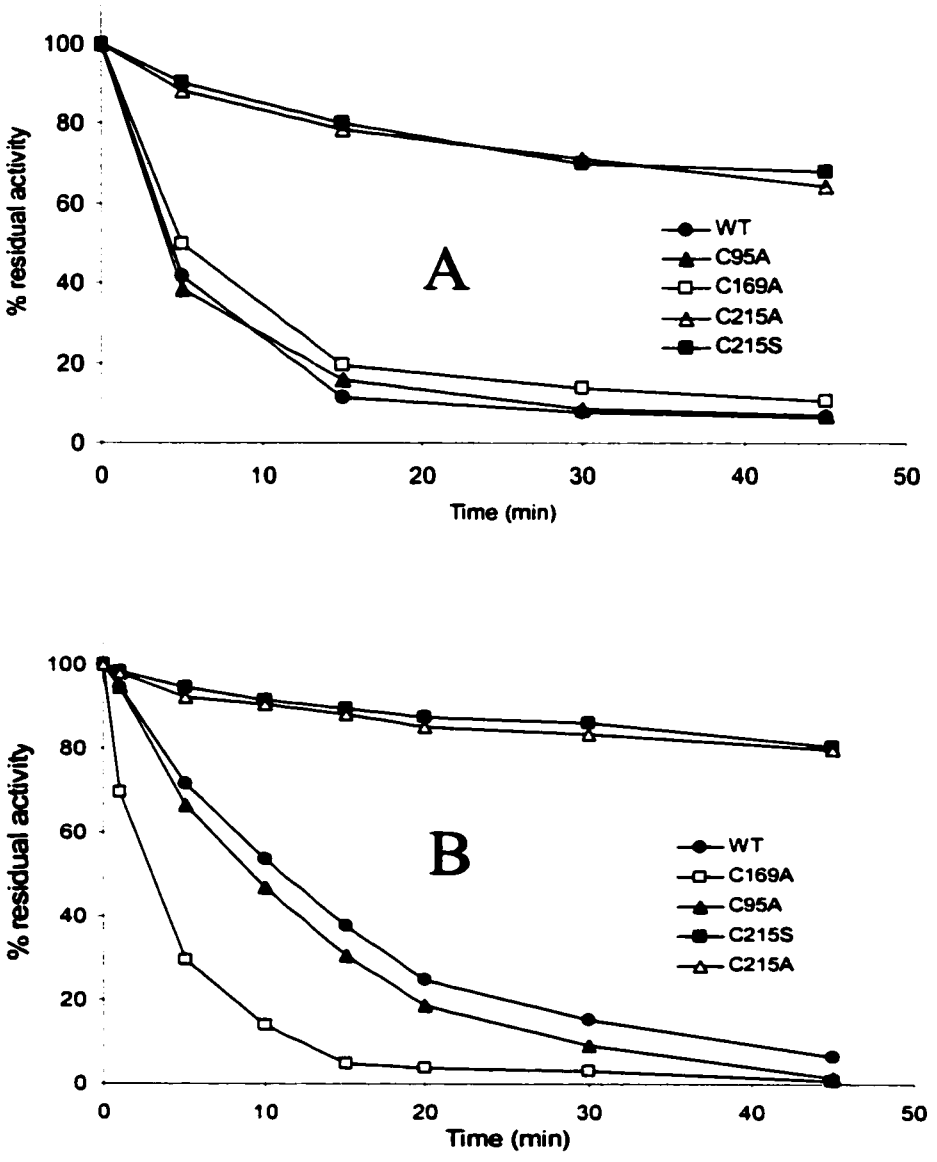

Fig. 2.20 Inactivation of CM (A) and PD (B) of WT and variant forms of CM-PD by DTNB.

WT and Cys variants (6.67 μM monomer; 20 μM Cys) in 50 mM NEM (pH 7.7), 1 mM EDTA and 25% glycerol were reacted with 1.75-fold excess DTNB (35 μM). CM and PD activity assays were performed as described in 2.1.5 (N=2).

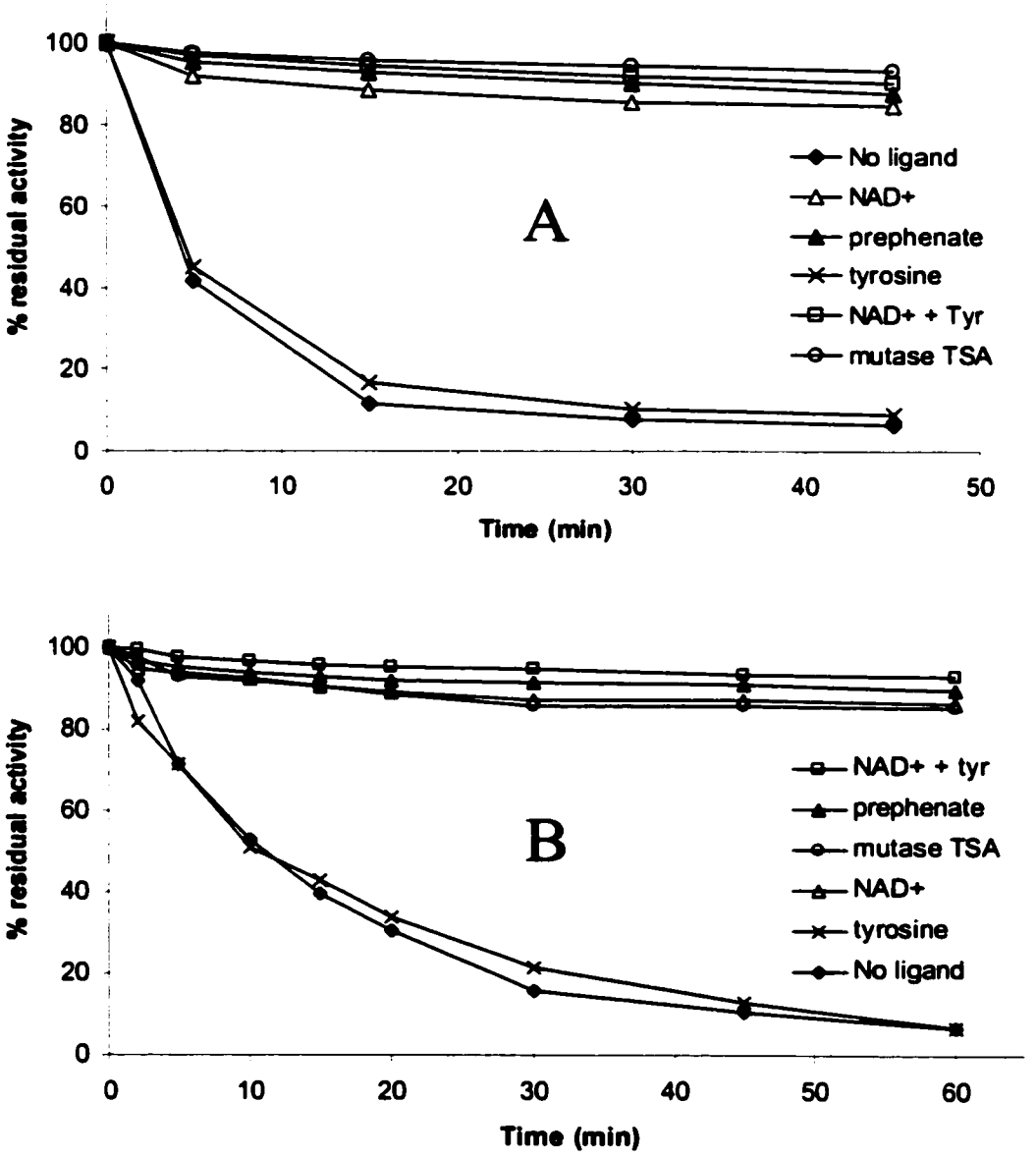

Fig. 2.21 The effect of different ligands on inactivation by DTNB of WT CM (A) and PD (B).

Ligands included: 2 mM NAD^+; 1 mM prephenate; 1 mM tyrosine; 2 mM NAD^+ + 1 mM tyrosine; 25 μM mutase TS analog. Conditions of inactivation and reaction activity assays were identical to Fig. 2.20 (N=2).

In both figures, we observe full protection against loss of CM and PD activities in the presence of NAD^+, *endo*-oxabicyclic diacid, prephenate and NAD^+ + tyrosine. In contrast, tyrosine alone did not afford protection since this ligand has poor affinity for the enzyme in the absence of NAD^+ (12, 13). Surprisingly, the TS analog, which is believed to bind specifically to the mutase site, protected the dehydrogenase against inactivation.

Similar experiments were conducted for variant proteins of CM-PD. The results obtained and compared to WT enzyme are shown in Fig. 2.22A and 2.22B. Again C95A and C169A showed similar degrees of inactivation by DTNB of both activities in the presence of various ligands to that of WT enzyme. On the other hand, C215A/S retained most of their respective activities after modification regardless if ligands were present or absent. These results indicate that Cys215 is at or near the binding site of prephenate, NAD^+ and perhaps *endo*-oxabicyclic diacid.

2.2.8.2 Chemical Modification of WT and Variant CM-PD by Iodoacetamide

Chemical modification studies were repeated on CM-PD using a less bulky Cys-specific reagent, iodoacetamide. This reagent is capable of forming an irreversible link with sulfhydryl groups thereby facilitating mass spectral analysis of the adduct and providing a direct correlation with enzyme inactivation and Cys reactivity.

The effect of iodoacetamide modification of WT CM-PD activity is shown in Fig. 2.23. The rate of inactivation increased with increasing iodoacetamide concentration (0-20 mM).

Fig. 2.22 The effect of different ligands on inactivation by DTNB of WT and Cys variant CM (A) and PD (B).

Ligands included: 1 mM prephenate; 2 mM NAD^+; 1 mM tyrosine; 2 mM NAD^+ + 1 mM tyrosine; 25 μM mutase TS analog. Conditions of inactivation and reaction activity assays were identical to Fig. 2.20. For presentation purposes, results for C215A and C215S (<5% variation) were averaged and presented together (N=1).

A

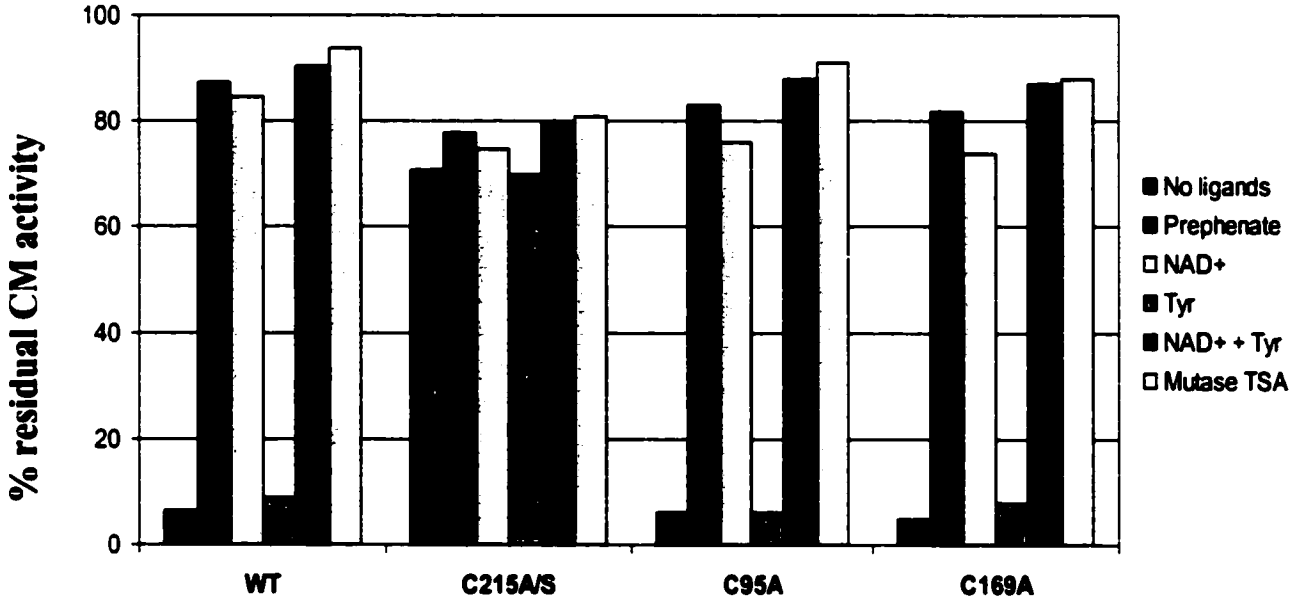
% residual CM activity
100
80
60
40
20
0
WT
C215A/S
C95A
C169A
No ligands
Prephenate
NAD+
Tyr
NAD+ + Tyr
Mutase TSA

B

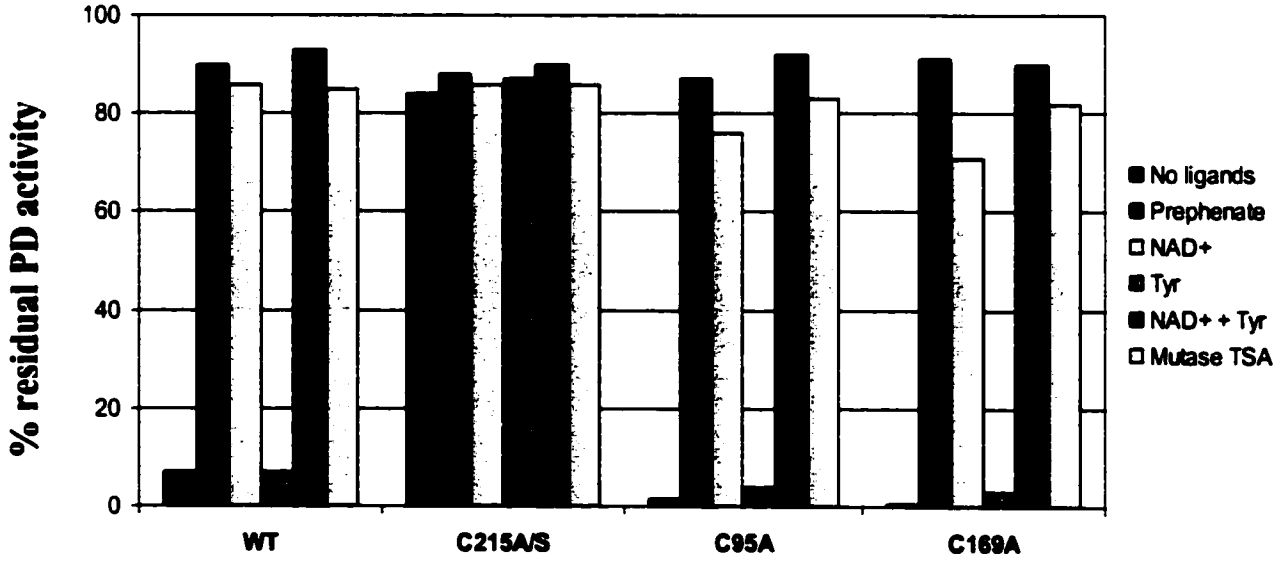
% residual PD activity
100
80
60
40
20
0
WT
C215A/S
C95A
C169A
No ligands
Prephenate
NAD+
Tyr
NAD+ + Tyr
Mutase TSA

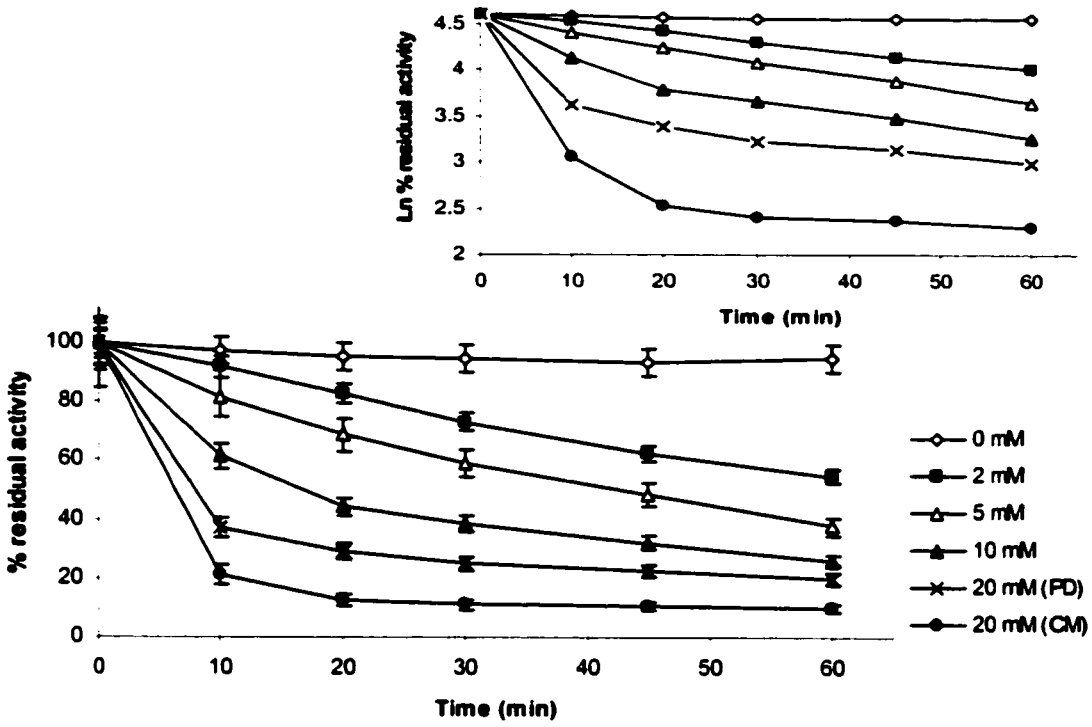

Fig. 2.23 Inactivation of WT CM-PD by iodoacetamide.

Enzyme (12 μM monomer) in 200 mM Tris, pH 7.5 and 2 mM EDTA was reacted with: 0 mM, 2 mM, 5 mM, 10 mM and 20 mM iodoacetamide at 25 °C. This figure illustrates the inactivation of PD at all concentrations and the inactivation of CM at 20 mM IAM. Activity assays were performed as described in 2.1.5. Plot of Ln % residual activity vs. Time (inset) (N=2).

The biphasic kinetics of inactivation (see inset) indicated the modification of at least two Cys affecting CM-PD activity; one fast reactive group and one or more slower reacting groups by iodoacetamide. As noted for the reaction with DTNB, inactivation of the mutase by iodoacetamide was faster and more complete than the dehydrogenase. A concentration of 10 mM iodoacetamide was used for the remaining modification experiments.

Inactivation of WT and variant CM and PD activities with 10 mM iodoacetamide is shown in Fig. 2.24A and 2.24B, respectively. In Fig. 2.24A, no significant loss of mutase activity was observed for C215A/S enzymes. These results paralleled those obtained with DTNB modification, indicating that Cys215 is the most reactive cysteine. WT enzyme along with C95A and C169A variants lost most of their activities after 60 min of reaction. Surprisingly, the inactivation of C95A variant with iodoacetamide was faster and more complete than WT enzyme even though the kinetic parameters for WT and C95A were nearly identical (Fig. 2.24A). Similar results were observed for the inactivation of PD of WT and variants (Fig. 2.24B).

Inactivation of WT CM and PD in the presence of various ligands is shown in Fig. 2.25A and 2.25B, respectively. In Fig. 2.25A, the mutase TS analog and NAD^+ + tyrosine provided the most protection followed by prephenate, and finally NAD^+ alone. This variation in the degree of protection afforded by the different ligands was not observed in the DTNB modification reaction where all ligands except tyrosine provided approximately the same degree of protection. This may be related to: (1) Different sizes

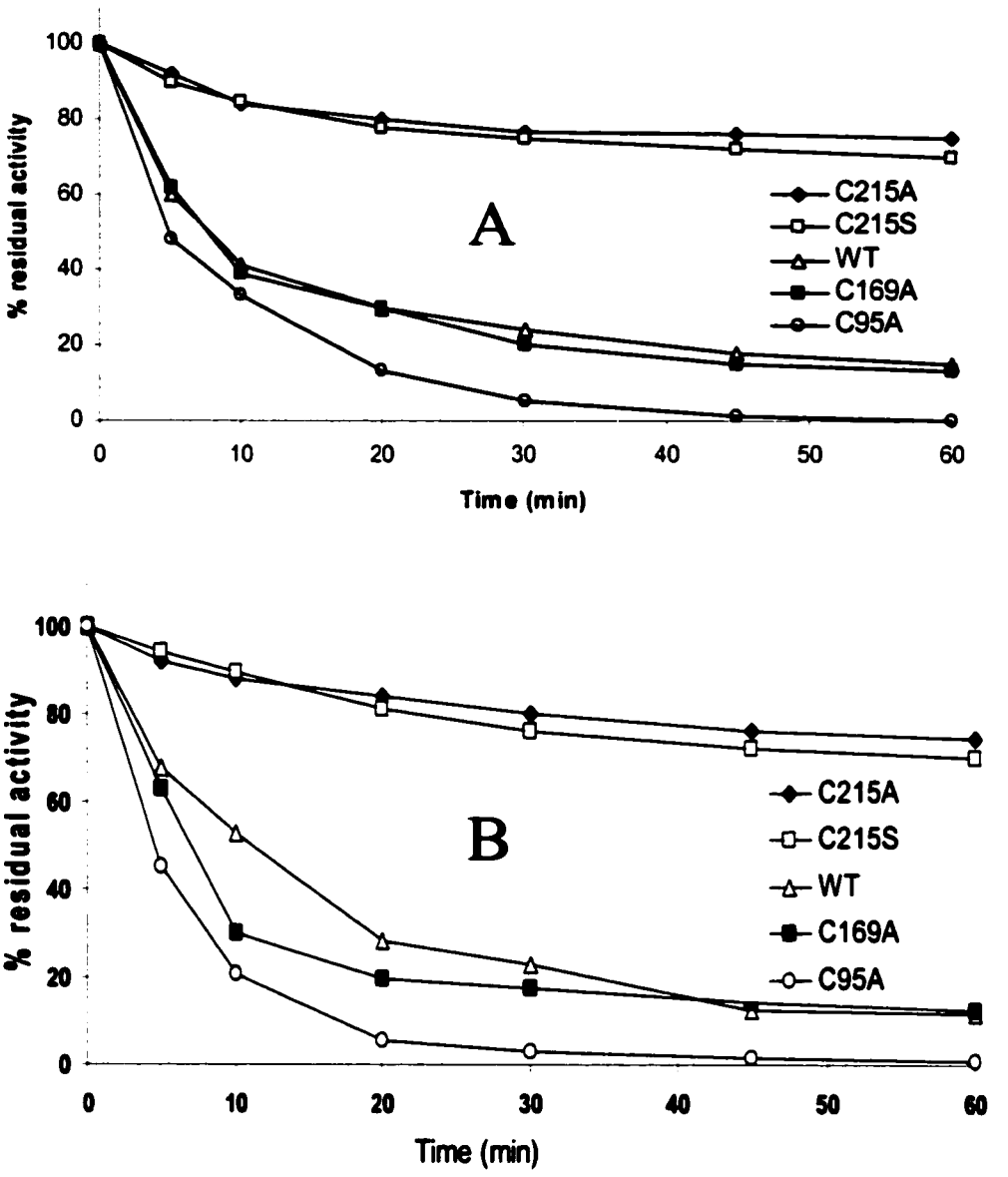

Fig. 2.24 Inactivation of WT and Cys variant CM (A) and PD (B) by iodoacetamide.

WT and Cys variants (12 μM monomer) in 200 mM Tris, pH 7.5 and 2 mM EDTA were reacted with 10 mM iodoacetamide at 25 °C (N=2).

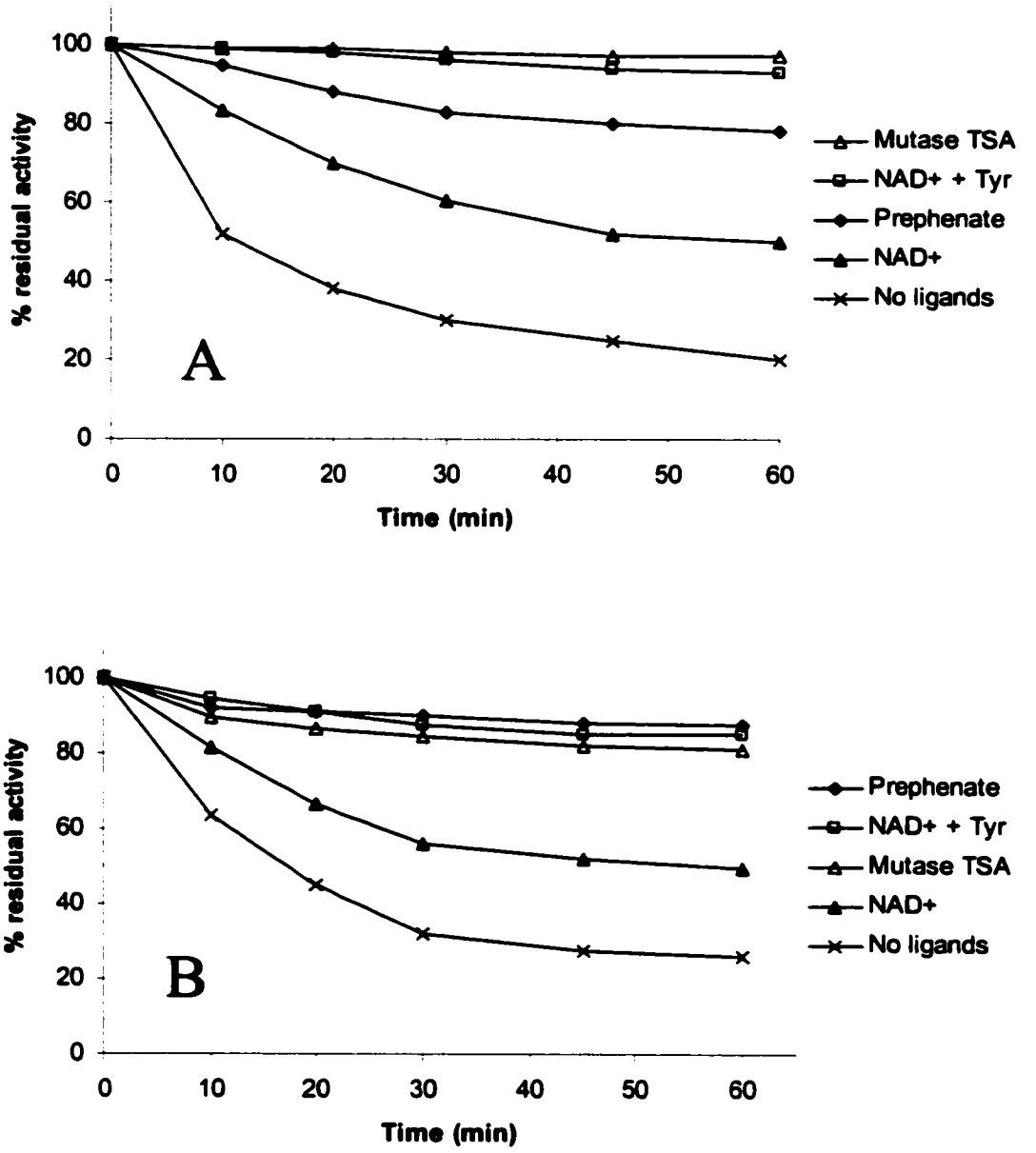

Fig. 2.25 The effect of different ligands on inactivation by iodoacetamide of WT CM (A) and PD (B).

Ligands used: 2 mM NAD^+; 1 mM prephenate; 2 mM NAD^+ + 1 mM tyrosine and 25 μM mutase TS analog (N=2).

of modifying reagents; DTNB is very bulky. (2) Iodoacetamide is not as group-specific as DTNB and has also been reported to react with His and Met enzymic groups (53, 68). In Fig. 2.25B, mutase TS analog, prephenate and NAD^+ + tyrosine provided the most protection of the dehydrogenase activity followed by NAD^+ alone.

2.2.8.3 Protection of Dehydrogenase Activity by *endo*-oxabicyclic diacid

In both DTNB and iodoacetamide alkylation reactions, the mutase transition state analog protected dehydrogenase activity against inactivation by cysteine specific reagents. To determine if the analog binds to the PD site, the dehydrogenase activity was recorded in the presence or absence of the transition state analog. For this purpose, WT CM-PD (5.5 μM) was assayed in 50 mM NEM (pH 7.7) containing 2 mM NAD^+, 40 μM prephenate and with or without 200 μM mutase TSA. The rate of reaction in the absence or presence of *endo*-oxabicyclic diacid was identical (data not shown) indicating that the chorismate analog does not inhibit dehydrogenase activity and hence does not interact with the PD site.

To determine if the mutase TS analog protects PD against alkylation by binding to the CM site, inactivation studies were performed using the CM-PD variant (K37Q). This mutant possesses WT dehydrogenase activity but mutase activity is completely abolished (26).

Lys37 of CM-PD is believed to interact with *endo*-oxabicyclic diacid based on the crystal structure of the mutase portion of *E. coli* CM-PDT complexed with this analog (42).

Hence it is expected that the K37Q variant would not bind *endo*-oxabicyclic diacid as well as WT enzyme. A series of protection experiments of PD WT and K37Q were conducted with various ligands including *endo*-oxabicyclic diacid. The results are shown in Fig. 2.26A for WT and 2.26B for K37Q. Not surprisingly, the TS analog protected PD site against inactivation by iodoacetamide whereas for K37Q, no protection was provided. These results indicate that the TS analog protected PD by binding to the CM site. Hence, binding of the analog to CM blocks or hinders modification of Cys215 thus preventing dehydrogenase inactivation upon incubation with either DTNB or iodoacetamide.

Prephenate, which acts as a substrate for the dehydrogenase reaction and as a product of the mutase reaction, should bind to both sites of the WT enzyme. However, prephenate interacts only with the dehydrogenase site of the K37Q variant (26). Surprisingly, prephenate did not markedly protect the K37Q variant (which has WT dehydrogenase activity) from inactivation by iodoacetamide. This indicated that the protective effect of prephenate against dehydrogenase inactivation was mainly provided by binding to the mutase site. Furthermore, incubation of K37Q in the presence of a higher concentration of mutase TS analog (200 μM) did not prevent the inactivation of the variant by iodoacetamide (Fig. 2.27).

2.2.9 Time-Dependent Modification with Iodoacetamide and Peptide Mapping of CM-PD Tryptic Digest

One of the main features of iodoacetamide is that it reacts irreversibly with sulfhydryl groups. This makes iodoacetamide an ideal candidate for protein modification followed

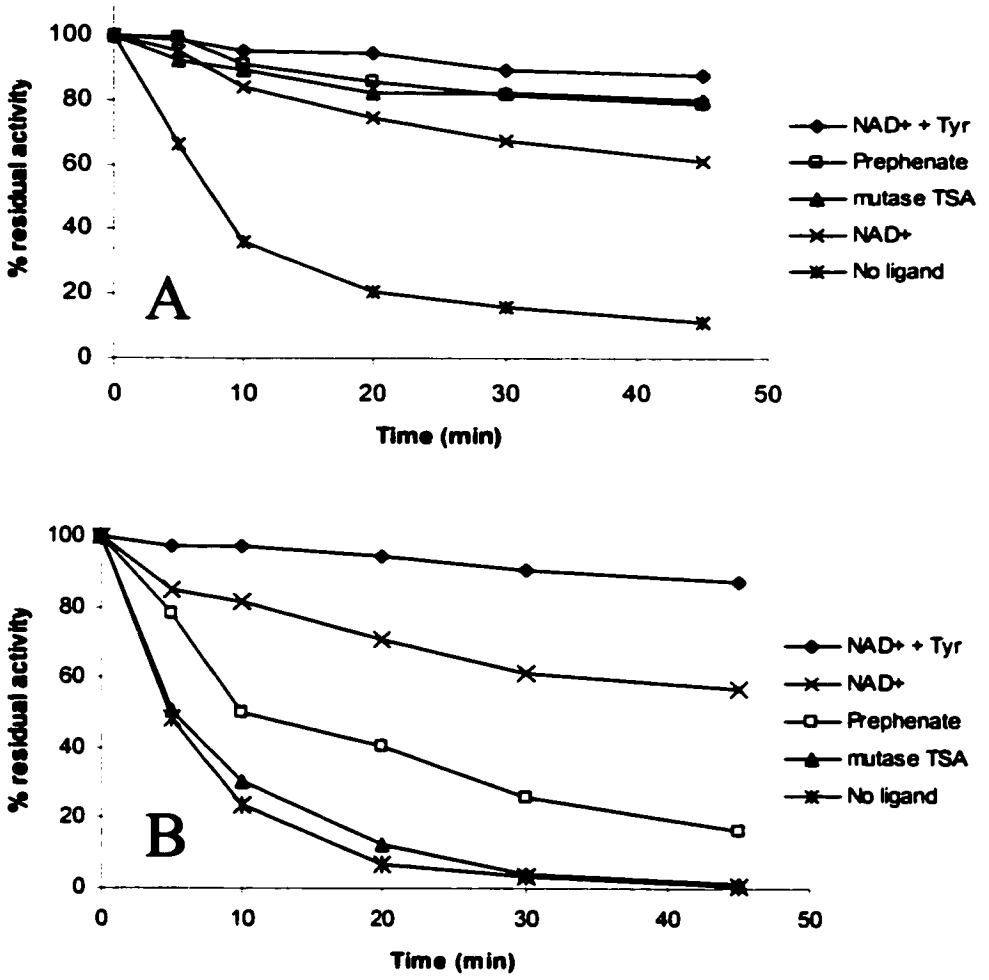

Fig. 2.26 The effect of different ligands on inactivation by iodoacetamide of WT (A) and K37Q (B) dehydrogenase.

WT and K37Q CM-PD (12 μM monomer) were incubated at 25 °C with 10 mM iodoacetamide in 200 mM Tris buffer (pH 7.5) and 2 mM EDTA in the presence or absence of various ligands. At different time intervals, 10 μl aliquots were assayed for PD activity as described in section 2.1.5. Ligands included: 1 mM prephenate; 2 mM NAD^+; 2 mM NAD^+ + 1 mM tyrosine; 25 μM mutase TS analog (N=2).

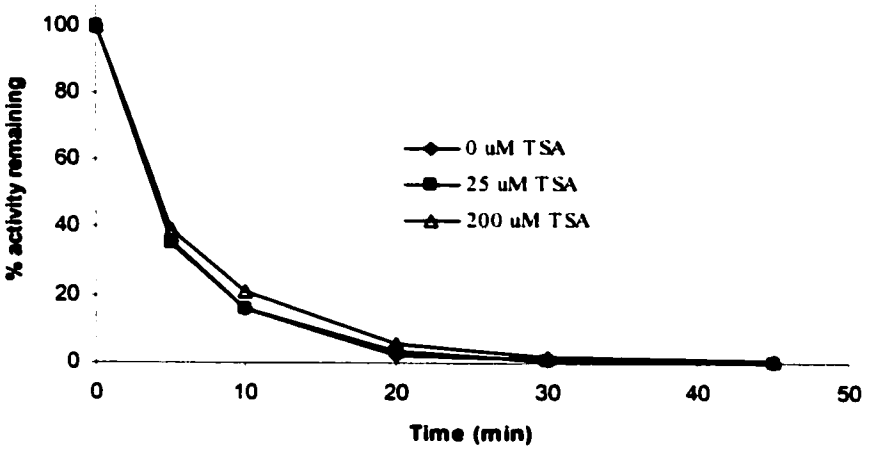

Fig. 2.27 Inactivation of K37Q PD activity in the presence of mutase TS analog.

K37Q CM-PD (12 μM monomer) was incubated at 25 °C with 10 mM iodoacetamide in 200 mM Tris buffer (pH 7.5) and 2 mM EDTA in the presence of mutase TS analog (25 μM and 200 μM). At different time intervals 10 μl aliquots were assayed for PD activity as described in 2.1.5 (N = 1).

by mass spectrometric analysis. Reaction of CM-PD with iodoacetamide for different time intervals will provide information about the reactivity and surface accessibility of the different Cys residues in CM-PD.

In this study, WT CM-PD was reacted for different times, the reactions were quenched with DTT, the modified proteins were digested with trypsin and the peptides analyzed by MS. It is expected that peptides containing Cys alkylated with iodoacetamide will yield a change in mass of +57 amu compared to the non-modified peptide. The results are shown in Fig. 2.28A and 2.28B. At t =3 min, the only modified peptide was P(210-218) shown as a singly charged peak at m/z 1117.512 (Fig. 2.28A). At t = 30 min, two other Cys (Cys95 and Cys169) were modified with the appearance of a doubly charged peak at m/z 1028.546 and a singly charged peak at m/z 1231.648 respectively (Fig. 2.28B). It is also important to note that at t = 30 min, Cys95 was alkylated to completion whereas Cys169 was present in both modified and non-modified forms. Taken together, the data implied that Cys215 is the most reactive or surface accessible followed by Cys95 and Cys169.

2.2.10 Cross-linking of WT CM-PD with Bifunctional Reagents

The purpose of this experiment was to determine if there are any cysteines at the monomer interface of dimeric CM-PD. When CM-PD was reacted with 5-fold excess of the Cys-specific bifunctional crosslinking reagent BMOE, the predominant species resolved was the monomer. However, a significant amount of higher molecular weight species was resolved by SDS-PAGE (Fig. 2.29A). This species migrated on the denaturing gel most often as two very close bands. Comparison of the Rf value of this

Fig. 2.28 Peptide fingerprint of WT CM-PD tryptic digest initially modified with iodoacetamide for 3 min (A) and 30 min (B).

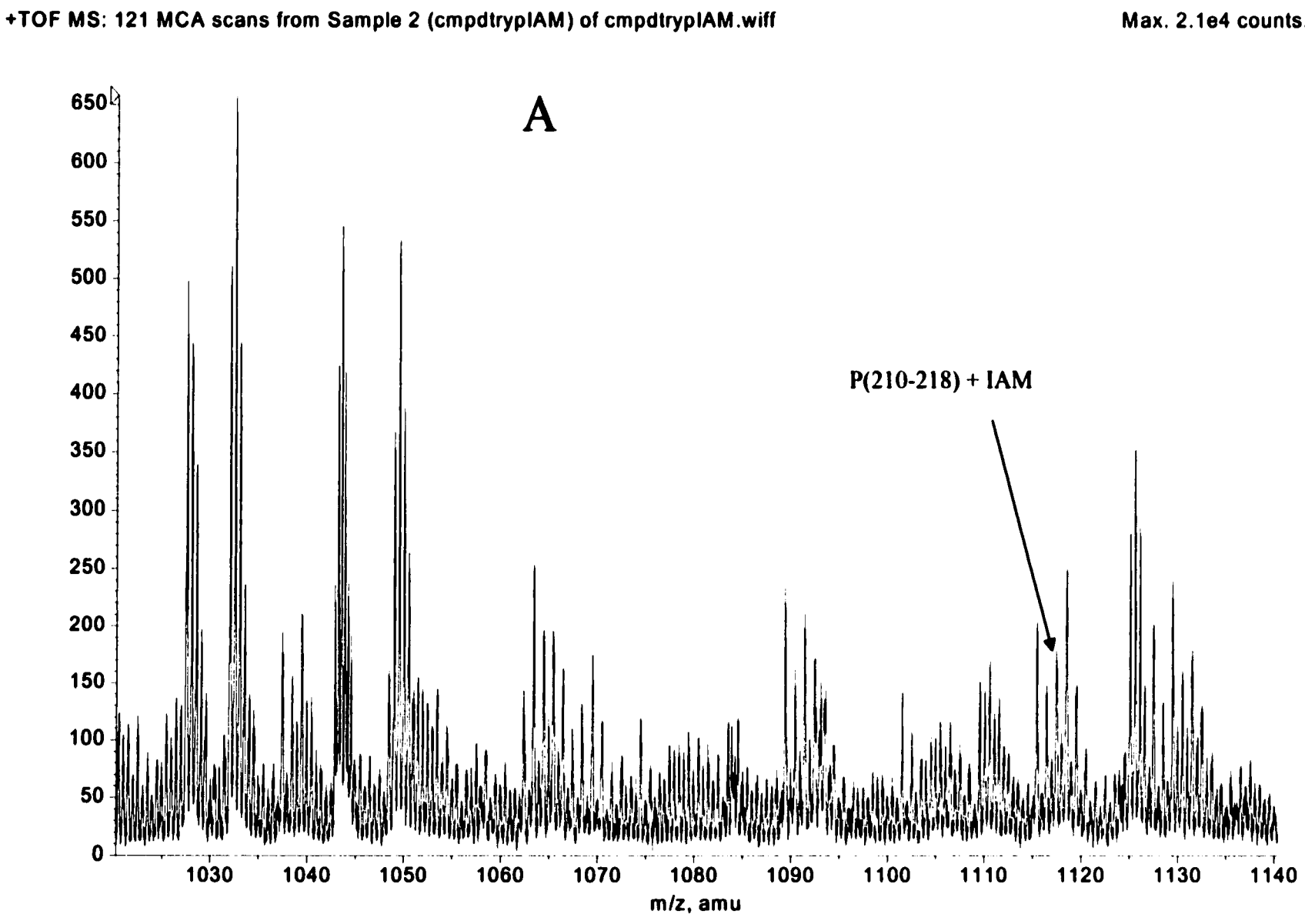
+TOF MS: 121 MCA scans from Sample 2 (cmpdtrypIAM) of cmpdtrypIAM.wiff
Max. 2.1e4 counts.
A
P(210-218) + IAM
650
600
550
500
450
400
350
300
250
200
150
100
50
0
1030
1040
1050
1060
1070
1080
1090
1100
1110
1120
1130
1140
m/z, amu

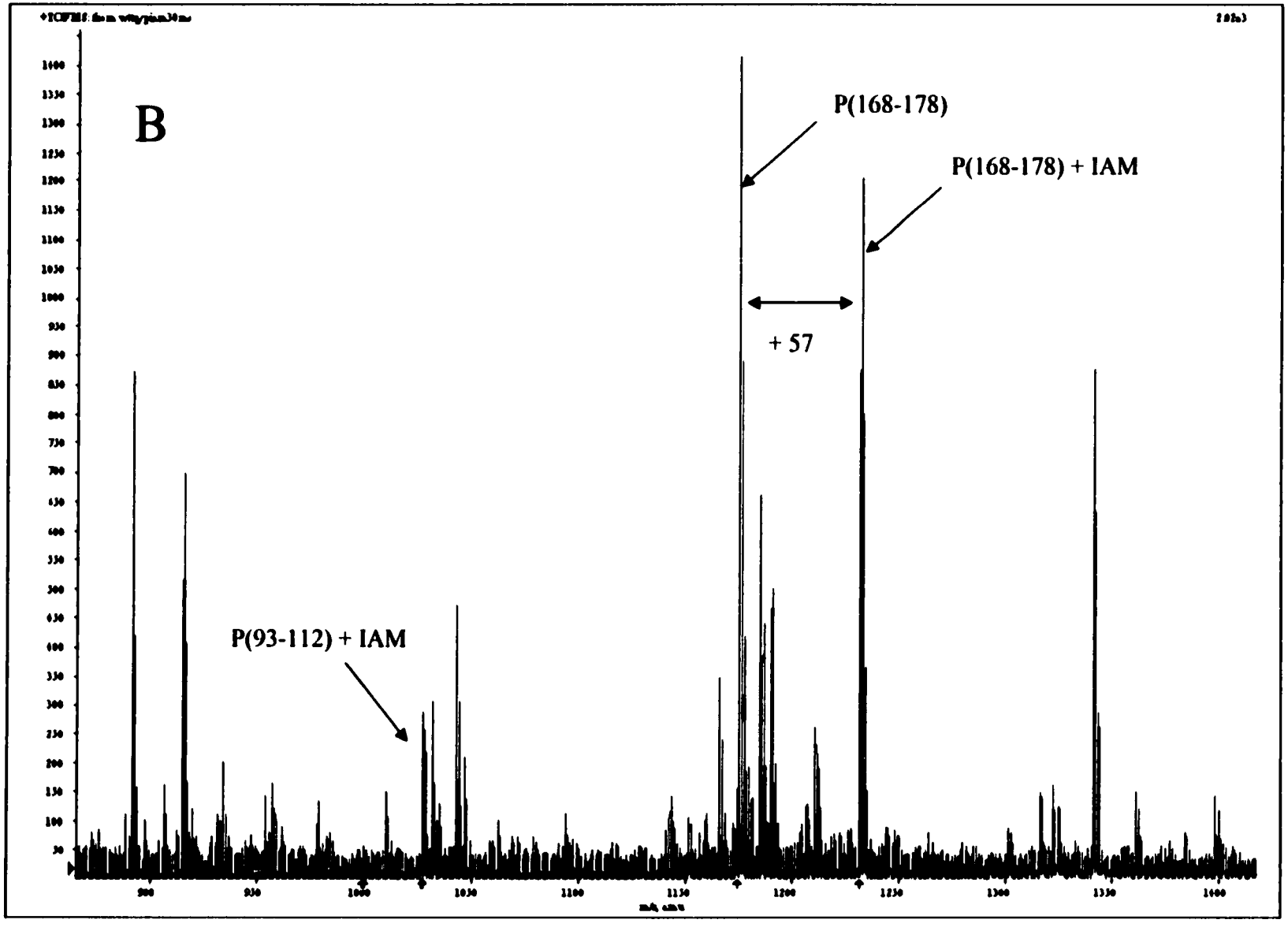
B
P(168-178)
P(168-178) + IAM
+ 57
P(93-112) + IAM

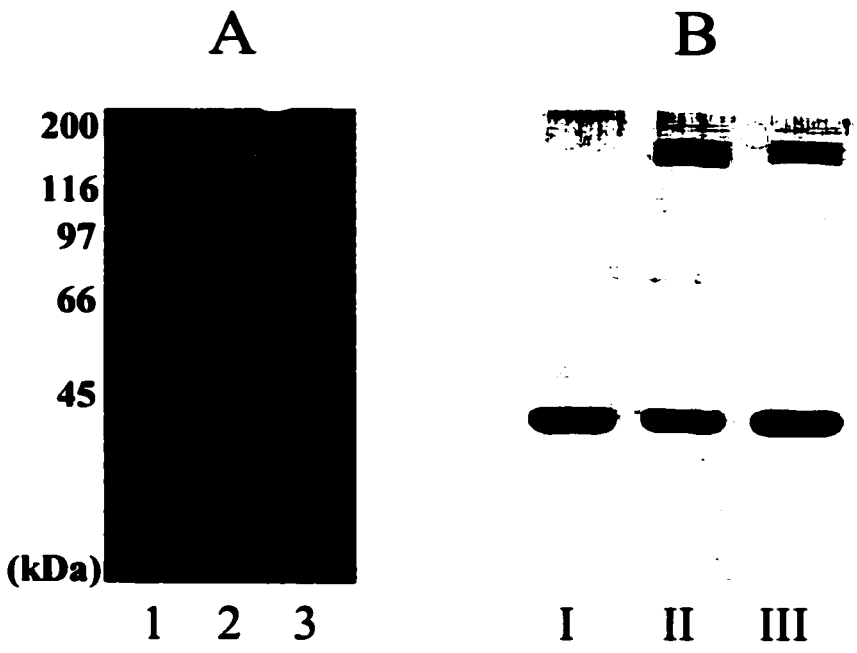

Fig. 2.29 SDS-PAGE analysis of WT CM-PD incubated with cross-linking reagents.

Analysis was performed under reducing conditions on a 15% polyacrylamide gel. Gels were silver stained as described in 2.1.4. Lane 1, MW standards; lane 2, CM-PD; lane 3, CM-PD + BMH. Lane I, CM-PD; lane II, CM-PD + BMH; lane III, CM-PD + BMOE

doublet relative to molecular weight standards was consistent with a tetramer of ~170,000 kDa (Fig. 2.29A). CM-PD undergoes oligomerization in the presence of NAD^+ + tyrosine (13). However, modification reactions conducted with BMOE and BMH (a related bifunctional reagent), in the presence of NAD^+ + tyrosine did not change the ratio of monomer to tetramer when compared to WT enzyme (S. Spetsieris, unpublished). A dimer was never observed on SDS-PAGE indicating that a Cys is not accessible for this type of reaction in the native form of the enzyme and/or it is not near the interface of the two monomers. The "arm length" between maleimide groups of the Cys-specific bifunctional reagents did not play a critical role as identical results were observed when using BMH which has a 6-Carbon bridge between maleimide groups, versus BMOE which possesses a 2-Carbon bridge (Fig. 2.29B).

2.3 DISCUSSION

2.3.1 A possible role for Cys215 in the mechanism of CM-PD

In the present investigation, we have studied the role of the cysteines in the function and structure of the *E. coli* CM-PD. Toward this goal, site-directed mutagenesis was conducted to define more precisely the role of the three Cys residues (Cys95, Cys169 and Cys215) in substrate binding and catalysis. Cys to Ala substitutions were introduced at all three positions in order to eliminate H-bonding capabilities at that position. In addition, a Cys215 to Ser change was made. Although Cys and Ser are relatively isosteric, the polar hydroxyl group of Ser is capable of forming stronger H-bonds compared to the sulfhydryl group of Cys.

The kinetic parameters obtained for the CM and PD reactions catalyzed by C95A and C169A variant proteins were similar to those obtained for WT enzyme (Table 2.2). Hence, it appears that Cys95 in the mutase portion of CM-PD does not contribute to the binding energy of the diaxial form of chorismate and of the transition state of the mutase reaction as proposed for Cys75 in the monofunctional CM from *B. subtilis* (76). Kinetic analysis of C75A variant of the monofunctional CM from *B. subtilis* has shown that the binding of both chorismate and the mutase TS analog are reduced by > 10 fold.

Replacing the sulfhydryl group of Cys215 with a methyl group (C215A) resulted in significant decreases in the binding of chorismate at the mutase site and prephenate at the

dehydrogenase site, and a moderate decrease in turnover number for both reactions compared to WT enzyme. Moreover, replacing Ala with Ser restored the dehydrogenase's affinity for prephenate to values comparable to the WT protein, highlighting the importance of the thiol group for the proper binding of the substrate. These results support the recent findings of Zhang *et al.* (55) who showed that C216A variant in the related bifunctional enzyme CM-PDT possessed a poor affinity for prephenate, which was restored with the Ser substitution.

In contrast to the PD reaction, replacing Ala with Ser further reduced the binding of chorismate at the mutase site suggesting that the presence of a polar group perturbed the proper binding of chorismate. In contrast, Zhang *et al.* (55) reported that the mutase activity and the Km for chorismate were not altered by the Cys216 to Ala substitution, supporting the idea that the reactions catalyzed by CM and PDT occur at distinct non-interacting sites (55). In summary, our observations suggest that Cys215 is the only Cys essential for the activity of both the mutase and the dehydrogenase of CM-PD and highlight the interdependence of the sites at which the two reactions occur.

Site-specific substitutions can alter the kinetic parameters of an enzyme catalyzed reaction by causing conformational changes in the protein structure. The far-UV CD spectra of WT and variants suggested that the amino acid substitutions did not impart any global secondary structural changes in the protein. However, the environment of tryptophans in C215A was slightly different than in the WT protein as determined by near UV-CD spectroscopy. These minor changes are difficult to interpret given that *E. coli*

CM-PD possesses 5 Trp in addition to 10 Tyr and 15 Phe. It is worth noting however that a Trp (Trp214) immediately precedes Cys215 in the primary sequence of CM-PD.

The pH dependence of the kinetic parameters V and $(V/K)_{prephenate}$ for the WT dehydrogenase reaction as performed in this study and others (22) indicated that a protonated group with a pK_a value of about 8.4 was essential for the binding of prephenate to the enzyme-NAD^+ complex. This value is close to that expected for a free Cys residue at neutral pH (45). However this titrating residue was not Cys215 as the $(V/K)_{prephenate}$ pH profiles for C215S and WT enzyme were essentially identical (Fig. 2.9). Our findings clearly indicated that the residue titrating with a pK of ~ 8.4 is still present when this cysteine is missing.

In the absence of a crystal structure, comparative modeling of the dehydrogenase using 6-phosphogluconate dehydrogenase as a template along with results from recent site-directed mutagenesis allow us to speculate on the role of Cys215. Interestingly, in the PD model, Cys215 was located in a pocket surrounded by residues which have been determined in the Turnbull lab to play a key role in prephenate binding (Arg294), catalysis (His197) and tyrosine binding (His257) (24, 26, T. Lee, unpublished). The close proximity of Cys215 to these residues (notably His197) suggested that this thiol group could be involved directly in the proper orientation of prephenate. The fact that both Km of prephenate and the turnover number are affected by the C215A mutation suggests that Cys215 may play an indirect role in correctly orienting the catalytic residue, His197. It should be noted, however, that only the NAD^+ binding domain is modeled with

confidence, so caution is advised when interpreting this structure. Moreover, the mutase domain could not be modeled together with PD since there is no crystal structure of the bifunctional enzyme. This capability would have helped us pinpoint the location of both active sites relative to each other and understand the role of Cys215 in the mutase reaction.

2.3.2 Defining the location of the Cys residues and their importance in enzyme activity by chemical modification studies

Reaction of CM-PD with the Cys modifying reagents DTNB and iodoacetamide support the conclusion drawn from site-directed mutagenesis that Cys at position 215 is important for both PD and CM activity.

Modification of WT CM-PD with DTNB and iodoacetamide resulted in the time-dependent loss of both mutase and dehydrogenase activities. This agreed with previous reports by Hudson *et al.* (13) using the aforementioned reagents and by Turnbull *et al.* (11) who monitored alkylation by the active site-directed reagent, iodoacetic acid. However, this was in contrast to the results obtained by Zhang *et al.* (55) and Gething *et al.* (54) in which modification of CM-PDT with DTNB and N-ethylmaleimide (NEM) resulted in the inactivation of only the dehydratase.

Extending these studies to the inactivation of variant forms of CM-PD by DTNB and iodoacetamide showed conclusively that it was Cys215, presumably at or near the active

site(s) that was essential for enzyme activity. The fact that C215A/S proteins retained > 75% residual mutase and dehydrogenase activities upon modification with Cys specific reagents (Fig. 2.20 and 2.24) supported the idea that the loss of both activities in the WT enzyme was due to the modification of the same group (Cys215).

However, modification of at least one Cys other than Cys215 contributed to the loss of CM-PD activity, since the kinetics of inactivation by iodoacetamide were biphasic presumably due to the modification of a fast reacting sulfhydryl (Cys215) and one or more slower reacting groups. Moreover, the mutase was more sensitive than the dehydrogenase to inactivation by both Cys modifying reagents (Fig. 2.19 and 2.23). Interestingly, the kinetics of inactivation of C169A and C95A were both biphasic implying that modification of either of these two Cys contributed to loss of enzyme activity. Although the Ala substitution at positions 95 and 169 did not affect the kinetic parameters of the enzyme catalyzed reaction, they did appear to affect their reactivity with the Cys modifying reagents. Inactivation of C169A dehydrogenase activity by DTNB was faster and more complete compared to WT enzyme. Clearly the Cys to Ala substitution resulted in changes that rendered the reactive group(s) more prone to modification by the different reagents. This result clearly demonstrates the necessity of combining site-directed mutagenesis with protein modification to better understand the function of the different residues under investigation.

In agreement with studies by Hudson *et al.* (16), incubation of WT CM-PD with DTNB resulted in the modification of 2 Cys/monomer, indicating that one Cys was inaccessible

or not reactive to modification by DTNB (Fig. 2.18). In the present study, identical studies with the Cys variants identified this sulfhydryl group as Cys169. Furthermore, alkylation of the enzyme with iodoacetamide followed by peptide mapping using mass spectrometry clearly identified Cys215 as the reactive and surface accessible Cys followed by Cys95 and Cys169 (Fig. 2.28). These findings are in agreement with peptide mapping experiments of Hudson *et al.* using radiolabeled iodoacetamide (16).

Comparison of the chemical modification of WT and variant forms of CM-PD in the absence and presence of substrates and substrate analogs have affirmed that only Cys215 is at or near the active site(s) of CM-PD. Incubation of the enzyme with prephenate, NAD^+ + tyrosine and mutase TS analog prior to inactivation with DTNB or iodoacetamide, led to the protection of both mutase and dehydrogenase activities. The degree of protection afforded by NAD^+ was less when inactivating the enzyme with IAM versus DTNB. This may reflect the fact that iodoacetamide is less bulky than DTNB and able to access the prephenate binding site in the presence of NAD^+. As expected the protective effect of NAD^+ was enhanced in the presence of tyrosine presumably by increasing the enzyme's affinity for this cofactor (12, 13). C169A and C95A variant proteins, which possess a Cys at position 215 could be protected against inactivation by these ligands whereas C215A and C215S were not (Fig. 2.20 and 2.24).

Similarly, preincubation of the enzyme with prephenate, NAD^+ + tyrosine, and mutase TS analog, prevented one Cys from being alkylated with DTNB. These results clearly indicated the presence of a reactive thiol group near or at the binding site of these ligands.

Similar studies with the Cys variants clearly identified this reactive sulfhydryl as Cys215. However, from the conclusion that Cys169 was buried and that Cys215 could be protected against modification by any one of the ligands, modification of C95A in the presence of ligands did not result in zero Cys modified per monomer as predicted (Fig. 2.16). This might arise if the substitution at position 95 caused a conformational change in the structure of this variant.

Surprisingly, the mutase TS analog protected the PD from inactivation by the Cys specific reagents. Moreover our kinetic studies indicated that this protection was afforded through binding to the mutase site and not the dehydrogenase site. In support of this idea was the finding that the dehydrogenase activity of K37Q (a CM-PD variant unable to bind the mutase TS analog) was inactivated by iodoacetamide in the presence of the analog (Fig. 2.27).

Based on all the results obtained in the studies by site-directed mutagenesis, comparative modeling and chemical modification, we propose a model where Cys215 is at the interface of both active sites. This would be consistent with the decrease in the enzyme's affinity for both chorismate and prephenate as observed by site-directed mutagenesis. The inactivation of both activities by modification with Cys specific reagents, notably iodoacetamide that is smaller than DTNB, also supports our hypothesis. Furthermore, the model is in keeping with the protective effect of *endo*-oxabicyclic diacid against inactivation of PD, assuming that the binding of the mutase TS analog to the CM site blocks the interaction of the modifying reagents with Cys215. Alternatively, the

interaction of the *endo*-oxabicyclic diacid at the mutase site could promote a conformational change in the enzyme propagated to the dehydrogenase site. However, binding of the analog to the enzyme does not elicit change in fluorescence or near UV-CD spectra, consistent with this idea (data not shown).

2.3.3 CM-PD is post-translationaly modified

This present study also reports the first MS analysis of *E. coli* CM-PD. The difficulty in analyzing CM-PD by MS is presumably due to the protein's surface hydrophobicity. This high hydrophobicity leads to a decrease in the tendency of the residues to ionize, which is essential for ESI-MS analysis. Sixty percent of the enzyme's 373 a.a. residues are large (L, I, V, M, F, Y, W) and small (A, G) non-polar groups with L, I, V alone constituting 26% of the total residues. Recent results from ANS coupled fluorescence experiments (J. Bonvin, unpublished) and the observation that CM-PD binds very tightly to phenyl Sepharose and to C_{18} reverse phase columns, highlight the fact that the protein's surface is highly hydrophobic.

MS has yielded an accurate determination of the molecular weight of the CM-PD subunit (41,042 Da). Furthermore, MS analysis of native and tryptic digests of the protein has been used in this study to verify the presence and identity of the site-directed variants.

MS analysis of CM-PD has also identified a post-translational modification common to many proteins. Deconvolution of the mass spectra of WT and variant enzyme yielded two

peaks with a difference in mass of 131 amu. These two peaks corresponded to the enzyme with or without the N-terminal methionine.

More than 60% of all proteins lose their N-terminal methionine (90). Among the various hypotheses concerning the crucial role of methionine removal is the idea that it allows further post-translational modifications and that it is linked to a molecular device, which governs the half-life of proteins (91). The extent of N-terminal methionine excision from *E. coli* proteins is governed by the side-chain length of the penultimate amino acid. The extent of cleavage decreases in parallel with increasing of the maximal side-chain length of the amino acid at position 2 (90). In *E. coli* CM-PD, the amino acid at position 2 is a valine. Studies by Meinnel *et al.* (92) have shown that when valine is the amino acid at position 2 in a series of different proteins, the extent of methionine cleavage was around 80%. This ratio was not observed in our studies, where the two peaks in the deconvoluted spectra of WT and Cys variants were of equal intensity. This could be explained if the overexpression of CM-PD in *E. coli* cells, leads to a high ratio of the bifunctional enzyme versus the enzyme responsible of cleaving the N-terminal residue, thus decreasing the extent of methionine cleavage.

CHAPTER 3

Determination of the pK_a of Lys37 in *E. coli* Chorismate Mutase - Prephenate Dehydrogenase

3.0 INTRODUCTION

Lys37 plays an important role in the mutase domain of chorismate mutase – prephenate dehydrogenase of *E. coli*. Sequence alignment with CM portion of CM-PD and CM-PDT shows a conserved Lys at position 37 and 39 respectively (13, 16). Overall, sequence identity between the different chorismate mutases is low. Nevertheless, the electrostatic environment is conserved (40, 41). Comparison of the crystal structures of the minimutase and monofunctional mutases from *B. subtilis*, *S. cerevisiae* show a cationic residue homologous to Lys37 which plays a key role in stabilizing the transition state of the mutase reaction. Furthermore, substituting Lys37 in *E. coli* CM-PD with Gln results in complete loss of CM activity (26). Similarly, site-directed mutagenesis of homologous residues of CM in other organisms results in inactive enzyme.

Earlier studies by Turnbull *et al.* (22) and more recently by K. Bull (unpublished) examining the pH dependence of $V/K_{chorismate}$ in mutase reaction of CM-PD established that a group with pK ~ 7.5 had to be protonated to assist in binding of chorismate and the TS analog to CM (Fig. 1.3).

The purpose of this chapter is to determine the pK_a of Lys37 of *E. coli* CM-PD as a goal towards identifying the catalytically important group whose ionization is observed in the V/K pH rate profile. This is achieved by following the pH dependence of the reactivity and inactivation by Lys-specific reagent TNBS.

3.1 EXPERIMENTAL PROCEDURES

3.1.1 Materials

CM-PD WT was prepared as previously described (2.1.3) whereas K37Q variant was prepared by D. Christendat (26). Chorismate, NAD^+ and *endo*-oxabicyclic diacid were prepared as previously described (2.1.1). 2,4,6-Trinitrobenzene Sulfonic Acid (TNBS) (5% w/v in methanol) and Glu-C protease from *Staphylococcus aureus* strain V8 were purchased from Sigma. NAP pre-packed Sephadex G-25 size exclusion buffer exchange columns were obtained from Amersham Biosciences. Acetonitrile (HPLC grade) was from Fisher. Trifluoroacetic acid (TFA) (HPLC grade) was from Pierce. All other chemical reagents were obtained commercially and were of the highest quality available.

3.1.2 Determination of Enzyme Activity and Concentration

CM and PD activities and protein concentrations were determined as previously described in 2.1.5.

3.1.3 Kinetics of Inactivation by TNBS

3.1.3.1 Inactivation Kinetics of WT CM-PD with TNBS

CM-PD (6 μM monomer) in 50 mM sodium phosphate, 25% glycerol (pH 7.2) was reacted with TNBS (20 μM or 200 μM) in the dark (foil around test tubes) at 25 °C. Control samples were incubated under the same conditions except that TNBS was omitted. At timed intervals after the addition of TNBS, aliquots (20-40 μl) of the reaction

mixture were assayed for CM and PD activities (substrate saturating) as described in 2.1.5.

3.1.3.2 Inactivation of CM-PD in the Absence or Presence of Mutase TS Analog

CM-PD (13 μM monomer) was dissolved in 50 mM sodium phosphate, 25% glycerol (pH 7.2), with or without mutase TS analog (25 μM), then incubated in the dark at 25 °C with 5-fold excess TNBS (65 μM) dissolved in the same buffer. Control samples were incubated under the same conditions except that TNBS was omitted. At timed intervals after the addition of TNBS, 20 μl aliquots of the reaction mixture were assayed for CM activity as described in 2.1.5.

3.1.3.3 pH-Dependent Modification of CM-PD with TNBS

CM-PD (4.5 μM monomer) was dissolved in 50 mM sodium phosphate, 25% glycerol (pH 6.0 – 8.5) or in 50 mM sodium pyrophosphate, 25% glycerol (pH 8.5 – 10.0) then incubated in the dark at 25 °C with ~3-fold excess TNBS (15 μM) dissolved in the same buffer at the same pH. Control samples were incubated under the same conditions except that TNBS was omitted. At timed intervals after the addition of TNBS, 40 μl aliquots of the reaction mixture were assayed for CM activity as described in 2.1.5. The slopes of the lines generated from a plot of ln % residual activity versus [TNBS] at each pH value were fitted to Eq. 3.1 using GraFit 3.0 to obtain a value for the pH-independent value of the observed rate constants, their maximum values, and for the acid dissociation constants (*Ka*). *H* is the hydrogen ion concentration.

$$k = k_{max} / [1 + (H/K_a)] \quad (3.1)$$

3.1.4 Mass Spectrometry

3.1.4.1 Verification of Amino Acid Substitution by Mass Spectrometry

WT CM-PD and K37Q were buffer exchanged into 0.1 M ammonium bicarbonate (pH 7.8). 100 µl aliquots (20 µg) of WT and K37Q were digested overnight at 37 °C with 20 µl (10 µg) of endoproteinase Glu-C from *Staphylococcus aureus* strain V8 (Sigma) dissolved in H_2O. Digestion was terminated by lyophilizing the reaction mixtures to dryness with a SpeedVac. The samples were then redissolved, just prior to analysis, with 50 µl of ACN:H2O (1:1) + 0.1% TFA and injected by direct infusion (4 µl/min) into a PE Sciex QSTAR Mass Spectrometer with an IonSpray source and a time-of-flight (TOF) mass analyzer (mass accuracy of ±0.01 amu), as previously described in 2.1.8.1.1.

3.1.4.2 Mass Spectral Analysis of WT CM-PD and K37Q Modified with TNBS

WT CM-PD (23 µM monomer) or K37Q in 50 mM sodium phosphate (pH 7.2) was incubated with 5-fold excess TNBS (110 µM) for 30 min in the dark at 25 °C. Control samples were incubated under the same conditions except that TNBS was omitted. At t = 30 min, the reaction mixtures were buffer exchanged into 0.1 M ammonium bicarbonate (pH 7.8). 100 µl aliquots (23 µg) of WT and K37Q protein were digested overnight at 37 °C with 20 µl (10 µg) of Glu-C endoprotease (Sigma). The reaction mixtures were then processed as described in 3.1.4.1.

3.1.4.3 Mass Spectral Analysis of CM-PD Alkylated in the Absence or Presence of Mutase Transition State Analog.

CM-PD (13 μM monomer) was dissolved in 0.1 M sodium phosphate (pH 7.0) in the presence or absence of 2-fold excess of mutase TS analog (25 μM) then incubated in the dark at 25 °C with 5-fold excess TNBS (65 μM) in the same buffer. After 5 min, the reactions were quenched by passing the mixtures on a NAP5 column into 0.1 M ammonium bicarbonate (pH 7.8). 100 μl of modified protein (30 μg) was digested for 18 h at 37 °C with 30 μl (15 μg) of Glu-C endoprotease. The reaction mixtures were then processed as described in 3.1.4.1.

3.1.4.4 Mass Spectral Analysis of pH-Dependent Modification of CM-PD with TNBS

CM-PD (10 μM monomer) in 50 mM sodium phosphate (pH 6.5 - 8.5), or in 50 mM sodium pyrophosphate (pH 10.0) was incubated in the dark at 25 °C with 5-fold excess TNBS (50 μM) in the same buffer. After 1 min, the reactions were quenched by passing the mixtures on a NAP5 column into 0.1 M ammonium bicarbonate (pH 7.8). 100 μl of modified protein (20 μg) was digested for 18 h at 37 °C with 10 μl (10 μg) of Glu-C endoprotease and processed as described in 3.1.4.1.

3.2 RESULTS

3.2.1 Inactivation of WT CM-PD with TNBS

Time-dependent inactivation of the mutase by TNBS is shown in Fig. 3.1. In the presence of 200 μM TNBS (30-fold excess of reagent to monomer) all mutase activity was lost after 10 min of reaction, whereas with 20 μM TNBS, the inactivation was much slower. The biphasic nature of inactivation at the higher concentration (200 μM) (see inset) indicated the alkylation of more than one reactive group.

When even higher concentrations of TNBS were used (500 μM), CM activity was lost too rapidly to conveniently monitor the time-dependent inactivation. TNBS is reasonably specific for Lys residues but will also alkylate Cys residues albeit at a much slower rate. Hence lower concentrations of TNBS (~3-5 fold excess of reagent to monomer) were used in all studies. Similarly, 25% glycerol was used to slow down the inactivation of the enzyme.

Fig. 3.2 illustrates the time-dependent inactivation of PD compared to CM. When a 3-fold excess of TNBS to CM-PD was used, mutase activity was markedly reduced whereas dehydrogenase activity was not affected by the alkylation reaction.

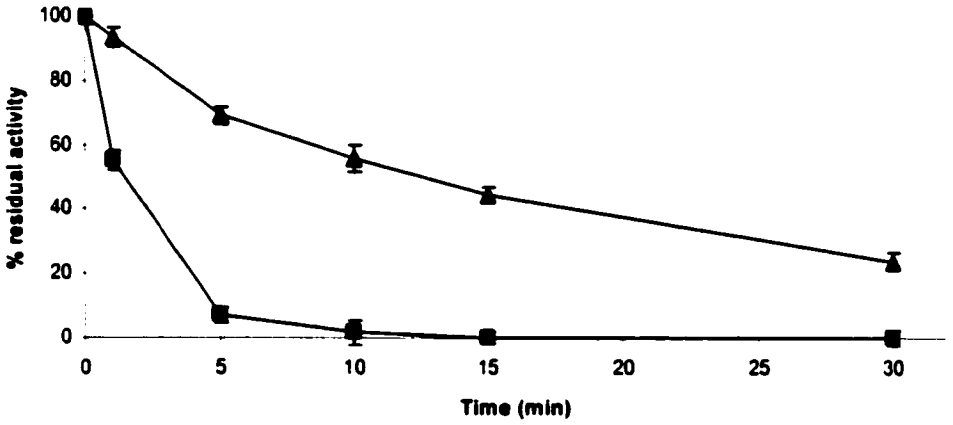

Fig. 3.1 Inactivation of CM by TNBS

WT CM-PD (6 μM monomer) was reacted with 20 μM (▲) and 200 μM (■) TNBS in 50 mM sodium phosphate, pH 7.2 plus 25% glycerol. At various time intervals, 20 μl aliquots were removed and assayed for mutase activity as described in 2.1.5 (N=2).

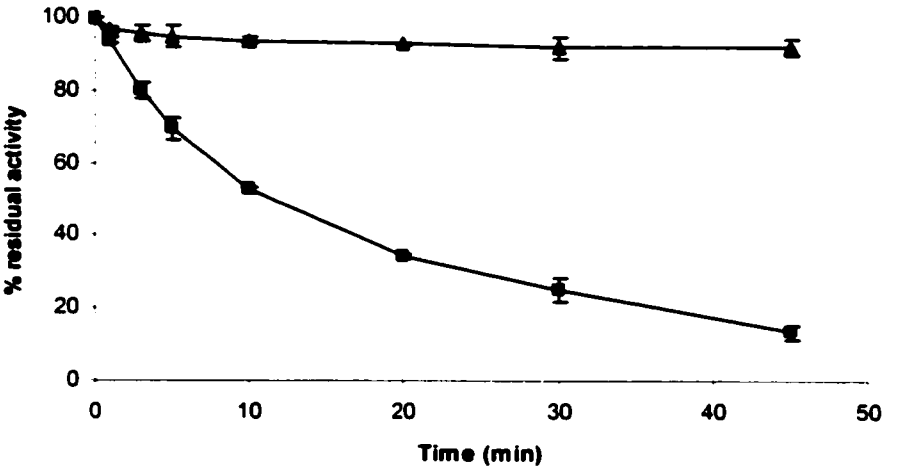

Fig. 3.2 Inactivation of WT CM-PD by TNBS

WT CM-PD (6 μM monomer) was reacted with 20 μM TNBS in 50 mM sodium phosphate, 25% glycerol (pH 7.2). At various time intervals 20 μl aliquots were withdrawn and assayed for mutase (■) and dehydrogenase (▲) activities as described in 2.1.5 (N=2).

3.2.2 Inactivation of CM-PD in the Absence or Presence of Mutase TS Analog

The purpose of this experiment was to determine if incubating CM-PD with mutase TS analog prevented time-dependent inactivation by TNBS. As shown in Fig. 3.3, in the absence of the TS analog, mutase activity was lost after 1 h of reaction, whereas in the presence of the analog the mutase was protected against inactivation. It is clear that the chorismate analog prevents the alkylation of residue(s) important for the catalytic mechanism of CM.

3.2.3 pH-Dependent Inactivation of CM-PD with TNBS

The inactivation of CM by TNBS was monitored as a function of pH in order to determine the pK_a of the enzymic group being modified. Inactivation reactions proceeded with a time-dependent loss of mutase activity over the pH range of 6.0-10.0 as shown in Fig. 3.4. The rate of inactivation was slow at lower pH values (pH 6.0-7.2) but rapidly increased at high pH values (pH 7.5-9.0). The kinetics of inactivation appeared slightly biphasic at the high pH values consistent with the participation of enzymic groups with different rates of reactivity. At pH 8.5, inactivation reactions conducted in either phosphate or pyrophosphate buffers showed a variation of less than 10%; the average of both data sets was plotted in Fig. 3.4. At pH 9.5 and 10.0 there was an unexpected decrease in the rates of inactivation by TNBS. Since TNBS is reported to be stable under alkaline conditions (75), this observation might be due to a pH-induced conformational change in the protein, limiting the reaction with the CM active site. Linear regression analysis was performed on all data points to obtain an approximation of the rate of inactivation at each pH value. Since biphasic kinetics were observed at the high pH

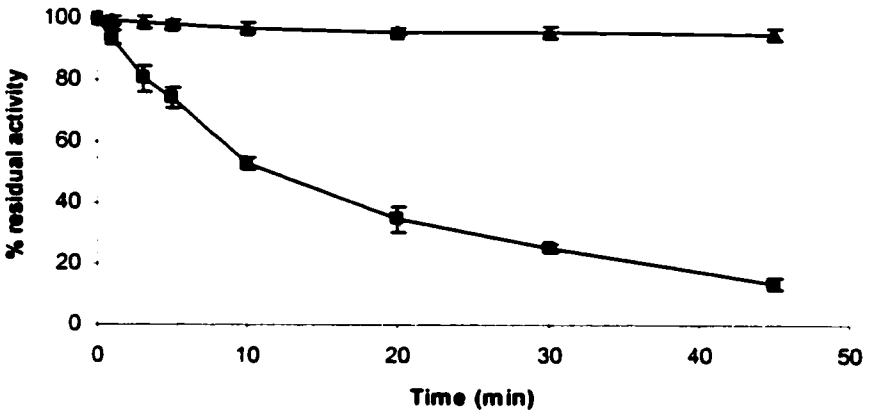

Fig. 3.3 Protection by mutase TS analog against alkylation of CM. WT CM-PD (13 μM monomer) was reacted with 5-fold excess TNBS (65 μM) in 50 mM sodium phosphate, 25% glycerol (pH 7.2), in the presence (▲) or absence (■) of 2-fold excess *endo*-oxabicyclic diacid (25 μM). CM was assayed as discussed in 2.1.5 (N=2).

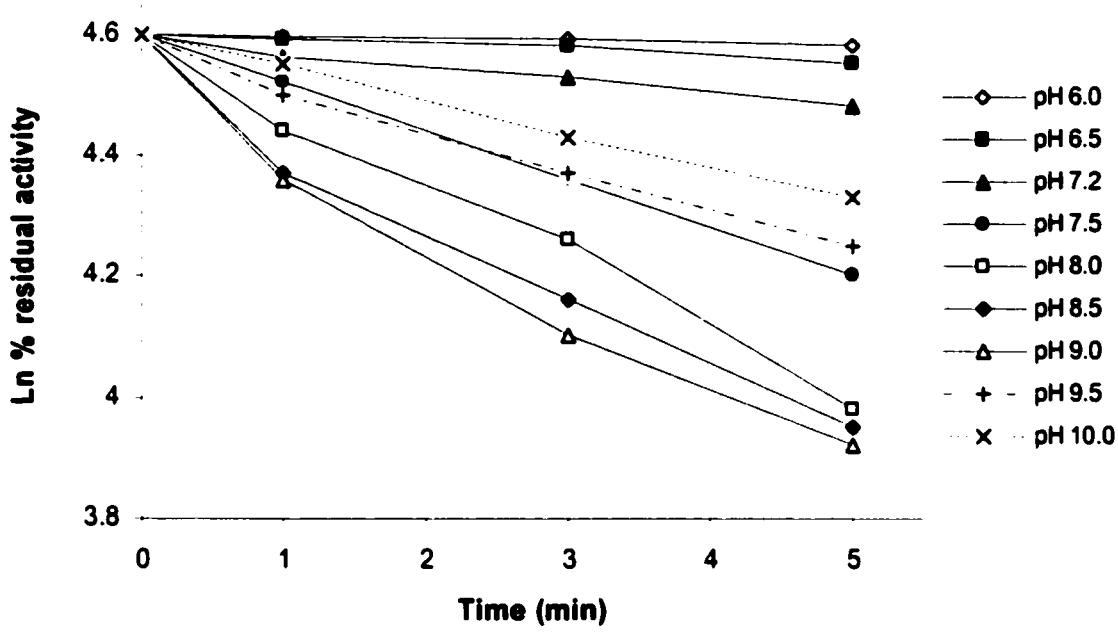

Fig. 3.4 Inactivation by TNBS of CM at various pH

WT CM-PD (4.5 μM monomer) was reacted at 25 °C with 3-fold excess TNBS (15 μM) in 50 mM sodium phosphate at pH 6.0, 6.5, 7.2, 7.5, 8.0, 8.5, or in 50 mM sodium pyrophosphate at pH 8.5, 9.0, 9.5, 10.0. Each buffer contained 25% glycerol. At timed intervals, 40 μl aliquots were assayed for CM activity as described in 2.1.5 (N=1).

values, linear regression was also performed on the data within the first minute of the reaction. For both data sets, the apparent pK_a of the reacting group was estimated by following the pH dependence of the rate constants for TNBS inactivation of the mutase. Over the pH range of 6.0-9.0, the ionization of a single group was observed (Fig. 3.5A and 3.5B). pK_a values of 7.48 ± 0.19 and 7.82 ± 0.07 were determined by fitting the data in A and B to Eq. 3.1, respectively.

3.2.4 Verification of Amino Acid Substitution by Mass Spectrometry

Glu-C protease-digested WT and K37Q CM-PD were analyzed by mass spectrometry and their spectra were compared in order to verify the mutation introduced by site-directed mutagenesis.

The number of detected peptides was approximately 80% for both proteins. Table 3.1 shows the list of all the peptides detected by MS. The peptide of interest, consisting of residues 36 to 48, was found in both spectra. Fig. 3.6 shows the region of the mass spectra containing the signal for P(36-48) for the WT CM-PD and K37Q variant. In both spectra, the peptide was present as a doubly charged species, as indicated by the isotope peaks, which are separated by 0.5 m/z. The molecular mass (M_r) of the peptides was calculated using Eq. 3.2, where (Z) is the number of charge and (M) is the peptide mass divided by the charge of the peptide (m/z).

$$Mr = (M + Z) / Z \qquad (3.2)$$

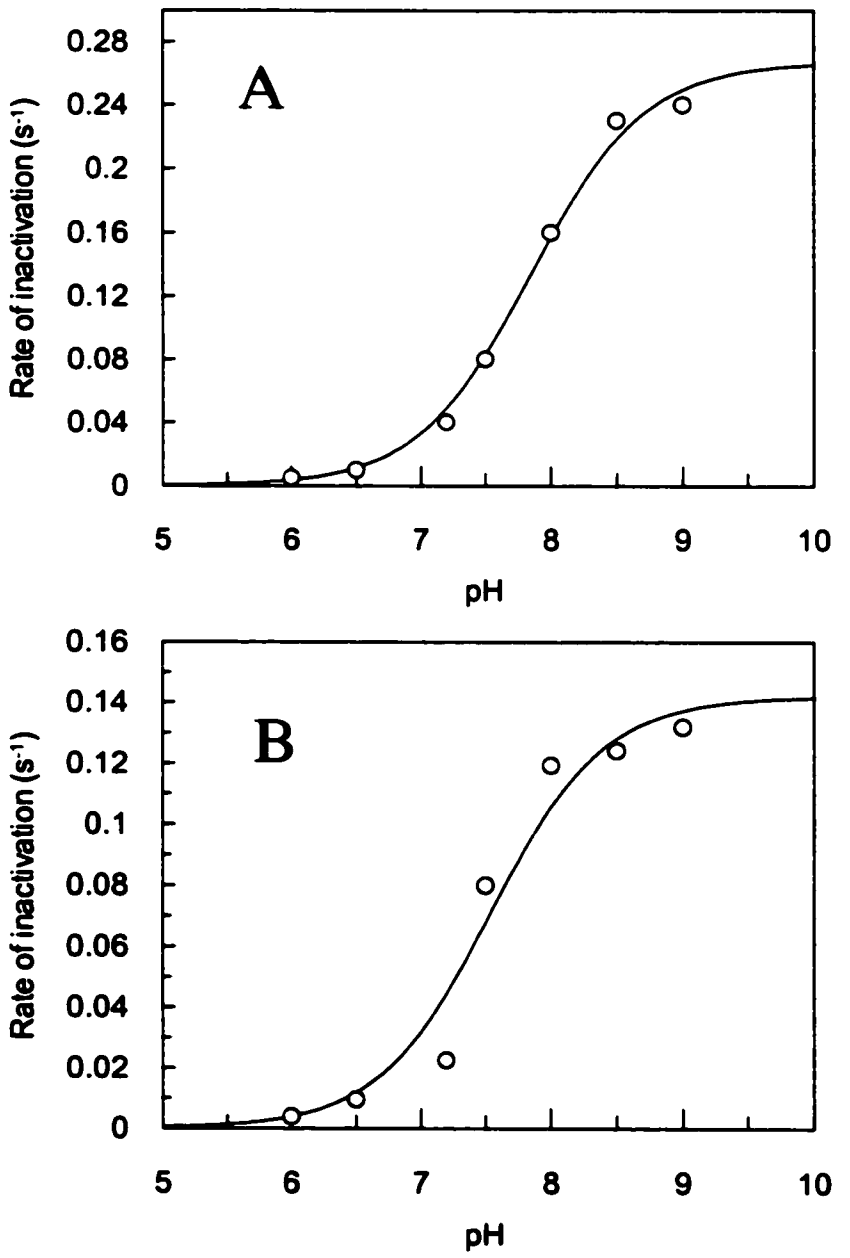

Fig. 3.5 pH-dependence of rate constant for inactivation by TNBS of CM

WT CM-PD (4.5 μM monomer) was reacted at 25°C with 15 μM TNBS in 50 mM sodium phosphate at pH 6.0-8.5 and in 50 mM sodium pyrophosphate at pH 8.5-9.0. At different time intervals over 1 min (**A**) and 5 min (**B**), aliquots were assayed for CM activity. The curves represent the best fit of the data to Eq. 3.1 (N=1).

Table 3.1 List of peptides generated by Glu-C[1] digestion of WT and K37Q CM-PD and detected by QSTAR ESI MS[2]

Mass	Position	Amino Acid Sequence
448.199	1-4	MVAE
1172.604	5-14	LTALRDQIDE
1594.977	15-28	VDKALLNLLAKRLE
430.243	29-32	LVAE
1503.848	**36-48**	**VKSRFGLPIYVPE (WT)**
1503.813	**36-48**	**VQSRFGLPIYVPE (K37Q)**
1090.555	51-60	ASMLASRRAE
1022.565	63-72	ALGVPPDLIE
1172.645	73-81	DVLRRVMRE
571.213	82-86	SYSSE
1649.917	116-129	KMLTLSGYQVRILE
955.444	222-228	AYQWFLE
1862.027	229-244	QIQVWGARLHRISAVE
601.307	271-275	NVQLE
1501.850	276-288	QLLALSSPIYRLE
2567.276	289-311	LAMVGRLFAQDPQLYADIIMSSE
1766.895	333-347	QGDKQAFIDSFRKVE
1669.727	348-360	HWFGDYAQRFQSE
1568.849	361-373	SRVLLRQANDNRQ

[1] Endoproteinase Glu-C from *Staphylococcus aureus* strain V8 hydrolyzes peptide bonds at the carboxyl side of glutamyl residues.

[2] Digestion of WT and K37Q CM-PD and analysis by MS are described in 3.1.4.1

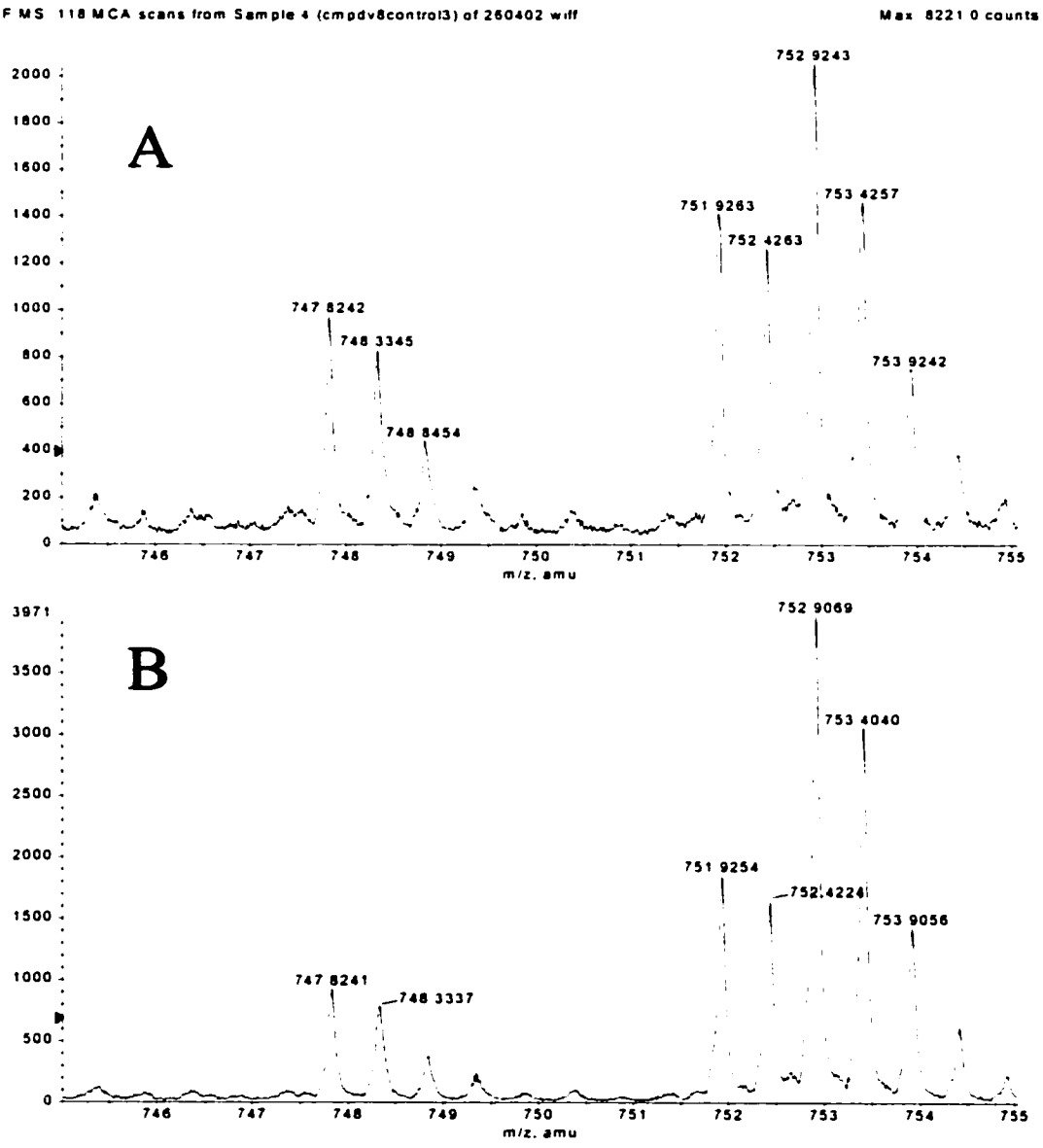

Fig. 3.6 ESI mass spectra of 470 pmol of WT and K37Q CM-PD digested overnight at 37 °C with Glu-C endoprotease (2:1). This figure illustrates the region of the mass spectra containing P(36-48) of (**A**) WT CM-PD resolved as a doubly charged peak (m/z 752.9243) and (**B**) K37Q CM-PD resolved as a doubly charged peak (m/z 752.9069).

This yields a molecular mass of 1503.8486 Da for WT enzyme and 1501.8138 Da for K37Q variant. The difference between these masses is 0.0348 Da, which is in excellent agreement with that predicted between Lys and Gln residues (0.0363 Da). This result also highlights the sensitivity of the QSTAR mass spectrometer (± 0.01 amu) to very small differences in mass.

3.2.5 Mass Spectral Analysis of WT and K37Q CM-PD Modified with TNBS

The purpose of this experiment was to determine if the loss of mutase activity correlates with the alkylation of Lys37 by TNBS. Fig. 3.7A and 3.7B show the spectra of Glu-C digested WT CM-PD unmodified and modified with TNBS using the same molar ratio of protein monomer to reagent as used for the inactivation reactions. However, in all MS studies, glycerol, was omitted from the reaction mixture since it prevented proper buffer exchange with the NAP columns and also since any residual glycerol (a non-volatile reagent) in the final sample would interfere with MS analysis.

The modification reaction was carried out for 30 min to ensure an adequate amount of adduct for detection. In Fig. 3.7A, the peak corresponding to the unmodified peptide containing Lys37 was identified at m/z 752.9243. CM-PD modified with TNBS for 30 min then proteolytically digested, yielded the mass spectrum shown in Fig. 3.7B. The peak corresponding to the Lys37 containing peptide was absent and a new doubly charged signal at m/z 858.4106 had appeared. This peak corresponded to the P(36-48) with an addition of 211 Da representing the molecular weight of a TNB adduct on a Lys residue.

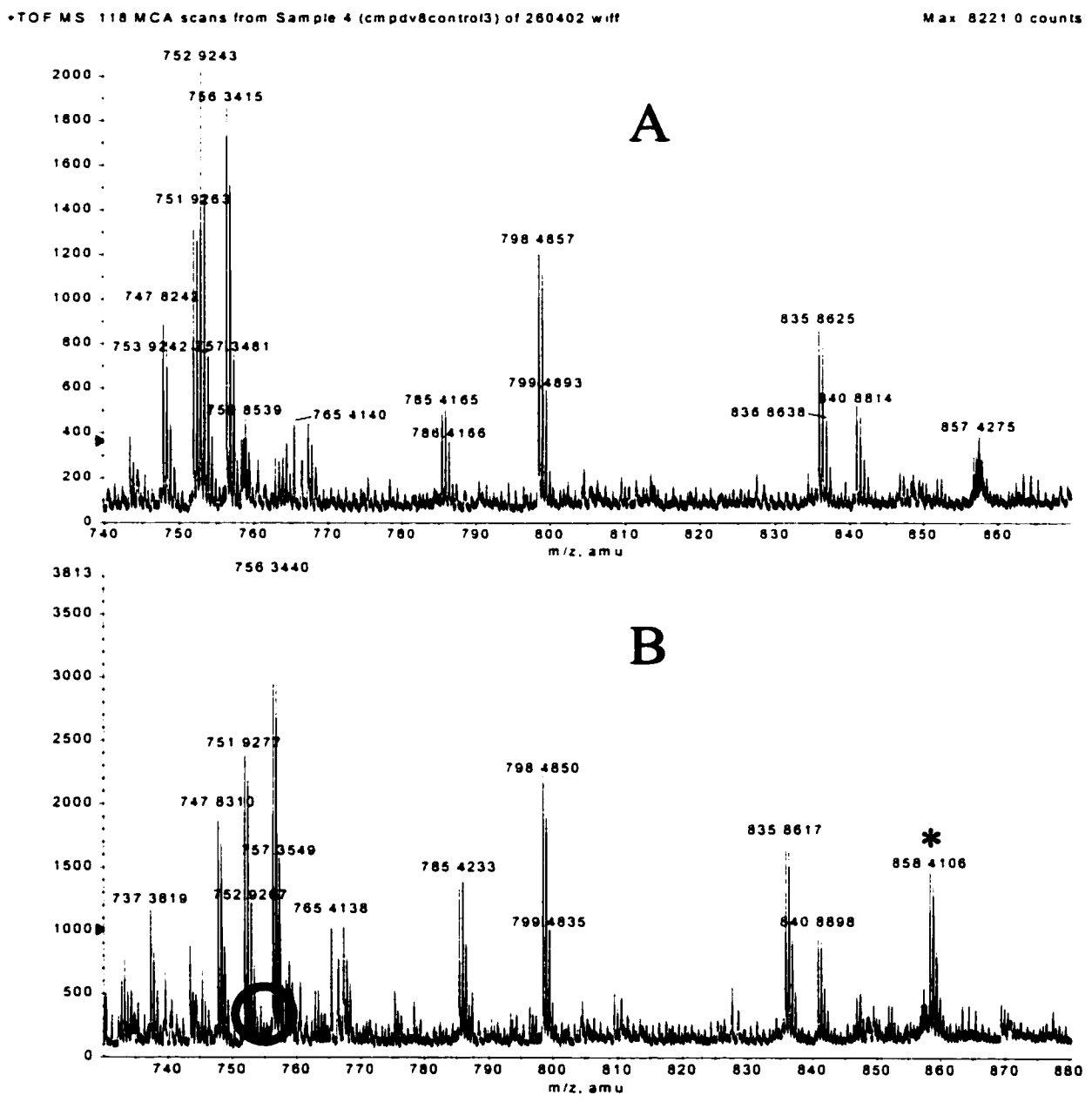

Fig. 3.7 ESI mass spectrum of WT CM-PD (547 pmol) unmodified (**A**) or modified with 5-fold excess TNBS for 30 min (**B**) and then digested overnight with Glu-C endoprotease (2:1). In **A**, the peak corresponding to the peptide containing Lys37 was observed at m/z 752.9243. In **B**, the peak corresponding to the unmodified peptide was not observed (circled portion) and a new doubly charged peak at m/z 858.4106 appeared (*). This peak corresponds to P(36-48) with a TNB adduct (+211 amu).

To verify that the peaks identified corresponded to P(36-48), the peptide mapping was repeated with K37Q variant protein. Fig. 3.8A and 3.8B show the spectra of K37Q CM-PD unmodified and modified with TNBS, respectively. In Fig. 3.8A, the peak corresponding to unmodified P(36-48) was identified at m/z 752.9069. In Fig. 3.8B, this same peak was still present (m/z 752.9107) but the corresponding modified peptide was absent. The fact that variant K37Q was not modified and the only lysine in P(36-48) is at position 37 clearly showed that the lysine modified by TNBS was Lys37.

3.2.6 Mass Spectral Analysis of CM-PD Alkylated in the Absence or Presence of Mutase TS Analog.

The purpose of this experiment was to determine if the extent of inactivation of the mutase in the presence of the TS analog correlated with the degree of modification of Lys37 observed by MS. Fig. 3.9A and 3.9B show the mass spectra of WT CM-PD reacted with TNBS in the absence or presence of the mutase TS analog then proteolytically digested with Glu-C, respectively. In Fig. 3.9A, both the unmodified and modified Lys37-containing peptides P(36-48) were identified at m/z of 752.9258 and 858.4106, respectively. The ratio of the intensity of the unmodified to modified signals was ~ 2. The same peaks were present for CM-PD reacted with TNBS in the presence of the TS analog (Fig. 3.9B). However, the intensity of the peak corresponding to the unmodified peptide had increased, and that of the modified peptide had decreased, to yield a ratio of 6.

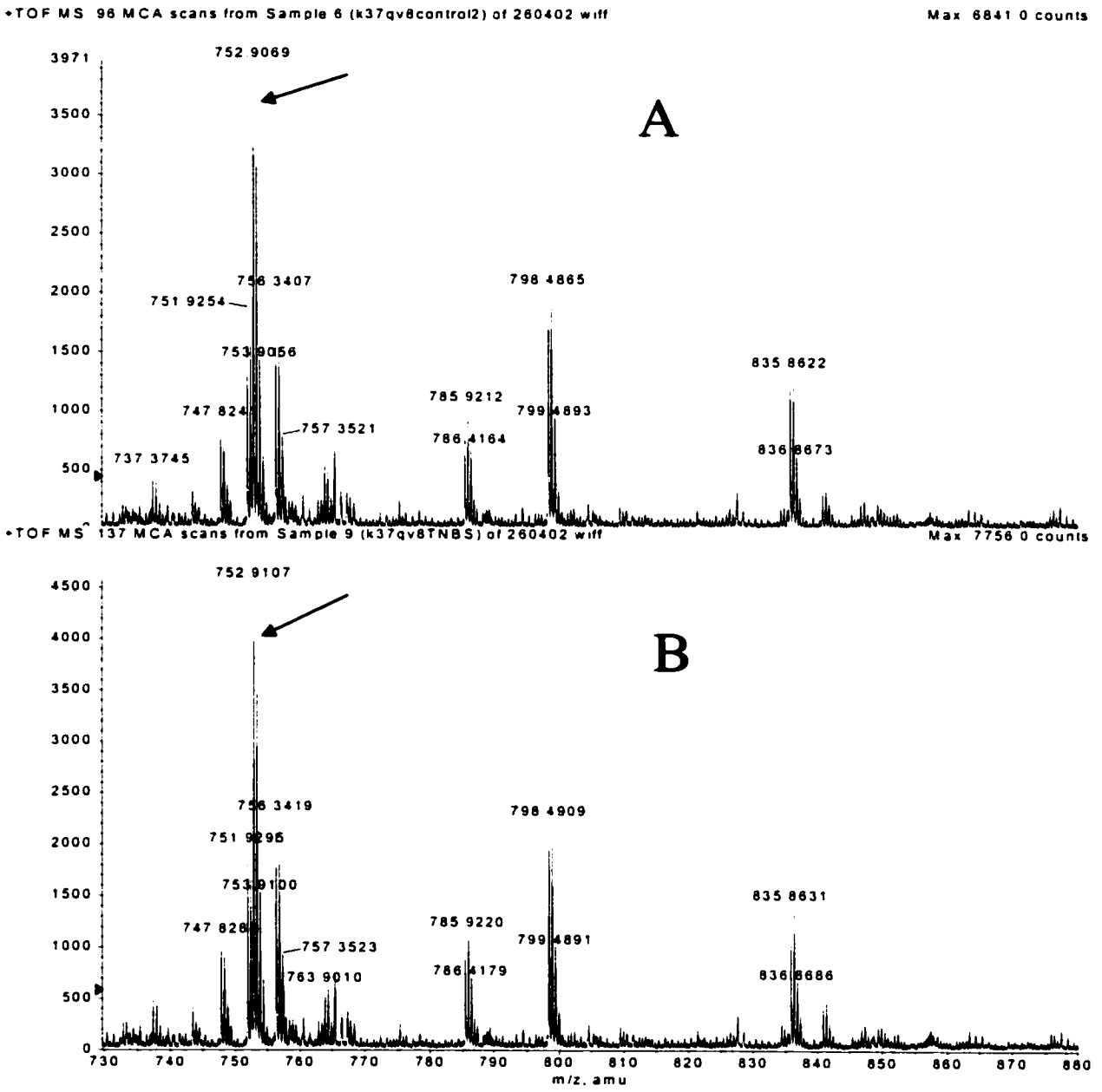

Fig. 3.8 ESI mass spectrum of K37Q CM-PD (547 pmol) unmodified (**A**) or modified with 5-fold excess TNBS for 30 min (**B**) and then digested overnight at 37 °C with Glu-C endoprotease (2:1). In both **A** and **B**, only the peaks corresponding to unmodified P(36-48) were observed at m/z 752.9069 and 752.9107, respectively (indicated by arrow).

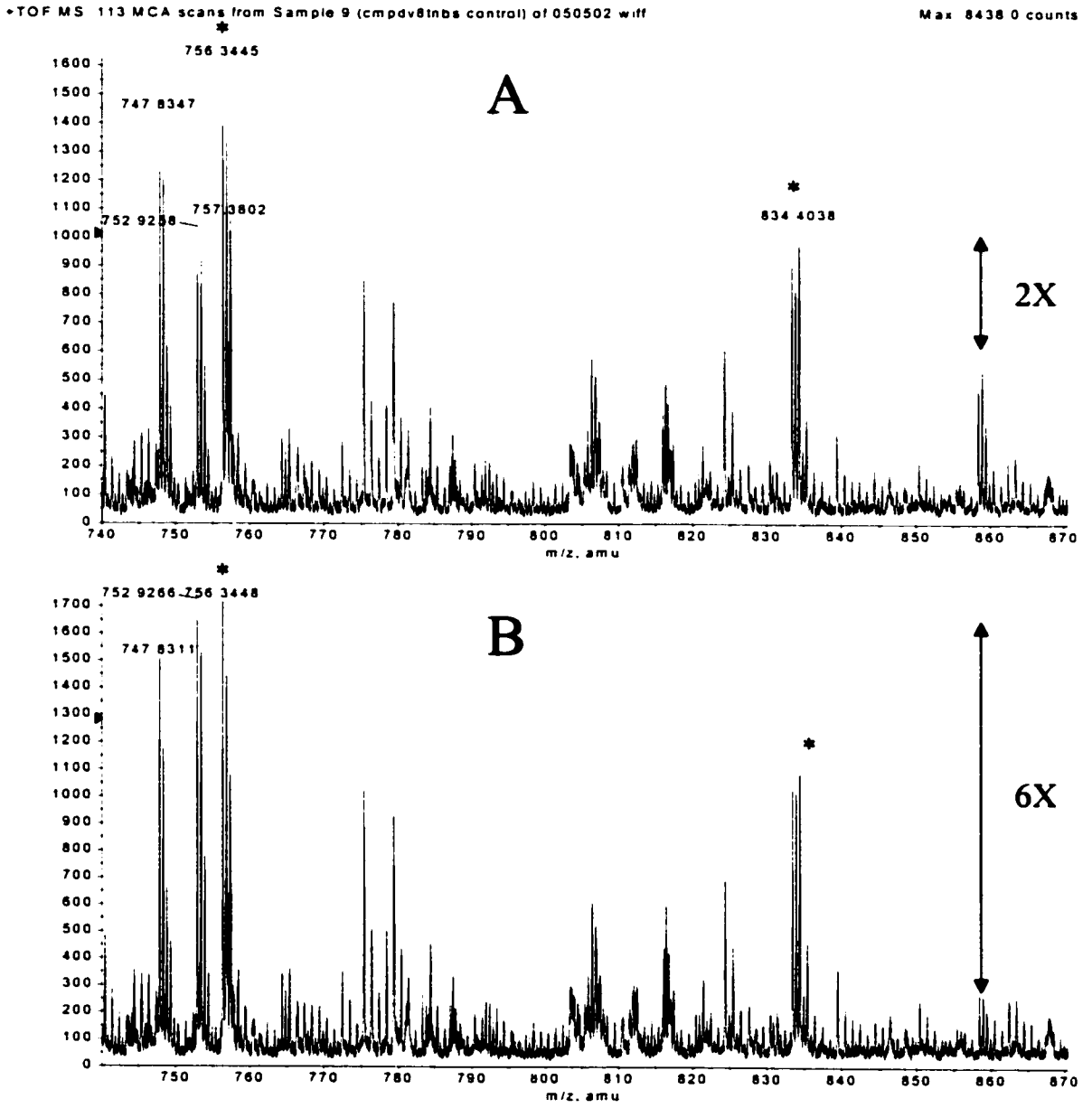

Fig. 3.9 ESI mass spectra of WT CM-PD modified with 5-fold excess TNBS in the absence (**A**) or presence (**B**) of 2-fold excess mutase TS analog, then digested overnight at 37 °C with Glu-C Endoprotease. The difference in the ratio of unmodified peptide (m/z 752.92) to modified peptide (m/z 848.41) in the absence or presence of the analog, respectively, indicated that Lys37 was protected from modification by the mutase TS analog. The internal standards were observed at m/z 834.40 and m/z 756.34 (*).

An important observation that helps correlate the changes in peak intensities with degree of protection by the mutase TS analog is the appearance in Fig. 3.9A and 3.9B of doubly charged peaks originating from other unrelated peptides of CM-PD. These peptides acted as internal standards, at m/z 834.40 and m/z 756.34 and showed identical intensities in both figures for the same number of scans (~115). It is clear from both figures that the only two peaks varying in intensity were the peaks under investigation.

3.2.7 Mass Spectral Analysis of pH-Dependent Alkylation of CM-PD with TNBS

The purpose of this experiment was to determine if the loss in mutase activity correlated with the extent of Lys37 modification at different pH values. The WT CM-PD was modified at pH 6.5, 7.2, 8.5 and 10, using the same conditions as for the inactivation experiments (without glycerol and samples after reaction with TNBS for 1 min), proteolytically digested, and analyzed by MS (Fig. 3.10). The mass spectra showed that the degree of alkylation increased with pH. At pH 6.5 and 7.2, there was an intense signal (m/z 752.91) corresponding to the unmodified peptide and a small peak (m/z 858.41) corresponding to the modified peptide. However, at pH 8.5 and 10.0, there was no signal at m/z 752.9, but the signal at 858.41 corresponding to the modified peptide was quite intense. It appeared that the modification of Lys37 was essentially complete by pH 8.5. These results suggest that the pK_a of Lys37 is between 7.2 and 8.5; the pH range from 8.5 to 10.0 represents the upper limit in the titration curve. The doubly charged peaks at m/z 798.47 and m/z 756.34 were used as internal standards since their intensity was relatively the same at the four different pH values.

Fig. 3.10 ESI mass spectra of WT CM-PD modified with 5-fold excess TNBS for 1 min in 50 mM sodium phosphate at pH 6.5 (**A**), 7.2 (**B**), 8.5 (**C**) and in 50 mM sodium pyrophosphate at pH 10.0 (**D**), then digested overnight at 37 °C with Glu-C endoprotease (2:1). At pH 6.5 and 7.2 (**A,B**), the unmodified and modified peptides were observed at m/z 752.91 and 848.41, respectively. At pH 8.5 and 10.0 (**C,D**), there was no signal for the unmodified peptide (circled portion) whereas a more intense signal corresponding to the modified peptide was observed at m/z 848.41 (indicated by arrow). The internal standards were observed at m/z 798.47 and m/z 756.34.

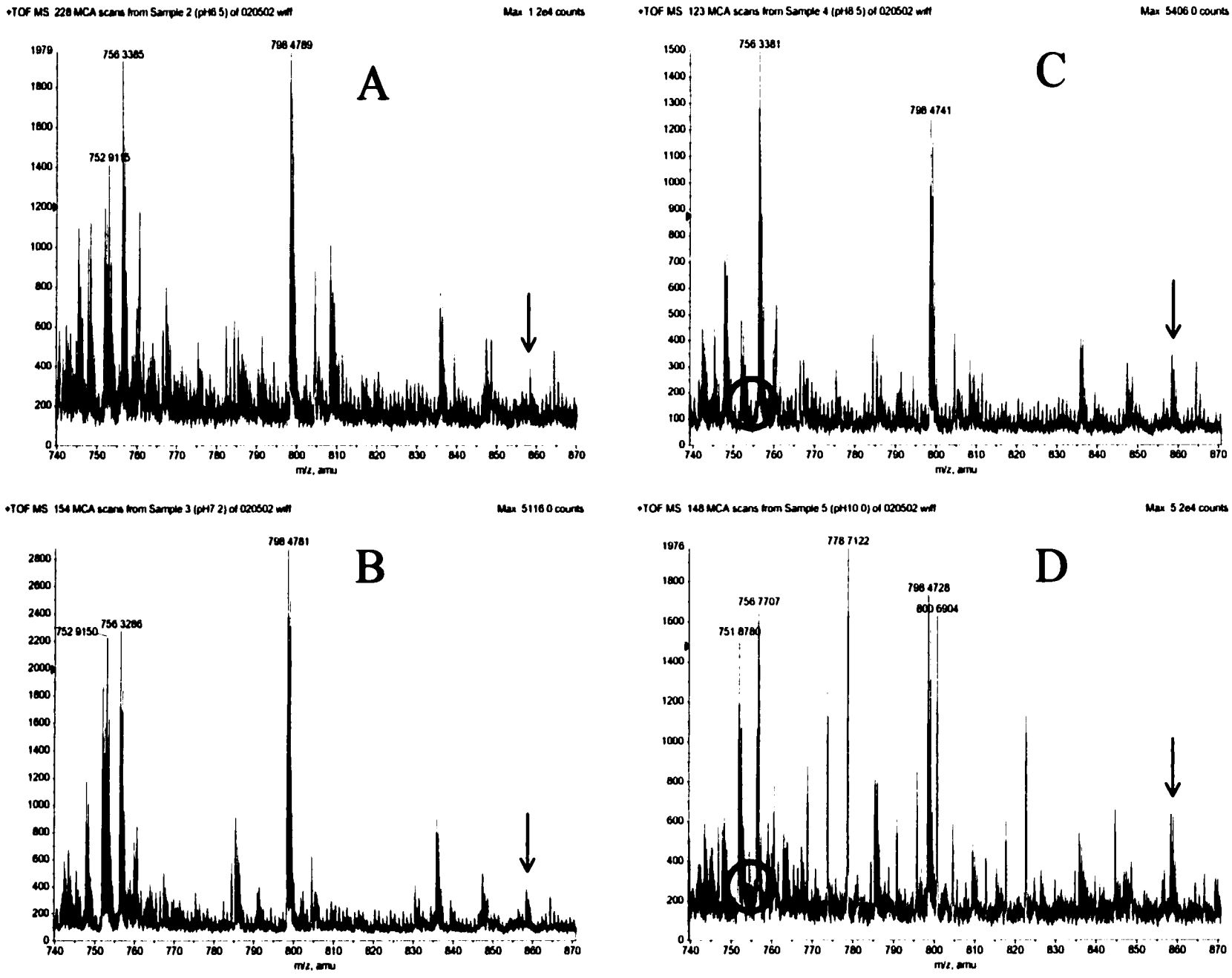
+TOF MS 228 MCA scans from Sample 2 (pH6 5) of 020502 wiff
Max 1 2e4 counts
A
756 3385
798 4789
752 9165
m/z, amu
+TOF MS 123 MCA scans from Sample 4 (pH8 5) of 020502 wiff
Max 5406 0 counts
C
756 3381
798 4741
m/z, amu
+TOF MS 154 MCA scans from Sample 3 (pH7 2) of 020502 wiff
Max 5116 0 counts
B
798 4781
752 9150
756 3286
m/z, amu
+TOF MS 148 MCA scans from Sample 5 (pH10 0) of 020502 wiff
Max 5 2e4 counts
D
778 7122
798 4728
756 7707
800 6904
751 8780
m/z, amu

3.3 DISCUSSION

In this chapter chemical modification studies and MS were conducted in parallel on WT and K37Q forms of CM-PD in order to determine the sensitivity of Lys37 towards modification with TNBS and to estimate the pK_a of this catalytically important residue in the CM reaction.

Results in this study showed that TNBS, a reagent that reacts reasonably specifically with Lys residues (75), rapidly inactivated the mutase (Fig. 3.1). Christendat and Turnbull (35) also reported that the reaction of CM-PD with the His modifying reagent diethyl pyrocarbonate (DEPC) led to the carbethoxylation of a Lys at a rate that was 50-100 times faster than normally observed for the reaction of an enzymic Lys with DEPC (93, 94). In the present study, interestingly, the dehydrogenase was not inactivated in a time-dependent fashion by reaction with TNBS, indicating the absence of a particularly reactive Lys at the PD site. In contrast, Christendat and Turnbull noted ~ 40% loss of dehydrogenase activity with TNBS reaction. However, this may be a consequence of the longer exposure to 20-fold molar excess of reagent to monomer CM-PD that was used compared to 45 min incubation with 3-fold excess used in the present study. It is worth noting that TNBS can react slowly with Cys residues (95, 96). However this seems unlikely in the present study since modification of Cys residues by sulfhydryl-specific reagents is expected to inactivate both CM and PD (Fig. 2.19 and 2.23).

Regrettably MS analysis of Glu-C digested fragments of the TNBS treated enzyme could not resolve the Cys-containing peptides. The two Cys-containing fragments, P(87-115) and P(157-221) were not observed in the MS spectrum of the digest. The high molecular weight of these two peptides, 3074.616 Da and 6849.636 Da, respectively, could explain their absence from the spectrum of the enzyme digest, since the sensitivity of the time-of-flight mass detector is low at the higher m/z range.

Inactivation of CM by TNBS was prevented by preincubation with stoichiometric amounts of *endo*-oxabicyclic diacid (Fig. 3.3), a compound that mimics the proposed transition state for the chorismate mutase reaction (40) and thus is expected to provide protection against modification of residues at the mutase active site. Similarly, preincubation of the enzyme with the product of the mutase rearrangement (prephenate) protected CM from inactivation (D. MacLauchlan, unpublished).

The mass spectrometric analysis of Glu-C digested fragments of WT and K37Q CM-PD after alkylation provided evidence that Lys37 was modified by TNBS. The absence of a modified peptide in the peptide map of K37Q clearly demonstrated that it is specifically Lys37 that was modified in the WT enzyme.

Our studies support the findings of Christendat and Turnbull (35) who identified Lys37 as the enzyme group that was exceptionally reactive with DEPC by differential peptide

mapping of TNBS treated CM-PD incubated in the absence and presence of DEPC (acting as a protective ligand).

Comparison of logV pH rate profiles between WT and H197N CM-PD allowed Christendat *et al.* to determine the pK_a of His197, an essential H-bond acceptor in the dehydrogenase reaction (26). This approach was not possible in the present study in order to determine the pK_a of Lys37 since the K37Q variant protein had no residual mutase activity. Instead a pK_a of ~ 7.5 was estimated for an enzymic residue that was particularly reactive with TNBS and whose modification resulted in a pH-dependent loss of CM activity (Fig. 3.4). These results correlated well with the pH-dependent modification of a Lys37 containing fragment of CM-PD (Fig. 3.10). Our preliminary MS studies, which were only performed at 4 different pH values (6.5, 7.2, 8.5 and 10.0), showed that alkylation of Lys37 was complete by pH 8.5. However, more experiments have to be repeated in the pH range 7.2 and 8.5 to better estimate the pK_a value. The pK_a value of ~7.5 agrees well with that determined for a protonated group titrating in the V/K pH rate profile for the mutase of WT CM-PD (22) and K. Bull (unpublished), implying that Lys37 possesses a pK_a of ~ 7.5, depressed because of its location in a positively charged active site (see Fig. 1.3). Such a result is in accord with the increased reactivity observed with TNBS and DEPC at neutral pH (Fig. 3.4) (35).

The work presented in this chapter provides one of the few examples reporting the titration of active site residues using chemical modification in conjunction with peptide mass mapping, and hence outlines the utility of this approach. Recently, Krekel *et al.* (97)

demonstrated by MS analysis that Cys115 of *Enterobacter cloacae* MurA was only alkylated by IAM at pH's > 7. Measurement of the enzymatic inhibition by IAM as a function of pH revealed a $pK_a \sim 8.3$.

4.0 FUTURE STUDIES

In the future, we would like to determine if TNBS is reacting with any of the three cysteines. This can be accomplished by quantifying the number of cysteines with DTNB after reacting the enzyme with TNBS. This can be checked also by reacting CM-PD with TNBS and then digesting the modified enzyme with trypsin and/or Glu-C endoprotease to verify the presence of an adduct on any of the Cys-containing peptides.

Second, we would like to "change" (Phe200) by site-directed mutagenesis at the putative dehydrogenase active site. Comparative modeling studies have located this group at the dehydrogenase active site. Phe200 can be important in binding substrates of the dehydrogenase reaction.

Finally, our preliminary studies for the determination of the pK_a of Lys37 done at four different pH's (6.5, 7.2, 8.5 and 10.0) have established the limits of the pK_a value. These early studies indeed suggest that the pK_a is depressed between 7.2 and 8.5. The MS studies have to be extended to include samples at 8 different pH's, which will allow us to narrow down the range of pK_a values. Furthermore, we will try to relate peak height or area to the susceptibility to alkylation by TNBS as a function of pH using an external standard (octapeptide; m/z 829) added to the digested protein before injection into MS. Matching the pK_a determined kinetically (pH rate profile) with the physical studies by MS will help us to conclude that this lysine is titrating in the pH rate profile.

5.0 REFERENCES

1. Pittard, J.T. and Gibson, F. (1970) *Curr. Topics Cell Reg.* **2**, 29-63.
2. Umbarger, H.E. (1978) *Ann Rev. Biochem.* **47**, 533-606.
3. Somerville, R.L. (1983) *Amino Acid Biosynthesis and Genetic Regulation*, Addison, Wesley Publishing Co. pp 351-378.
4. Brown, K.D. (1968) *Genetics* **60**, 31-48.
5. Gibson, F. and Pittard, J. (1968) *Bacteriol Rev* **32**, 465-492.
6. Dosselaere, F. and Vanderleyden, J. (2001) *Crit Rev Microbiol* **27**, 75-131.
7. Camakaris, H. and Pittard, J. (1973) *J. Bacteriol* **115**, 1135-1144.
8. Hudson, G.S. and Davidson, B.E. (1984) *J. Mol. Biol.* **180**, 1023-1051.
9. Yanofsky, C. (1988) *J. Biol. Chem.* **263**, 609-612.
10. Koch, G.L., Shaw, D.C. and Gibson, F. (1971) *Biochim. Biophys. Acta.* **229**, 795-804.
11. Turnbull, J. and Morrison, J.F. (1990) *Biochemistry* **29**, 10255-10261.
12. Heyde, E. and Morrison, J.F. (1978) *Biochemistry* **17**, 1573-1580.
13. Hudson, G.S., Howlett G.J. and Davidson B.E. (1983) *J. Biol. Chem.* **258**, 3114-3120.
14. Powell, J.T. and Morrison, J.F. (1978) *Eur. J. Biochem.* **87**, 391-400.
15. SampathKumar, P. and Morrison, J.F. (1982) *Biochim. Biophys. Acta.* **702**, 204-211.
16. Hudson, G.S., Wong, V. and Davidson, B.E. (1984) *Biochemistry* **23**, 6240- 6249.

17. Turnbull, J., Cleland, W.W. and Morrison, J.F. (1990) *Biochemistry* **29**, 10245-10254.

18. Christendat, D. Ph.D. Thesis (1998) Concordia University.

19. Koch, G.L.E., Shaw, D.C. and Gibson, F. (1972) *Biochim. Biophys. Acta*, **258**, 719-730.

20. Heyde, E. (1979) *Biochemistry* **18**, 2766-2775.

21. Sampathkumar, P. and Morrison, J.F. (1982) *Biochim. Biophys. Acta.* **702**, 212-219.

22. Turnbull, J. Cleland, W.W. and Morrison, J.F. (1991) *Biochemistry* **30**, 7777-7782.

23. Vincent, S., Chen, S., Wilson, D.B. and Ganem, B. (2002) *Bioorg. Med. Chem. Lett.* **12**, 929-931.

24. Christendat, D. and Turnbull, J. (1999) *Biochemistry* **38**, 4782-4793.

25. Christopherson, R.I., Heyde, E and Morrison, J.F. (1983) *Biochemistry* **22**, 1650-1656.

26. Christendat, D., Saridakis, V.C. and Turnbull, J. (1998) *Biochemistry* **37**, 15703-15712.

27. Liu, D.R., Cload, S.T., Pastor, R.M. and Shultz, P.G. (1996) *J. Am. Chem. Soc.* **118**, 1789-1790.

28. Zhang, S., Kongsaeree, P., Clardy, J., Wilson, D.B., and Ganem, B. (1996) *Bioorg. Med. Chem.* **4**, 1015-1020.

29. Gorisch, H. and Lingens, F. (1974) *Biochemistry* **13**, 3790-3794.

30. Andrews, P.R., Smith, G.D. and Young, I.G. (1973) *Biochemistry* **12**, 3492-3498.

31. Sogo, S.G., Widlanski, T.S., Hoare, J.H., Grimshaw, C.E., Berchtold, G.A. and Knowles, J.R. (1984) *J. Am. Chem. Soc.* **106**, 2701-2703.

32. Copley, S.D. and Knowles, J.R. (1987) *J. Am. Chem. Soc.* **109**, 5008-5013.

33. Delany, J.J., Padykula, R.E. and Berchtold, G.A. (1992) *J. Am. Chem. Soc.* **114**, 1394-1399.

34. Herbert, S., Chao, I. and Berchtold, G.A. (1982) *Biochemistry* **21**, 2778-2781.

35. Christendat, D. and Turnbull, J. (1996) *Biochemistry* **35**, 4468-4479.

36. Gray, J.V. and Knowles, J.R. (1994) *Biochemistry* **33**, 9953-9959.

37. Davidson, M.M, Gould, I.R. and Hillier, I.H. (1996) *J. Chem. Soc. Perkin Trans.* **2**, 525-532.

38. Xue, Y., Lipscomb, W.N., Graf, R., Schnappauf, G. and Braus, G. (1994) *Proc. Natl. Acad. Sci.* **91**, 10814-10818.

39. Chook, Y.M., Ke, H. and Lipscomb, W.N. (1993) *Proc. Natl. Acad. Sci.* **90**, 8600-8603.

40. Lee, A.Y., Stewart, J.D., Clardy, J. and Ganem, B. (1995) *Chem. Biol.* **2**, 95- 203.

41. Lee, A.Y., Karplus, P.A., Ganem, B. and Clardy, J. (1995) *J. Am. Chem. Soc.* **117**, 3627-3628.

42. Bartlett, P.A. and Johnson, C.R. (1985) *J. Am. Chem. Soc.* **107**, 7792-7799.

43. Bartlett, P.A., Nakagawa, Y., Johnson, C.R., Reich, S.H. and Luis, A. (1988) *J. Org. Chem.* **53**, 3195-3210.

44. Turnbull, J.L. Ph.D. Thesis (1988) Australian National University.

45. Voet, D., Voet, J.G., Pratt, C.W. *Fundamentals of Biochemistry*. New York: Wiley (80).

46. Hermes, J.D., Tipton, P.A., Fisher, M.A., O'Leary, M.H., Morrison, J.F. and Cleland, W.W. (1984) *Biochemistry* **23**, 6263-6275.

47. Addadi, L. Jaffe, E.K. and Knowles, J.R. (1983) *Biochemistry* **22**, 4494-4501.

48. Guilford, W.J., Copley, S.D. and Knowles, J.R. (1987) *J. Am. Chem. Soc.* **109**, 5013-5019.

49. Llewellyn, D.J. and Smith, G.D. (1979) *Biochemistry* **18**, 4707-4714.

50. Christopherson, R.I. and Morrison, J.F. (1985) *Biochemistry* **25**, 1116-1121.

51. Christopherson, R.I. (1985) *Arch. Biochem. Biophys.* **240**, 646-654.

52. Kenyon, G.L., and Bruce, T.W. (1997) *Methods Enzymol.* **47**, 407-430.

53. Lundblad, R.L. (1995) *Techniques in Protein Modification*, CRC Press, London, 107.

54. Gething, M.J., Davidson, B.E. (1977) *Eur. J. Biochem.* **78**, 111-117.

55. Zhang, S., Wilson, D.B., and Ganem, B. (2000) *Biochemistry* **39**, 4722-4728.

56. Pohnert, G., Zhang, S., Husain, A., Wilson, D.B., Ganem, B. (1999) *Biochemistry* **38**, 12212-12217.

57. Chook, Y.M., Gray, J.V., Ke, H. and Lipscomb, W.N. (1994) *J. Mol. Biol.* **240**, 476-500.

58. Nagel-Starczynowska, G. and Kaletha, K. (1993) *Biochim. Biophys. Acta.* **1164**, 261-267.

59. Liao, T.H., Ho, H.C. and Abe, A. (1991) *Biochim. Biophys. Acta.* **1079**, 335-342.

60. Esmann, M., Sar, P.C., Hideg, K. and Marsh, D. (1993) *Anal. Biochem.* **213**, 336-348.

61. Turk, T. and Macek, P. (1992) *Biochim. Biophys. Acta.* **1119**, 5-10.

62. Davis, D.A., Dorsey, K., Wingfield, P.T., Stahl, S.J., Kaufman, J., Fales, H.M., and Levine, R.L. (1996) Biochemistry 35, 2482-2488.

63. Peredo, A.G., Saint-Pierre, C., Adrait, A., Jacquamet, L., Latour, J.M., Michaud-Soret, I., and Forest, E. (1999) *Biochemistry* **38**, 8582-8589.

64. Gadda, G., Banerjee, A., Dangott, L.J., and Fitzpatrick, P.F. (2000) *J. Biol. Chem.* **275**, 31891-31895.

65. Ellman, G.L. (1959) *Arch. Biochem. Biophys.* **82**, 70-77.

66. Riddles, P.W., Blakeley, R.L. and Zerner, B. (1983) *Meth. Enzymol.* **91**, 49-60.

67. Riddles, P.W., Blakeley, R.L. and Zerner, B. (1979) *Anal. Biochem.* **94**, 75-81.

68. Gurd, F.R.N. (1972) *Meth. Enzymol.* **25**, 424.

69. Ouimet, P.M. and Kapoor, M. (1999) *Biochem. Cell. Biol.* **77**, 89-99.

70. Freitag, D.G., Ouimet, P.M., Girvitz, T.L. and Kapoor, M. (1997) *Biochemistry* **36**, 10221-10229.

71. Sinz, A. and Wang, K. (2001) *Biochemistry* **40**, 7903-7913.

72. White, P., Pelletier, A., Brault, K., Titolo, S., Welchner, E., Thauvette, L., Fazekas, M., Cordingley, M.G. and Archambault, J. (2001) *J. Biol. Chem.* **276**, 22426-22438.

73. Goldfarb, A.R. (1966) *Biochemistry* **5**, 2570.

74. Goldfarb, A.R. (1966) *Biochemistry* **5**, 2574.

75. Habeeb, A.F.S.A. (1966) *Anal. Biochem.* **14**, 328.

76. Cload, T.S., Liu, D.R., Pastor, R.M., and Schultz, P.G. (1996) *J. Am. Chem. Soc.* **118**, 1787-1788.

77. Rieger, C.E. and Turnbull, J. (1996) *Prep. Biochem.* **26**, 67-76.

78. Dudzinski, P.K. and Morrison, J.F. (1976) *Prep. Biochem.* **6**, 113-121.

79. Dawson, C.M.R., Elliott, C.D., Elliott, H.W. and Jones, M.K. (1986) *Data for Biochemical Research*. 3rd edition. Oxford Science Publications, Clarendon Press.

80. Bhosale, S.B., Rood, J.L., Sneddon, M.K. and Morrison, J.F. (1982) *Biochim. Biophys. Acta* **717**, 6-11.

81. Maruya, A., O'Connor, M.J. and Backman, K. (1987) *J. Bacteriol.* **169**, 4852-4853.

82. Laemmli, U.K. (1970) *Nature* **227**, 680-685.

83. Sampathkumar, P. (1978) Ph.D. Thesis. Australian National University.

84. Ellis, K.J. and Morrison, J.F. (1982) *Methods Enzymol.* **87**, 405-426.

85. Johnson, W.C.Jr. (1992) *Methods Enzymol.* **210**, 426-447.

86. Bates, P.A. and Sternberg, M.J.E. (1999) *Proteins, Suppl* **3**, 47-54.

87. Wilkins, M.R., Gasteiger, E., Sanchez, J.C., Appel, R.D., Hochstrasser, D.F. (1999) *Curr. Biol.* **6**, 1543-1544.

88. Aponte, R. (2002) M.Sc. Thesis. Concordia University.

89. Fruchter, R.G. and Crestfield, A.M. (1967) *J. Biol. Chem.*, **242**, 5807-5812.

90. Sherman, F., Stewart, J.W. and Tsunasawa, S. (1985) *BioEssays* **3**, 27-31.

91. Flinta, C., Persson, B., Jornvall, H. and Heijne, G. (1986) *Eur. J. Biochem* **154**, 193-196.

92. Meinnel T., Mechulam, Y. and Blanquet, S. (1993) *Biochimie* **75**, 1061-1075.

93. Wells, M.A. (1973) *Biochemistry* **12**, 1086-1093.

94. Holbrook, J.J. and Ingram, V.A. (1973) *Biochem. J.* **131**, 729-738.

95. Coffee, C.J., Bradshaw, R.A., Goldin, B.R., and Frieden, C. (1971) *Biochemistry* **10**, 3516-3526.

96. Goldin, B.R. and Frieden, C. (1971) *Biochemistry* **10**, 3527-3534.

97. Krekel, F., Samland, A.K., Macheroux, P., Amrhein, N., Evans, J.N. (2000) *Biochemistry* **39**, 12671-12677.